Molecular Dissection of Reovirus Outer Capsid Digestion During Entry

by

Thais Pontin Bernardes

A Thesis submitted to the Faculty of Graduate Studies of

The University of Manitoba

in partial fulfilment of the requirements for the degree of

MASTER OF SCIENCE

Department of Medical Microbiology and Infectious Diseases

University of Manitoba

Winnipeg, MB

Canada

I hereby declare that I am the sole author of this thesis.

I authorize the University of Manitoba to lend this thesis to other institutions or individuals for the purpose of scholarly research.

Thais Pontin Bernardes

I further authorize the University of Manitoba to reproduce this thesis by photocopying or by other means, in total or in part, at the request of other institutions of individuals for the purpose of scholarly research.

Thais Pontin Bernardes

The University of Manitoba requires the signatures of all persons using or photocopying this thesis. Please sign below, and give address and date.

TABLE OF CONTENTS

ACKNOWLEDGEMENTS

LIST OF FIGURES

LIST OF TABLES

LIST OF COPYRIGHTED MATERIAL

LIST OF ABBREVIATIONS

14SO$_4$	sodium tetradecyl sulphate
AF405	Alexa Fluor 405
AF408	Alexa Fluor 488
BSA	bovine serum albumin
CHT	α-chymotrypsin
CNS	central nervous system
CPE	cytopathic effect
cryoEM	cryo-microscopy
D-buffer	dialysis buffer
DAPI	4'6-diamidino-2-phenylindole
DOC	sodium desoxycholate
dsRNA	double-stranded RNA
E-64	cysteine-protease inhibitor
ECL	enhanced chemiluminescence system
EM	electron microscopy
ESB	electrophoresis sample buffer
FCM	flow cytometry
FCS	fetal calf serum
FITC	fluorescein isothiocyanate
FSC	forward scatter
HO buffer	homogenization buffer
HSR	hypersensitive region
ISVP	infectious (or intermediate) subviral particles
JAM	junction adhesion molecule
mAb	monoclonal antibody
MALDI-TOF	matrix-assisted laser desorption/ionization time of light
MEM	minimal essential medium
MOI	multiplicity of infection

mRNA	messenger RNA
MRV	mammalian reovirus
MβCD	methyl-β-cyclodextrin
NH_4Cl	ammonium chloride
NTPase	nucleoside triphosphatase
NTR	non-translated region
ORF	open reading frame
PBS	phosphate buffered saline
pen-strep	penicillin-streptomycin
PFU	plaque forming units
PKR	protein kinases
PMSF	phenylmethylsulfonyl fluoride
PVDF	polyvinylidene fluoride
RdRp	RNA-dependent RNA polymerase
RNA	ribonucleic acid
SDS-PAGE	sodium dodecyl sulphate polyacrylamide gel electrophoresis
SSC	side scatter
T1L	reovirus serotype 1 Lang
T2J	reovirus serotype 2 Jones
T3D	reovirus serotype 3 Dearing

ABSTRACT

Reovirus is the prototypic member of the family *Reoviridae* and well known as a respiratory and enteric virus that consists of 10 segments of double stranded RNA. Eight structural proteins are organized into two concentric capsids that surround the viral genome, where three of them (µ1, σ1 and σ3) are found in the outermost capsid layer and are responsible for events leading to cell entry. After interaction of σ1 with the host cell, virus is internalized by clathrin-mediated endocytosis. The acidic environment found within the endosome causes conformational changes in the viral proteins which eventually lead to generation of an infectious (or intermediate) subviral particle named "ISVP". The ISVP may also be formed extracellularly by proteases; consequently, susceptible host cells can be infected not only with intact viruses, but also with ISVPs. The ISVP differ from intact virus in that σ3 is completely removed and µ1 is cleaved into 2 smaller peptides (δ and ϕ). In addition, infectious entry of viruses, but not of ISVPs, is blocked by various inhibitors, including cysteine protease inhibitor E-64, acidification inhibitors such as ammonium chloride and chloroquine, and clathrin- or caveolae-mediated endocytosis inhibitors like chlorpromazine and methyl-β-cyclodextrin. Cleavage of reovirus outer capsid protein σ3 has been shown to be essential for virus internalization, whereas cleavage of its associated µ1 protein is needless when generating ISVP-like particles. The hypothesis presented here that there is a threshold of σ3 digestion required to allow the particle to bypass entry blockers has motivated this study, and the correlation of the reovirus population with the virus infectiousness was essential for this thesis conclusion. Results demonstrated that cleavage of σ3 is a multistep process

which is differently processed within the same population. By combining protease and detergent to the digestion of virions, data from this work showed distinct particles generated along the transition pathway. Particles digested for less than 7 minutes contained significant amounts of non-cleaved σ3 and, therefore, were not able to bypass entry blockers. Particles digested for more than 7 minutes contained approximately 25% of remaining σ3; however, infectivity was not inhibited by any chosen inhibitor. Until now, studies involving flow cytometry and specific antibodies to discriminate the reovirus population have not been applied to the family *Reoviridae*. When these tools were applied to this study they (1) provided a novel information about the reovirus population, (2) suggested that between virus and ISVP there is a gradual yet heterogeneous proteolysis of particles, and (3) demonstrated that infectiousness of reovirus particles may rely on ISVP only, and not on a group of particles as first thought. These findings mean that an *in vitro* infection of reoviruses may be accompany by the presence of different particles, which are proteolytically processed during the transition pathway to turn into a more infectious unit, called ISVP and proposed here as the determinant particle for reovirus penetration into cell. The approaches taken for this thesis work can be extended for studies of reovirus replication and pathogenesis. Moreover, it may help to shed some light on the development of safe and effective oncolytic agents.

1. INTRODUCTION

1.1. Mammalian reovirus

The mammalian reoviruses (also called reovirus or MRV) are the prototypic members of the *Orthoreovirus* genus from the family *Reoviridae* (Hadžisejdić et al, 2006). The family currently consists of 12 genera, two of which infect vertebrates only and others that infect vertebrates, invertebrates and plants (Kobayashi et al, 2006; Schiff et al, 2007; Lal et al, 2009). The family includes the highly contagious and relatively resistant rotavirus, an important agent that causes $20 - 40\%$ of child hospitalizations due to gastroenteritis worldwide (Rivest et al, 2004). Unlike the medically significant rotavirus, reovirus is relatively non-pathogenic in humans (Norman & Lee, 2000). It infects virtually every child in the first few years of life but the symptoms of its infection are usually very mild (Parashar et al, 1998; Stoeckel & Hay, 2006). Indeed, the acronym reovirus was coined by Sabin in 1959 to describe a virus that can be isolated from the <u>r</u>espiratory and <u>e</u>nteric tracts, but due to its lack in pathogenicity it was considered, hence, an <u>o</u>rphan virus (Sabin, 1959; Fields, 1985; Norman & Lee, 2000; Stoeckel & Hay, 2006). Although reovirus may be harmful to young children and neonates, more than half of healthy adults aged 20-30 years who have been exposed to this virus are seropositive (Selb & Weber, 1994; Norman & Lee, 2000). Currently, studies on reovirus are getting even more attention, not only for "basic" academic, but also on the medical area, where reovirus has been used as a potential agent for the treatment of cancer. Despite the fact that "normal" and "healthy" cells are more resistant to reovirus, the virus has been shown to successfully replicate in numerous transformed cells (Strong et al,

1998; Alain et al, 2002), exploiting the *ras* pathway and thus; leading to the cancer cell death (Hashiro et al, 1977; Tyler et al, 2001; Norman et al, 2004; Lal et al, 2009). During the past few years, several authors have described MRV as a broad infectious agent and a valuable tool to illustrate the cellular susceptibility to viruses (Morin et al, 1996; Tyler et al, 2001; Norman et al, 2004; Coombs, 2006; Kobayashi et al, 2006; Schiff et al, 2007). For instance, much of what is currently known about reovirus came from detailed studies involving viral reassortants, temperature-sensitive mutants, recoating of subviral particles, electron cryo-microscopy (cryoEM) and X-ray crystallography (Yin et al, 1996; Baker et al, 1999; Hazelton & Coombs, 1999; Jané-Valbuena et al, 1999; Liemann et al, 2002; Mendez et al, 2003; Coombs, 2006; Dryden et al, 2008). Considering structural details of individual proteins is fundamental when studying viral particles. Hence, delineating the precise requirements for events that positively or negatively affect the particle infectivity and its morphogenesis might be a future key in the development of new antiviral drugs and more specific oncolytic agents (Hermann & Coombs, 2004; Aghi & Martuza, 2005; Coombs, 2006; Lal et al, 2009).

1.2.   Reovirus structure

The *Reoviridae* family is comprised of non-enveloped particles (60 to 85 nm in diameter) consisting of segmented double-stranded (ds) RNA arranged inside a multi-layer icosahedral shell (Van Regenmortel & Fauquet, 2000; Tyler et al, 2001; Schiff et al, 2007). Reovirus genome is composed of 10 gene segments which are enclosed by two protein shells; termed inner capsid (or core) and outer capsid (Figure 1) (Joklik, 1981; Jiang & Coombs, 2005; Kobayashi et al, 2007). Five structural proteins
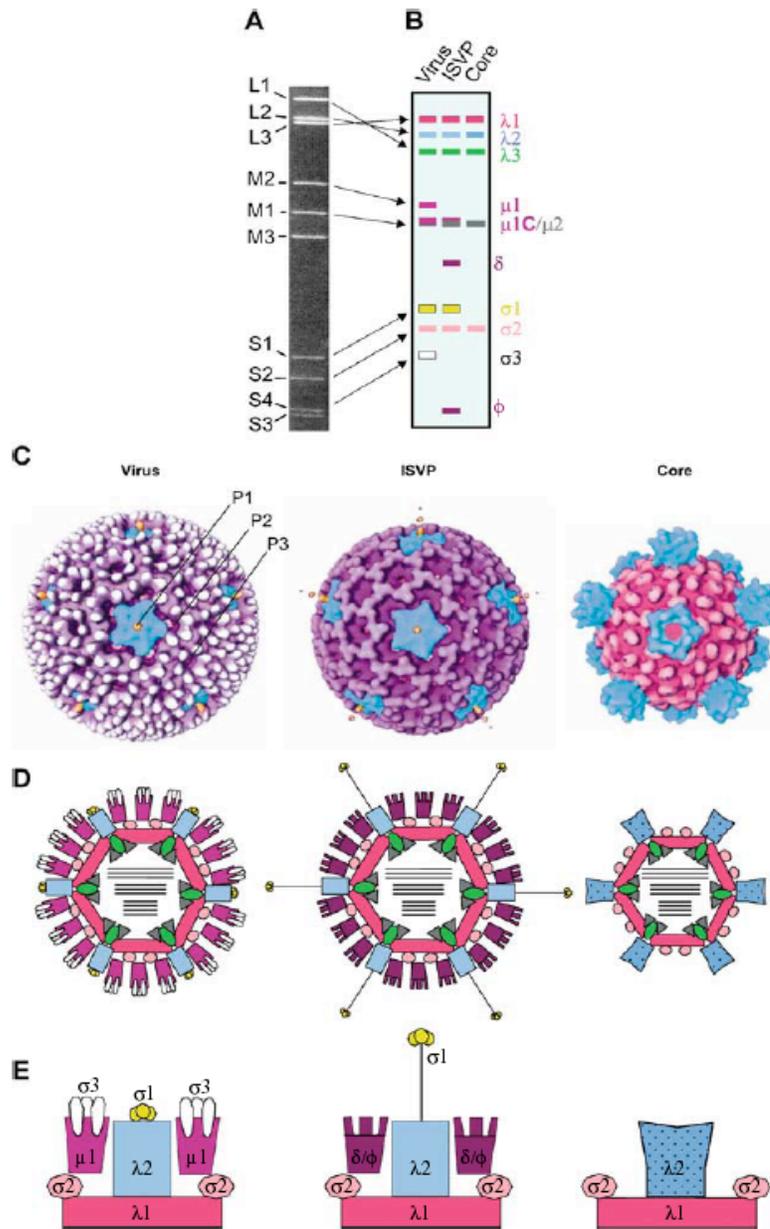
Figure 1. Mammalian reovirus type 1 Lang genome, protein locations and structure. **A.** Genome representation of MRV T1L in 10% SDS-PAGE containing all ten gene segments (L, large; M, medium; S, small genes) which encode the proteins highlighted in B (*arrows*). **B.** Protein profiles of virus, ISVP and core in a typical SDS-PAGE; note the presence of all eight structural proteins in virus, the absence of σ3 and cleavage of μ1 (into δ and φ) in ISVP, and the further absence of σ1 in core particle. **C.** CryoEM illustration of virus, ISVP and core. Images were colour coded to facilitate comparison of colors in B, D and E and examples of solvent channels P1, P2 and P3 are indicated. **D-E.** Detailed exemplification of each reoviral particle showed in C; note the conversion and/or the removal of proteins from one particle to the other. *Thick solid lines* in D indicate each gene segment described in A. Modified from (Coombs, 2006). Permission kindly granted from © Springer Science + Business Media on January 7, 2011.

5

(λ1, λ2, λ3, μ2, and σ2) organize the inner capsid, which is an active multienzyme complex that includes the viral genome and all the components required for transcription, methylation, and capping of its progeny messenger RNA (Coombs, 1998; Hadžisejdić et al, 2006). In addition to the core, the outer capsid is composed of three extra proteins (μ1, σ1, and σ3), which in turn complete the eight structural proteins necessary to form a full reovirus particle (Figure 1) (Dryden et al, 1993). Results from electron microscopy and SDS-PAGE have indicated that each structural protein is encoded by its own gene segment. These are divided according to their size as large (L1, L2, L3), medium (M1, M2, M3) and small (S1, S2, S3, S4) segments (Schiff et al, 2007). The three large segments correspond to about 3.8 – 3.9 kilobase pairs (kbp), the three medium to about 2.2 – 2.3 kbp, and the four small segments to about 1.2 – 1.5 kbp, all gather in a total genome of 23.6 kbp (Shatkin et al, 1968; Mustoe et al, 1978; Coombs, 2006). The number-based scheme applied to describe the segments within each gene class (i.e. L1-L3) has been related to their migration in the Tris/acetate-buffered gel system, which differ depending on the virus strain (Schiff et al, 2007). Since first isolation in the 1950s, three serotypes of reovirus have been classified based on neutralization and hemagglutination-inhibition tests (Ramos-Alvarez & Sabin, 1958; Sabin, 1959; Rosen, 1962; Lerner et al, 1963; Nibert et al, 1990; Norman & Lee, 2000). An isolate from a healthy child is the prototype strain for reovirus type 1, commonly described as reovirus type 1 Lang (T1L). Isolates from children with diarrhea are the prototype strains for reovirus types 2 and 3, respectively known as type 2 Jones (T2J) and type 3 Dearing (T3D) (Sabin, 1959; Stanley, 1967; Schiff et al, 2007). The major difference among the three reovirus strains has been genetically related to the S1 gene, which encodes the viral

attachment protein σ1 (Barton et al, 2001a; Clark et al, 2006). Each reovirus genome

segment consists of a small 5' non-translated region (NTR), an open reading frame

(ORF), a 3' NTR; and all of which are of different lengths (Coombs, 2006). Conserved

nucleotide regions have been described at the extreme 5' end (GCUA) and at the extreme

3' end (UCAUC) of all plus sense strands of reovirus genome. Additionally, regions

located near the segment ends and which extend to the protein-coding regions, are usually

more conserved than those located in the internal sequence region (Schiff et al, 2007).

1.3.   Inner shell

The core (i.e. the inner shell or inner capsid) is the inner-most complex of proteins

found in a reovirus particle. It features icosahedral symmetry and has a diameter of about

52 nm, not counting the extra 5.5 nm extension of λ2 proteins (i.e. core spike "turrets")

(Dryden et al, 1993; Coombs, 2006). As briefly described, the reovirus core contains five

of the total eight structural proteins present in a virion (Figure 1) (Reinisch et al, 2000).

Internally, core is composed of transcriptase complexes enclosed by 60 dimers of a 142

kDa protein, λ1 (Harrison et al, 1999; Schiff et al, 2007). Externally, it is connected by

turrets of 12 pentamers of λ2, a 144 kDa protein; and decorated with nodules of 150

monomers of σ2, a 47 kDa protein (Wiener et al, 1989; Reinisch et al, 2000; Coombs,

2006; Schiff et al, 2007). The remaining two structural proteins - λ3 and μ2 - are

respectively, an internal 142 kDa protein (12 copies) that is considered the virion RNA-

dependent RNA polymerase (RdRp); and an enigmatic 83 kDa protein (~24 copies),

which has an influence on nucleoside triphosphatase (NTPase) and on viral transcription,

perhaps, through interactions with λ1 and λ3 RdRp (Yin et al, 1996; Dryden et al, 1998;

Zhang et al, 2003). Several studies have proposed that λ1 protein is a zinc metalloprotein that not only has ATPase activity, but also exhibits a non-specific affinity for single-stranded or double-stranded RNAs (Bisaillon & Lemay, 1997; Bisaillon et al, 1997; Lemay & Danis, 1994). Despite that, the specific role of both λ1 and μ2 proteins in the viral mRNA synthesis is not as thoroughly defined as the role of λ2 protein. The turrets are believed to serve as conduits through which nascent transcripts of mRNAs are extruded from the cores (Mendez et al, 2008). Moreover, λ2 manifests methyltransferase and guanylyltransferase activities; thus, is required for capping of mRNAs (Dryden et al, 1993; Coombs, 2006). Both σ2 and λ2 reside at radial positions, atop the λ1 shell, and between the inner and outer capsid of virions (Schiff et al, 2007). The σ2 protein is not directly related to any enzymatic activity, but is thought to act as a stabilizing clamp required to support the core shell (Xu et al, 1993; Dryden et al, 1998; Reinisch et al, 2000). Like σ2, the strategic position of λ2 may be particularly important for holding shells together. Featuring an extended conformation, λ2 span from the core into the outer capsid, and hence; it may act as an important sustainability device for a full reovirus particle (Schiff et al, 2007).

1.4.   Outer shell

The outermost complex of proteins found in reovirus particle is essentially composed of 600 copies of each of the two major proteins, μ1 and σ3; and 36 copies of the cell attachment protein, σ1 (Lee et al, 1981; Cashdollar et al, 1985; Nibert et al, 1991a; Dryden et al, 1993; Chandran et al, 2002). Multiple copies of these three reovirus structural proteins appear to be arranged in a T=13*l* icosahedral lattice (Nibert et al,

1991a; Dryden et al, 1993; Hadžisejdić et al, 2006). The role of this outer layer is to mediate cell tracking, penetration or disruption, and finally, deposit of the transcriptionally active core into the cell cytoplasm (Chandran et al, 2002; Odegard et al, 2004; Zhang et al, 2005; Zhang et al, 2006). Considering that µ1 protein (76 kDa, 200 trimers per particle) is usually present in its autolytic fragments µ1N (4 kDa, myristoylated) and µ1C (72 kDa), it has been proposed that cleavage of µ1 is a key step during viral penetration into cells (Chandran et al, 2002; Odegard et al, 2004). Moreover, trimers of µ1 are intimately connected to monomers of σ3 protein (41 kDa, 600 copies). Their association form heterohexamer complexes ($\mu1_3\sigma3_3$) that provide stability to the shell while protecting µ1 from proteolytic agents (Zhang et al, 2006; Schiff et al, 2007). Besides protecting the outer proteins from the extracellular environment, σ3 decorates the primary lattice of proteins and regulates some viral activities (Chandran & Nibert, 1998; Chandran et al, 2002). For instance, σ3 has dsRNA-binding capacity and acts as an antagonist of cell protein kinases (PKR). By inhibiting the interferon pathway and counteracting the host antiviral responses, σ3 allows the virus translation and its consequent spread (Olland et al, 2001). The last protein to complete the viral outer shell is a minor component which is manifested at the fivefold icosahedral vertex as oligomeric complex of σ1 subunits (Nibert et al, 1991a; Dryden et al, 1993). σ1 protein has been shown to assume both folded and extended conformation in viral particles. In the latter, σ1 expand as much as 40 nm out from viral particle, an advantage that confer virus a receptor-recognition (junction adhesion molecule, JAM) and tropism towards its target cells (Weiner et al, 1977; Lee et al, 1981; Barton et al, 2001a; Clarke & Tyler, 2003). There are three distinct types of channels present in a full reovirus particle. They

are located across the inner and outer capsid layers and are known as P1, P2 and P3 (Figure 1). P1 is present in a total of twelve channels and is formed by turrets of λ2 at the fivefold vertices. P2 and P3 are each present in a number of 60 channels, which are respectively surrounded by four or six subunits of σ3 protein (Dryden et al, 1998; Coombs, 2006). The function of these channels is not well understood; however, there has been speculation that channels may be required for conformational changes involving proteins like µ1 during viral penetration and infection of cells, or to allow nucleotides to enter particles for transcription (Schiff et al, 2007).

1.4.1. Mu 1 – reovirus penetration protein

Protein µ1 is the primary translation product of the reovirus M2 gene segment (Chandran et al, 2002; Coombs, 2006). Trimers of µ1 are assembled in dimensions of 10 × 8 × 7 nm with each of its subunits fully embracing each other as they coil counter clockwise from base to tip (Liemann et al, 2002). A complete subunit of µ1 has been described to have a Z shape composed of four domains (Figure 2). Three; domains I, II, III are primarily α-helical, while the forth, and most distal domain, is a canonical jelly-roll β-barrel, as similarly seen in capsids of other animal viruses (e.g. picorna-, noda-, and tetraviruses) (Guglielmi et al, 2006). These domains are essential for µ1 protein-to-protein interaction (Liemann et al, 2002; Guglielmi et al, 2006). For instance, domain I is the base of the trimer that interacts with core surface proteins. Moreover, it is the domain that contains the conserved autocatalytic cleavage site of the protein (Liemann et al, 2002). Domain II is basically the structure of µ1, with a long and horizontal α-helix that is oriented almost parallel to the trimer base. Moreover, the myristoyl group is found

located in one of the domain II segment (Liemann et al, 2002). Domain III is composed of five α-helices and a small β strand. Two of the five α-helices are believed to form a complex to which σ3 assembles (Liemann et al, 2002). Domain IV has two β sheets and forms the head of the µ1 trimer. An extended surface of domain IV participates in the heterohexamer interactions of µ1-µ1 or µ1-σ3 proteins (Liemann et al, 2002). Interactions with its protector protein σ3 are usually presented in a 1:1 combination (Schiff et al, 2007). The complex involves a central µ1 trimer with three monomers of σ3 connected to its upper half (Figure 2). This heterohexamer formation accounts for a great proportion of the reovirus outer capsid. Besides the interaction with σ3, µ1 also interacts with viral proteins present on core shell (Dryden et al, 1993; Reinisch et al, 2000). Two hundred trimers of µ1 are situated atop the 150 monomers of σ2. Additionally, at some position these trimers are connected side-to-side with two adjacent λ2 subunits (µ1.Q trimer) (Zhang et al, 2005). These contacts are believed to anchor µ1 layer in the core capsid, stabilizing the outer capsid structure, and limiting conformational changes triggered during entry (Smith et al, 1969; Zhang et al, 2005). In virions, full-length µ1 is 708-amino-acids-long. µ1 undergoes several cleavages during replicative cycle yielding a myristoylated amino-terminal fragment, µ1N; and a carboxy-terminal fragment, µ1C (Nibert et al, 1991b; Coombs, 2006,). The µ1C cleavage is supported by electrophoresis of purified virions, which demonstrates that 95% of µ1 appears in its cleaved form at 72 kDa. Also, detection of an additional µ1 fragment, µ1N (4 kDa), was achieved via high resolution SDS-PAGE. Cleavage of the latter has been proposed to occur between amino acids Asn_{42} and Pro_{43}, and is believed to be an in gel artifact due to sample manipulation (Dryden et al, 2008). Nevertheless, the asparagine residue is also found in close
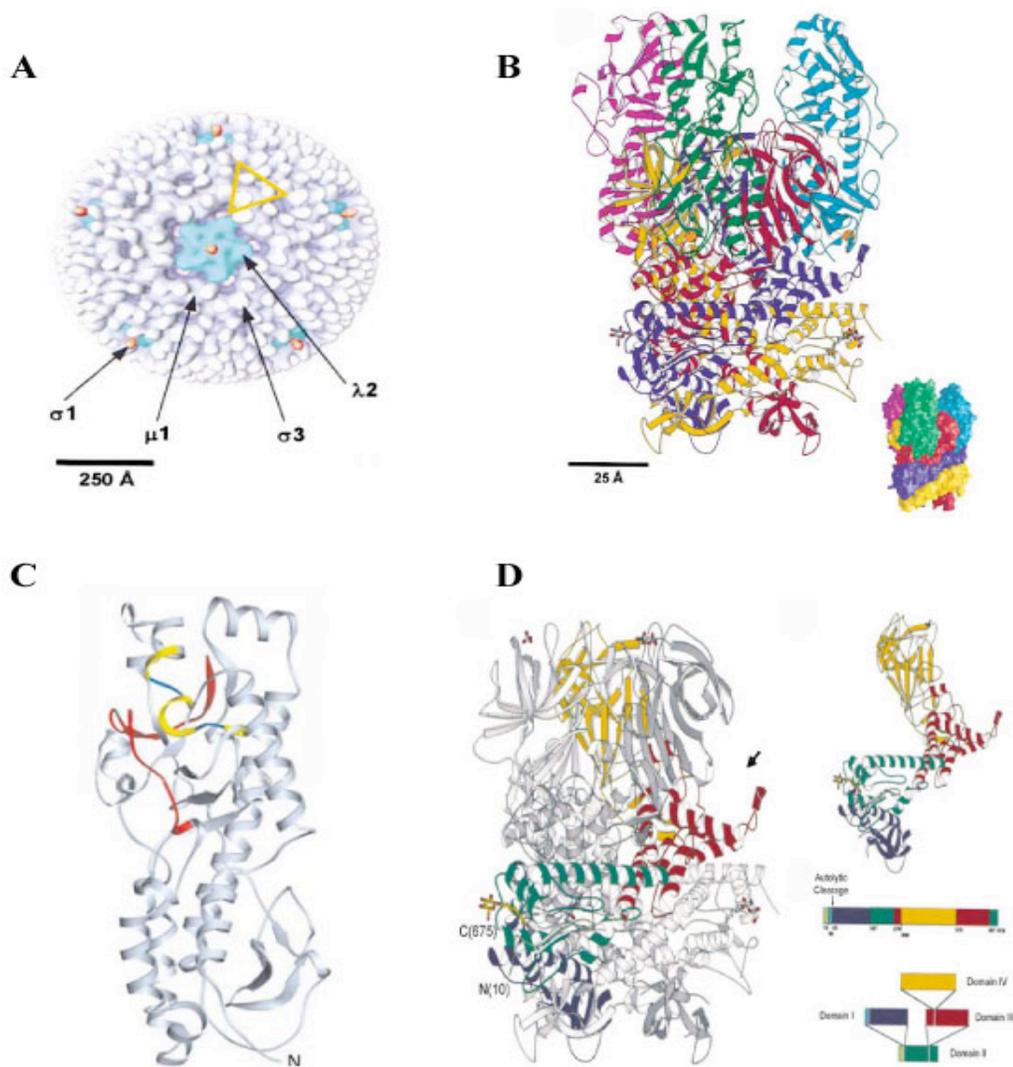
Figure 2. Structure of the µ1/σ3 heterohexamer and its subunits. A. Demonstration of reovirus particle and the four surface-exposed proteins, of which only µ1 and σ3 are further described. **B.** Side view of the $\mu1_3\sigma3_3$ heterohexamer. The bottom of the complex interacts with σ2 proteins present in core layer. Three σ3's (colored in green, cyan and magenta) sits on top of µ1 trimer (colored in red, violet and yellow). The three µ1 subunits wrap around each other as they twist 360°. Two subunits of µ1 are the contacts for each monomer of σ3. **C.** Side view of σ3 structure. **D.** On the left, µ1 trimer shown without bound σ3. On the upper right, a diagram illustrates one µ1 subunit. On the bottom right, the domain segmentation of the amino acid sequence. Domains are color coded according to one µ1 subunit in the 3D-structure (domain I, light and dark blue [µ1N, µ1C]; domain II, light and dark green [µ1N, µ1C]; domain III, red; domain IV, yellow). All domains are shown within the central domain II. Domain II holds domains I and III, and domain III equally contains domain IV. The other 2 subunits of µ1 are shown in gray. The arrow indicates the σ3 binding site. Adapted from (Liemann et al, 2002) and (Guglielmi et al, 2006). Permission kindly granted from both © Elsevier and © Springer Science + Business Media on January 7, 2011.

proximity to the N-terminal side of other animal viruses (e.g. avian reo-, polio-, rhino-, picornaviruses, etc.). This suggests that N-myristoylation and the autocatalytic cleavage of structural proteins may play an important role during viral replication (Nibert et al, 1991b; Odegard et al, 2004; Nibert et al, 2005; Zhang et al, 2005; Noad et al, 2006). One of the initial steps in reovirus penetration is marked by removal of σ3 protein, which in consequence, exposes μ1 to the cellular environment (Sturzenbecker et al, 1987; Bodkin et al, 1989; Nibert & Fields, 1992; Ebert et al, 2002). Briefly, the disassembly process is a key step in conformational rearrangements in μ1 protein (Nibert et al, 1991b; Chandran & Nibert, 1998; Chandran et al, 2002; Odegard et al, 2004). Cleavage of μ1N/μ1C allows the release of its myristoylated N-terminal peptide (μ1N), which probably interacts with the cell membrane (Zhang et al, 2006). The fact that μ1N has an addition of C14 fatty acid groups that may increase its hydrophobicity strongly supports this interaction proposal (Nibert et al, 1991b; Hruby & Franke, 1993; Chandran et al, 2002; Chandran et al, 2003; Odegard et al, 2004). Moreover, recent studies have found μ1N in association with red blood cell membranes and have suggested that this portion itself is sufficient for pore formation in cells (Nibert et al, 2005; Ivanovic et al, 2008). Related to that, Mendez and colleagues (2003) have published that proteolysis of the C-terminus of μ1 precedes σ3 digestion when virus is treated with trypsin and analysed by mass spectrometry. Also, earlier studies have found that specific monoclonal antibodies react against μ1 when in contact with full reovirus particles (Hayes et al, 1981; Virgin IV et al, 1994). Significance of these cleavages (μ1N/μ1C) is not fully understood yet; nevertheless, it suggests that μ1 is probably exposed on the surface of the reovirus particle and even more, supports that cleavage of μ1 is a prerequisite for reovirus penetration. The subsequent steps that allow

virus translocation into cytoplasm are still to be described.

1.4.2. Sigma 3 – reovirus protector protein

The full-length σ3 is a 365-amino acid long, N-terminally acetylated protein encoded by the S4 genome segment (Giantini et al, 1984; Kedl et al, 1995; Mendez et al, 2003). It is a major outer capsid protein that protects virus from environment proteolysis and forms a sheltering cap for µ1 protein (Nibert et al, 1991a; Guglielmi et al, 2006). The σ3 protein folds into a two-lobed cylindrical structure with a length of 7.6 nm and a diameter of 4.7 nm (Olland et al, 2001). The large C-terminal lobe is made of ~225 residues organized around several α-helices, short β-sheets, and large loops that are exposed on the virion surface. The small N-terminal lobe stabilizes the σ3 dimer via a conserved α-helical region that is the contact to other major outer capsid protein, µ1 (Figure 1 and 2) (Nason et al, 2001; Olland et al, 2001; Liemann et al, 2002). A non-conserved side is positioned close to P2 and P3 solvent channels and features large loops. The protein contains a zinc finger motif and binds zinc in its small lobe. This has been suggested as a requirement for proper particle folding and stability while maintaining the separation of motifs that further bind to dsRNA (Giantini et al, 1984; Schiff et al, 1988; Danis et al, 1992; Mabrouk & Lemay, 1994; Olland et al, 2001). The σ3 protein is the first one removed during entry of the infectious particle (Guglielmi et al, 2006). Its cleavage and subsequent disassembly has been chiefly accepted as one of the most important steps in reovirus early infection (Sturzenbecker et al, 1987; Baer & Dermody, 1997; Mendez et al, 2003; Golden et al, 2004). Coombs' group have extensively studied the digestion of σ3 by SDS-PAGE and mass spectrometry (Mendez et al, 2003;

Hadžisejdić et al, 2006). Together with others, they have proposed the cleavage in a central specific hypersensitive region (HSR) that continues bidirectionaly towards the protein's termini until all protein has been digested (Ebert et al, 2002; Jané-Valbuena et al, 2002; Mendez et al, 2003). Depending on the reovirus strain (e.g. T1L and T3D), the HSR can be located in different regions (amino acid residues 238–244 in T1L and 208–213 in T3D), modifying the protein cleavage pattern and its susceptibility to proteases (Jané-Valbuena et al, 1999; Jané-Valbuena et al, 2002). Moreover, Hadžisejdić and collaborators (2006) have shown that cleavage rate and digested products may also differ depending on the protease used and whether detergent is applied to the *in vitro* proteolysis. Previous reports have shed light on the mechanisms of σ3 cleavage and viral disassembly by using mutant reoviruses achieved by persistent infections of murine cells. The resultant viruses had a tyrosine-to-histidine single mutation at amino acid 354, near the carboxy-terminus of σ3. The mutation increased the viral proteolysis, led to σ3 structural rearrangements comparable to *in vivo* reactions (due to low pH environment in the digestive system), and in contrast to wild-type reoviruses, yielded a particle resistant to viral entry blockers (e.g. acidification inhibitors [ammonium chloride] and proteolysis inhibitors [E-64]) (McCrae & Joklik, 1978; Mustoe et al, 1978; Dermody et al, 1993; Baer & Dermody, 1997; Wetzel et al, 1997; Baer et al, 1999; Ebert et al, 2001; Wilson et al, 2002). Moreover, passage of wild-type reovirus in the presence of E-64 selects resistant viruses that have mutations in S4 gene, which encodes the σ3 protein (Ebert et al, 2001). The provided results demonstrated that mutations in σ3 protein allow variant reoviruses to bypass pharmacologic inhibitors, and indicate that indeed, σ3 cleavage at C-terminus has a major function during viral disassembly. However, the detailed pathway

from disassembly to virus internalization has yet to be unveiled; hence, the reason for this study. Non-structural functions were also attributed to the outer capsid protein σ3. For instance, the protein shuts down host protein synthesis and counteracts host defenses (i.e. interferon activation) by binding to cytoplasmic dsRNA at C-terminus residues 234 and 297 (Huismans & Joklik, 1976; Sharpe & Fields, 1982; Imani & Jacobs, 1988; Schiff et al, 1988; Miller & Samuel, 1992; Denzler & Jacobs, 1994; Beattie et al, 1995; Schiff, 1998; Olland et al, 2001). Moreover, the interaction of σ3 with dsRNA is independent of RNA sequence but dependent on duplex length (Huismans & Joklik, 1976). Mutational analysis has demonstrated that absence of zinc-binding sites decreases the intracellular stability and also interrupts the σ3 interaction with protein µ1 (Mabrouk & Lemay, 1994; Olland et al, 2001). Nevertheless, the loss of zinc does not seem to affect the way σ3 binds to dsRNA (Olland et al, 2001). Regarding the σ3 N-terminal, reports have shown that it contains an acetyl group and it may also serve to stabilize the structure or to promote protein complex assembly (Cumberlidge & Isono, 1979; Berger et al, 1981; Tercero & Wickner, 1992; Nguyen et al, 2000). Another speculation is that N-terminal acetylation may be involved in the differentiation of the roles σ3 plays during the virus life cycle (Polevoda & Sherman, 2000). However, the precise activity of this acetylated molecule is still not completely understood.

1.5. Reovirus proteolysis and morphological forms

The virion is the main virus progeny released from dead, dying, or disrupted cells in tissue culture or animal models (Schiff et al, 2007). The partial uncoating of virion leads to two well-known reovirus-derived particles: infectious (or intermediate) subviral

particles and cores (Shatkin & Sipe, 1968; Smith et al, 1969; Joklik, 1972; Shatkin & LaFiandra, 1972; Borsa et al, 1973). As described in detail in Table 1, the prime difference between virions and ISVPs is the lack of outer capsid protein σ3 and the cleavage of μ1 into 2 fragments; the 59 kDa N-terminal fragment δ and 13 kDa C-terminal fragment φ (Joklik, 1972; Shatkin & LaFiandra, 1972; Nibert & Fields, 1992; Dryden et al, 1993; Coombs, 1998; Reinisch et al, 2000; Chandran et al, 2003). The further lack of outer capsid proteins σ1 and μ1 fragments is what subsequently differentiates core from ISVP particles (Figure 1) (Joklik, 1972; Nibert et al, 1991a; Nibert & Fields, 1992; Dryden et al, 1993; Schiff et al, 2007). Protease digestions of virions can generate both ISVPs and cores under *in vitro* conditions that mimic the forms that participate in the *in vivo* infection and replication (Schiff et al, 2007). ISVP* is a recently identified uncoating of ISVP that has been referred to also play a role in both *in vitro* and *in vivo* infections (Joklik, 1972; Chandran et al, 2002; Chandran et al, 2003; Zhang et al, 2006). This distinct form of ISVP includes conformational changes in μ1 that further exposes δ fragments to proteolysis. The structural changes also promote shedding of σ1 by rearrangements in λ2 that release σ1. Consequently, Nibert's group have described that ISVP*, and not ISVP, must be the particle which penetrates the cytoplasm and precedes the core form (Chandran et al, 2002; Chandran et al, 2003; Zhang et al, 2006). Nonetheless, the morphologies of the three common reovirus forms were described via negative-stain electron microscopy (EM). Virions are generally spherical but contain flattened areas around the five-fold axes. ISVPs are shown even more spherical than virions; however, they are clearly identified by the conformation of proteins μ1 and σ1, which appear respectively jagged and extended by long fibers, on the

17

surface of ISVP particles (Figure 1) (Furlong et al, 1988). Cores are identified by the prominent turrets ($\lambda 2$ protein), which after removal of virus outer capsid proteins are seen to project out from the particle's surface (Figure 1) (Jiang & Coombs, 2005). To obtain reovirus-derived particles, virions are grown in murine cells and after several extraction procedures; they are finally purified by centrifugation with CsCl density gradient (Mendez et al, 2000; Berard & Coombs, 2009). The resultant virion particles have a density of about 1.36 g/ml (Table 1). When tested for infectivity by plaque assay, a virion particle:plaque forming units (PFU) ratio around 50:1 to 500:1 is usually seen. The high ratio has been suggested to be caused by defective particles that are measured via OD_{260} but are incapable of a productive infection (Schiff et al, 2007). To understand more about these reovirus particles and therefore, the virus structure; proteases (e.g. trypsin and chymotrypsin), temperature, and time, are often combined to create the best *in vitro* condition to convert virions into ISVPs or cores (Smith et al, 1969; Joklik, 1972; Shatkin & LaFiandra, 1972; Sturzenbecker et al, 1987; Furlong et al, 1988, Nibert & Fields, 1992; Mendez et al, 2003; Hadžisejdić et al, 2006). ISVP and cores seem to play important roles during viral disassembly and infection (Middleton et al, 2002). For instance, cores are active at the *in vitro* transcription and are thought to represent the primary particles that access the host cytosol to deliver the plus-strand RNAs for translation and packaging (Joklik, 1972; Borsa et al, 1973; Borsa et al, 1981; Jiang & Coombs, 2005). Additionally, cores are poorly infectious particles. Since they lack the outer-capsid proteins $\sigma 1$ (attachment protein) and $\mu 1$ (penetration protein) that mediate the viral entry, the hypothesis that cores are less capable of infection and therefore, are delivered to cell's cytoplasm via proteolysis of other reovirus particles (e.g. ISVPs)

Table 1. Differences and Similarities of the Common Reovirus Particles.

Features	Virion	ISVP	Core
Outer capsid proteins			
σ3	Present	Absent	Absent
σ1	Present	Present (extended)	Absent
μ1/μ1C	Present	Present (fragments δ + φ)	Absent
λ2	Present	Present	Present
Inner capsid proteins	Present	Present	Present
Infectivity in culture	+	++	−
Infectivity in presence of entry blockers (e.g. acidification or protease inhibitors)	−	+	−
Interaction with membrane bilayers	No	Yes	No
Diameter (nm)	85	80	60
Density in CsCl (g/ml)	1.36	1.38	1.43
Molecular weight (MDa)	127	103	49

seems to be relevant (Silverstein et al, 1970; Silverstein et al, 1972; Borsa et al, 1979; Borsa et al, 1981; Jiang & Coombs, 2005). On the other hand, ISVPs contain all the necessary proteins for a successful infection. In fact, ISVPs appear to be specifically required for *in vitro* infections in mouse models and are more infectious than other reovirus forms; presumably due to the extended conformation of its σ1 attachment protein. An exception is found in some isolates such as T3D, which have a σ1 sensitive to protease cleavage, thus, demonstrates loss in infectivity (Joklik, 1981; Amerongen et al, 1994; Schiff et al, 2007). While the identification of these reovirus-derived intermediate particles has provided a good model of reovirus entry, a better understanding of the molecular requirements and the structural transitions that allow these particles to enter cells is still needed.

1.6. Reovirus infection and dissemination

For a virus to produce systemic infection, it needs first to spread from its primary site of infection and replication, and then travel to distant target tissues (Tyler et al, 1986). The reovirus natural portal of entry is the host's respiratory and enteric tracts (Sabin, 1959). To deeply understand the essential steps in reovirus infection, newborn mice have been extensively used as a model to investigate the reovirus pathogenesis. Due to their exquisite sensitivity, mice are usually infected with strains T1L and T3D via enteric tracts (Wolf et al, 1981; Rubin et al, 1985; Bodkin et al, 1989; Organ & Rubin, 1998). Following peroral inoculation, the reovirus outer capsid proteins pass through the low pH in the stomach and finally reach the intestine, where they encounter pancreatic proteases such as trypsin or chymotrypsin (Golden et al, 2002). Within this rough

environment, the viral outer capsid proteins begin to be processed. Then, removal of σ3

protein and structural modifications in viral proteins (µ1 → δ/ϕ) turn virions into ISVPs

(Bodkin et al, 1989; Liemann et al, 2002). Both virions and ISVPs are thought to adhere

and penetrate into intestinal tissue via microfold (M) cells overlying Peyer's patches

(Amerongen et al, 1994; Wolf et al, 1981). Virus is subsequently transported across the

cell membrane via receptor-mediated endocytosis and delivered to the basolateral surface

(Wolf et al, 1987). In detail, the first step in the virus infectious cycle is the attachment to

receptors (e.g. JAMs) present on the surface of the host cells (Figure 3, step 1). The

reovirus protein that mediates this process, σ1, has a globular head at the C-terminus that

allows binding to junctional adhesion molecule-A, and residues in its tail that link to a

carbohydrate that has not been fully determined (Lee et al, 1981; Barton et al, 2001c;

Chappell et al, 2002; Antar et al, 2009). In contradiction to reovirus T1L, T3D also binds

sialic acid at a midpoint region of the σ1 tail (Chappell et al, 1997; Barton et al, 2001b).

After engaging receptors, the virion is internalized via clathrin-mediated endocytosis and

disassembled within minutes due to acidic pH and proteases (e.g. cathepsin B and L)

found within the endosome (Figure 3, step 2) (Borsa et al, 1979; Borsa et al, 1981;

Sturzenbecker et al, 1987; Ebert et al, 2002; Ehrlich et al, 2004). Studies using

pharmaceutical agents that block this endosomal acidification (e.g. chloroquine and

ammonium chloride), or inhibit lysosome proteases (e.g. E-64), have been shown to

restrict the infectivity of intact virions. Thus, low pH and viral proteolysis is a

requirement for reovirus infection (Sturzenbecker et al, 1987; Ebert et al, 2001). The

disassembly process promotes virion to ISVP conversion by removal of σ3 protein,

extension of σ1 fibers, and cleavage of µ1 into two particle-associated peptides, δ and ϕ

(Figure 3, step 2 and 3) (Silverstein et al, 1972; Borsa et al, 1981; Sturzenbecker et al, 1987; Dryden et al, 1993; Liemann et al, 2002). Alternatively, ISVPs formed extracellularly may also enter cells by direct penetration through the plasma membrane (Figure 3, 3a) (Borsa et al, 1979; Golden et al, 2002). Evidence for this is the infection of intact virions and ISVPs in the presence of acidification or protease inhibitors. While virions are inhibited by these antiviral agents, ISVPs produce a successful infection being able to bypass viral entry blockers (Sturzenbecker et al, 1987; Baer & Dermody, 1997; Odegard et al, 2004; Nibert et al, 2005). Lately, a novel intermediate particle named ISVP* has been described, which follow ISVP digestion by the loss of σ1 protein, as well as the conformational changes in µ1. By becoming ISVP*, virus is released from endosome to deliver the transcriptionally active core into the cell's cytosol (Figure 3, step 4) (Chandran et al, 2002; Chandran et al, 2003; Odegard et al, 2004; Nibert et al, 2005). The resulting core particle marks the final stage of the uncoating process in cell cytoplasm, where the remainder of the replicative cycle occurs (Coombs, 2006; Kobayashi et al, 2007). The RdRp produces 5'capped, non-polyadenylated mRNA from each gene segment during primary transcription (Faust et al, 1975). Only four (L1, M3, S3 and S4) genes are initially transcribed in mRNA and respectively translated by host ribosomes in proteins λ3, µNS, σNS and σ3 (Figure 3, step 5 and 6). Thereafter, the four newly produced proteins promote the transcription of all the remaining six genes through a mechanism that has not been clearly defined (Figure 3, step 7). Early mRNAs are subsequently translated into full complement of virus proteins (Figure 3, step 8). Proteins are sent with the 10 different mRNA molecules into a non-membrane viral-inclusion region in the cytoplasm, where the minus-strand is synthesized and the progeny's dsRNA

22

is produced (Figure 3, step 9 and 10). Packaged particles that contain the dsRNA play a role in secondary transcription and the majority of mRNAs are then produced. Finally, virions are assembled to contain one copy of each of the ten progeny genes and are released from cytosol by cell lysis (Figure 3, final steps) (Coombs, 2006). Both reovirus strains T1L and T3D disseminate systemically to reach the central nervous system (CNS). The difference among their pathogenesis is that reovirus T1L spreads from the intestine to the mesenteric lymph and spleen via hematogenous routes, leading to nonlethal hydrocephalus, whereas reovirus T3D spreads from the intestine to the myenteric plexus to the vagus nerve via neural routes, infecting neurons and causing lethal encephalitis (Weiner et al, 1980; Kauffman et al, 1983; Tyler et al, 1986; Morrison et al, 1991; Barton et al, 2001c; Antar et al, 2009). The gene that mediates the neurovirulence differences between these two serotypes is the S1 genome segment, which encodes for the attachment protein σ1 (Weiner et al, 1977; Weiner et al, 1980; Tyler et al, 1986).

1.7. Significance of the research

Little is known about the molecular requirements and structural transitions that allow a non-enveloped virus, such as mammalian reovirus, to enter cells. Therefore, this early step in reovirus infection has been extensively studied by many groups in North America (Wolf et al, 1981; Dryden et al, 1993; Morin et al, 1994; Coombs, 1998; Jané-Valbuena et al, 1999; Agosto et al, 2006; Hadžisejdić et al, 2006; Danthi et al, 2008). One of the main reasons for studying this virus in special is the fact that reovirus is a safe virus to work with and a good model to understand the pathogenesis of more virulent
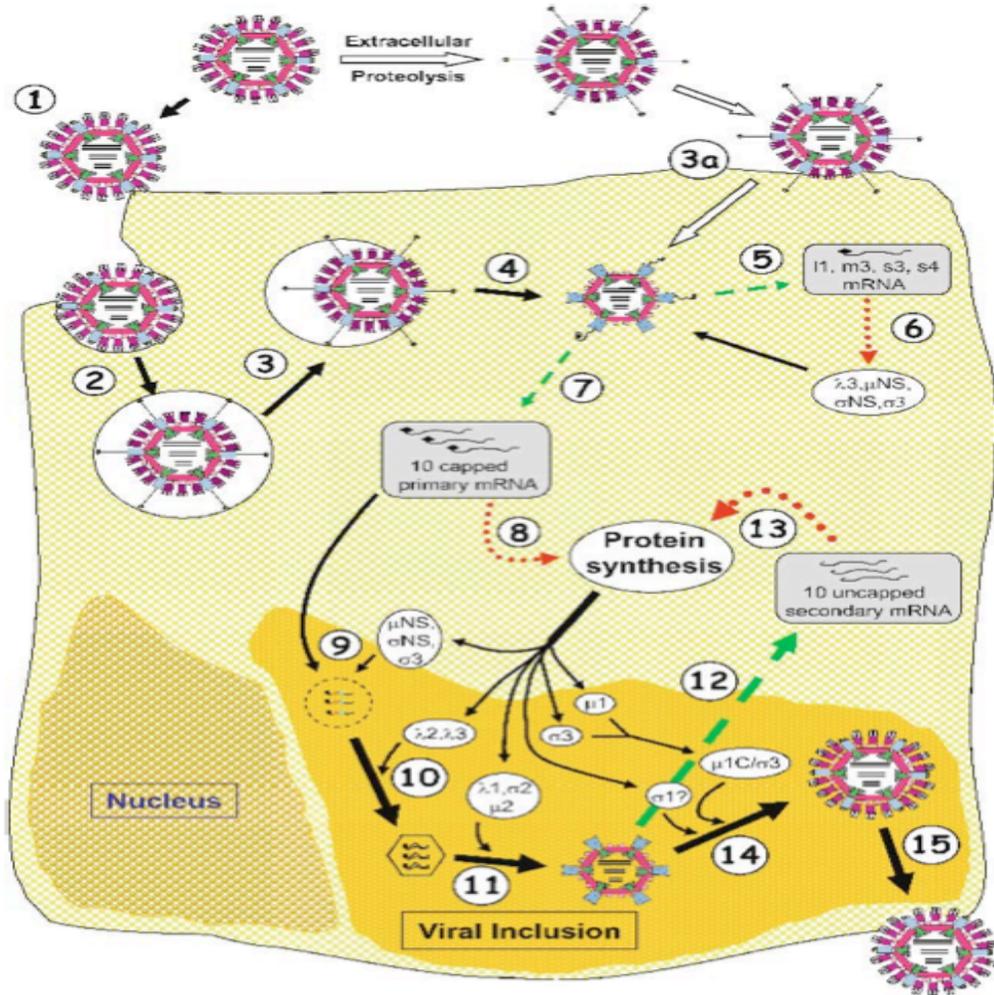
Figure 3. Mammalian reovirus replicative cycle. Diagrammatic representation of the various steps known to be involved in a successful reovirus infection: (*1*) binding of virions or ISVPs (when proteolysis occurs extracellularly), (*2*) entry/internalization via receptor-mediated endocytosis, (*3*) membrane interaction to allow ISVP release from endosome or directly by penetration in cell membrane (*3a*), (*4*) uncoating of ISVP under conditions (low pH or enzymatic reaction) that remove viral outer capsid proteins and release the transcriptionally active core particle into cytoplasm, (*5*) initial pre-early transcription and capping of mRNA, (*6*) initial pre-early translation by host ribosomes to produce viral proteins, (*7*) primary capped transcription, (*8*) primary translation of four proteins only - λ3, µNS, σNS, σ3 - out of the ten dsRNA genes that will be transcribed by unknown mechanisms, (*9*) assortment of mRNA segments into genome sets, (*10 – 14*) synthesis of negative RNA strands that generate progeny dsRNA, secondary transcription and translation, assortment and assembly of progeny proteins, (*15*) newly formed virions are release through cell lysis by a mechanism not well understood. An alternate penetration particle named ISVP* has been recently described (Chandran & Nibert, 1998; Chandran et al, 2002; Odegard et al, 2004) to play a role at probably step (*4*) of this figure. Figure taken from (Coombs, 2006). Permission kindly granted from © Springer Science + Business Media on January 7, 2011.

non-enveloped viruses such as rotavirus, a highly contagious pathogen that causes numerous cases of gastroenteritis hospitalizations (Rivest et al, 2004). Additionally, reovirus has been getting even more attention due to its ability to infect and kill transformed cells; thus, it may be valuable as a novel anti-cancer therapy (Coffey et al, 1998; Norman et al, 2004; Thirukkumaran et al, 2010). The principle of every successful infection is based on viral entry and subsequently, the replication and release of the viral progeny. A precise understanding of how reovirus proteins first interact with the host cell membrane still remains unclear in reovirus research. Studies have documented the importance of reovirus protein σ3 in the early steps of the infection and also as a marker to differentiate two important infectious forms of reovirus; virion and ISVP. The protein is a crucial factor when testing the infectivity of these two particles in the presence of acidification and protease inhibitors. As described in the literature review, virions are blocked by the presence of these pharmacological agents, whereas ISVPs are not. Moreover, cleavage of reovirus outer capsid protein σ3 has been appointed as essential for virus internalization, whereas cleavage of its associated µ1 protein is needless when generating ISVP-like particles. Therefore, the hypothesis presented in this thesis is that there is a threshold of σ3 digestion required to allow the particle to bypass entry blockers. Understanding the molecular requirements that allow the reovirus particle to bypass viral entry inhibitors may be a key in unveiling the first steps taken in the reovirus infection.

1.8.   Rationale and objectives of this study

The success of a reovirus infection is completely dependent on its three morphological forms (i.e. virion, ISVP and core), which relate to the amount of various

proteins present on the virus structure (Table 1). While there is mounting evidence that a conformational change in reovirus structural proteins is a key step during entry, some details about these specific rearrangements leading to virus internalization are still controversial. Nibert's group have described an improved protocol to access the molecular alterations on virus outer capsid protein σ3. By inclusion of the alkyl detergent $14SO_4$, they were able to separate the cleavage of protein σ3 from the cleavage of protein μ1, which appear to be fundamental on studying virus infection but occur simultaneously in previous tested conditions (Chandran & Nibert, 1998). The same protocol was tested by Coombs' group and indeed, it has been useful to clarify the important steps taken during the virion to ISVP transition pathway (Hadžisejdić et al, 2006). Previous studies have shown that intact virions digested for a brief time had an initial cleavage situated in the σ3 hypersensitive region (Ebert et al, 2002; Jané-Valbuena et al, 2002; Mendez et al, 2003). When tested in the presence of the acidic protease inhibitor, E-64, these particles were described as sensitive to the blocker most likely because the presence of σ3 fragments inhibit the μ1 function in membrane penetration. However, when ISVP was tested under the same conditions, it has shown strong resistance to the lysosomal protease inhibitor (Jané-Valbuena et al, 2002). These findings imply that there is a need of σ3 digestion to allow the functional virion → ISVP switch. However, the precise amount of σ3 processing required to allow the particle to bypass the entry blocker (i.e. enhanced ISVP infectivity) is still unknown. As indicated, it is believed that molecular changes at the virion-to-ISVP pathway are facilitated by acidic pH and acidic-dependent proteases. Therefore, combining different techniques by treating the virus with detergent and protease, then consequently infecting cells in the presence of acidification or proteolysis

inhibitors may help filling the gap about the reovirus molecular content in the early infection. The objective of this study, hence, was to mimic the virus infection by developing a gradual protein cleavage on the virus' external proteins. Moreover, it aimed to demonstrate the relationship between reovirus population according to the amount of σ3 remaining on the virus surface and the resultant effect of this protein content on the reovirus-derived particle/population infectivity. Identifying the structural and functional changes during the virus-to-ISVP transition pathway may have dramatic ramifications regarding proteolytically-mediated infections in general; besides contributing to the improvement and design of viral vectors used in oncolytic delivery purposes.

2. MATERIALS AND METHODS

2.1. Cells

Murine L929 cells were grown in either suspension or monolayer cultures at a concentration of $4 \times 10^5 - 5 \times 10^5$ cells per ml. Cells were maintained in Joklik's modified minimal essential medium (MEM; Gibco, Grand Island, NY, USA) supplemented with 5% fetal calf serum (FCS; HyClone Laboratories Inc., Logan, UT, USA), and 2 mM l-glutamine. Suspension cultures were counted on a daily basis to maintain the optimum level of cell concentration. Fresh supplemented MEM was used to adjust the final volume and replace the necessary nutrients to cells. Similarly to the suspension cells, monolayers were grown in a temperature of 37°C with a humidified atmosphere of 5% CO_2 in air.

2.2. Viral particles

Reovirus strain type 1 Lang (T1L) is a laboratory stock. T1L was grown in mouse L929 cells either in suspension at 33°C or in a cell culture monolayer at 37°C with 5% CO_2 atmosphere. Infection media were supplemented with 100 U/ml of penicillin, 100 μg/ml of streptomycin sulphate and 100 μg/ml of amphotericin-B.

2.2.1. Passaging

The wild type stocks of reovirus strain T1L were amplified in a series of passages. These typical passages were performed in flasks containing a monolayer of mouse fibroblast cells and medium. The monolayer was primarily grown in T25 Corning flasks

(Corning Inc., Corning, NY, USA) in a total volume of 5 ml. To achieve that, L929 cells were plated at approximately 4×10^5 cells/ml and incubated overnight to reach 90% cell confluency. Medium was removed from the T25 flask on the next day, and a volume of 0.5 ml of P_0 virus stock was inoculated into the flask allowing the virus-to-cell adsorption. The infection was held at room temperature for one hour, with periodic rocking every 10 – 15 minutes. After adsorption, 4.5 ml of fresh completed MEM (supplemented with penicillin:streptomycin [pen-strep] and Amphotericin-B) was pipetted into the flask. The infected monolayer was placed in 37°C incubator with 5% CO_2 in air, and examined daily for cytopathic effect (CPE). Flasks were transferred to the -80°C freezer when about 85% of detectable changes in the host cells (i.e. cell rounding, swelling or shrinking, death, detachment, etc.) were noticed. Then, they were frozen and thawed three times to collect the P_1 cell lysate. A second infection was carried out in a T75 Corning flask to continue the process of virus passaging. Fresh L929 cells were plated as described above but in a total volume of 15 ml. An aliquot of 0.5 ml from the P_1 cell lysate was used to infect the T75 cells on the following day. The virus adsorption and infection, the flask incubation, and the inspection for the CPE effect were all done in the same manner to generate the P_2 cell lysate. If necessary during growth time, ⅔rds of media was removed from the T75 flask and replaced with fresh supplemented MEM. After CPE effect was detected, cells were harvested and the P_2 cell lysate was held at 4°C for virus titration.

2.2.2. Titration

Plaque forming units assays, also known as plaque assays, were used to quantify infectious virus particles. L929 cells were plated onto 6-well cell culture plates (Corning Inc., Corning, NY, USA) at a concentration of 4×10^5 cells/ml and plates were incubated at 37^oC with 5% CO_2 atmosphere for one overnight to reach the 90% cell confluency. The day of cell culture was called day zero. On day 1, serial 1:10 dilutions of viral stocks were made in gel saline (137 mM NaCl, 0.2 mM $CaCl_2$, 0.8 mM $MgCl_2$, 19 mM HBO_3, 0.1 mM $Na_2B_4O_7$, 0.3% [wt/vol] gelatin). Growth media was removed from the sub-confluent L929 monolayer and 100 μl of every dilution were inoculated onto two wells; therefore, cells were twice infected to have an average of both wells. The virus-to-cell adsorption was taken for one hour in room temperature and plates were rocked every 10 – 15 minutes to maintain the cells moist. After adsorption, cells were overlaid with 3 ml of a 50:50 ratio of 2% Bacto-Agar (Becton Dickinson & Co., Franklin Lakes, NJ, USA) and $2 \times$ Medium 199 (supplemented with 6% FCS, 2 mM ι-glutamine, 100 U/ml penicillin, 100 μg/ml streptomycin sulfate, and 1 μg/ml amphotericin-B). Then, the 6-well culture plates were incubated at 37°C in a 5% CO_2 atmosphere. On day 3, the infected monolayers were fed with 1.5ml of fresh completed Medium 199/Agar overlay, and returned to the incubator. Plates were daily inspected for viral plaques, but stained usually around day 5 with a 0.03% neutral red solution (made in a 1:1 ratio of 2% Bacto-Agar and $2 \times$ phosphate buffered saline [PBS: 274mM NaCl, 0.6mM KCl, 1.6mM Na_2HPO_4, 0.2mM KH_2PO_4). After 18 hours of staining, plates were taken from the incubator and plaques were counted on a white lamp box. Viral titer was finally calculated according to the average of plaques taken from each virus dilution and only plaques between 20 and 200 were statistically considered as results. The virus' infectivity

was then expressed by the formula $\frac{\# plaques}{dil^n \times V} = PFU/ml$, where dil^n; described the

dilution factor, and V; the volume of diluted virus inoculated to the well.

2.2.3. Amplification

Large amounts of purified reovirus T1L were obtained through a massive infection of L929 cells. These were grown in suspension at 37°C until they reached the desired volume and the concentration needed; generally 6.5×10^8 cells. The cell suspension was poured into 250 ml conical tubes (Corning Inc., Corning, NY, USA) and centrifuged at $350 \times g$ for 7 minutes at 4°C (IEC Centra GP8R refrigerated centrifuge; Thermo Electron Co., Milford, MA, USA). The supernatant media was then transferred to a glass roller bottle and the cell pellet was re-suspended in few millilitres of pre-adapted media. The desired concentration of cells was adjusted to 2×10^7 cells/ml after the addition of P$_2$ virus stock. The infectious particles were added at a multiplicity of infection (MOI) of 5 PFU/cell. Then, cells and viruses were kept in the 33°C water bath for 1 hour with constant swirling of the tube. During this adsorption time, the glass roller bottle containing 250 ml of pre-adapted media was filled up to 1 L with fresh completed MEM supplemented with pen-strep and amphotericin-B. The bottle was then placed into the 33°C spinning water bath to equilibrate the media temperature. After adsorption time, cells and viruses were transferred to the roller bottles where the final concentration of cells was not greater than 6.5×10^5 cells/ml. The infection device was maintained in constant spinning at 33°C for 65 hours. After this time, cells were centrifuged at $500 \times g$ for 20 minutes (IEC Centra GP8R refrigerated centrifuge; Thermo Electron Co., Milford, MA, USA) and infected cells re-suspended in 12 ml of homogenization buffer (HO

buffer; 10 mM Tris [pH 7.4], 250 mM NaCl, 10 mM b-mercaptoethanol). The homogenate was then transferred to a 30 ml COREX tube and the final volume was recorded. At this point, samples could be frozen and stored at -80°C or used immediately for viral purification.

2.2.4. Purification

When stored at -80°C, the suspension was immediately thawed and sat in ice throughout the process of virus purification. Cell clumps and membranes were disrupted by a small probe on a Vibra-Cell sonicator (Sonics & Materials Inc., Danbury, CT, USA). At this step, sonication was set to 10 seconds at mid-range (35 - 40%) duty cycle. The protein dissociation and cell lysis was further processed by the addition of $1/50^{th}$ of sample volume of 10% sodium desoxycholate (DOC; Thermo Fisher Scientific, Waltham, MA, USA) detergent. Samples were then vortexed and placed in ice for 30 minutes. After reaction time, the solvent 1,1,1,2,3,4,4,5,5,5-decafluoropentane (Vertrel-XF; DuPont, Wilmington, DE, USA) was pipetted in a volume equal to $2/5^{th}$ of the sample volume. The suspension was then re-emulsified for 40 seconds and the addition of solvent Vertrel-XF was repeated once more, as well as the sonication process for 40 seconds. Thereafter, samples were centrifuged at $9,616 \times g$ for 10 minutes in a fixed-angle rotor (JA-25.50; Avanti J-30I Centrifuge; Beckman Coulter, Brea, CA, USA). The top aqueous phase was taken with a plastic pipette and the noted volume was transferred to a fresh COREX tube. The remaining organic phase was consequently discarded. The extraction was repeated as highlighted above, however, adding $9/10^{th}$ of Vertrel-XF of the sample volume per tube. Solutions were re-emulsified and phases were once again

separated under the same centrifuge conditions. The resultant top phase was layered onto a 1.2 – 1.4 g/ml cesium chloride gradient which was pre-established in a SW-28 tube (Beckman Coulter, Brea, CA, USA). Finally, the completed gradient was installed in the JS-24.38 swinging-bucket rotor (Avanti J-30I Centrifuge; Beckman Coulter, Brea, CA, USA) and ultracentrifuged overnight ($\geq$ 6 hours) at 87,275 $\times$ g units. On the next day, the SW-28 tube was taken from the rotor and a typical blue band formed by virus particles within the gradient was collected through a puncture made in the bottom of the tube. Before loading the virus in the dialysis tube, its density was determined as approximately 1.36 g/ml by refractometer (Baush & Lomb, Rochester, NY, USA). Then, virus was extensively dialysed against 3 or more sets of dialysis buffer (D-buffer; 150 mM NaCl, 15 mM $MgCl_2$, 10 mM Tris [pH 7.4]) to completely remove the cesium chloride solution from the tube. After dialysis, the purified virus particles were quantified using a Spectronic Genesys 5 spectrophotometer (Milton Roy Co., Rochester, NY, USA) where 1 OD_{260} = 2.1 $\times$ 10^{12} particles or 185 µg of protein per ml. Viral particles were adjusted to 1 $\times$ 10^{13}/ml and stored in appropriate vials at -80°C. Finally, virus' titer was taken by plaque assay to determine if particles were biologically infectious.

2.2.5. Proteolysis

The digestion of reovirus outer-capsid proteins, σ3 and µ1, was accomplished by two slightly different procedures. The first was made from aliquots of digested particles collected at various time intervals and called here, virion-to-ISVP transition particles. The second, known as ISVP, was made by a longer digestion of the intact particles. The PTC-100 programmable thermal controller (MJ Research, Waltham, MA, USA) was set

according to the protocol described in the next section to promote the generation of these different particles.

2.2.5.1. Virion-to-ISVP particles

Virion-to-ISVP transition particles were generated by an *in vitro* digestion of purified virus. Solutions of TLCK-treated α-chymotrypsin (CHT) (Sigma-Aldrich Co., Saint Louis, MO, USA) were prepared in D-buffer (pH 7.4) to a final concentration stock of 500 μg/ml and stored at -80°C. The detergent, tetradecyl sulfate sodium salt ($14SO_4$; Sigma-Aldrich Co., Saint Louis, MO, USA), was dissolved in distilled water to a final concentration stock of 10 mM. Aliquots of 1×10^{13} virus particles/ml were digested in the presence of 1 mM of detergent $14SO_4$ and 10 μg/ml of protease α-chymotrypsin. After protease addition, tubes were immediately vortexed and transferred to the PTC-100 programmable thermal controller (MJ Research, Waltham, MA, USA) which was set to a constant temperature of 32°C. When the desired time point lapsed, tubes were immediately chilled in an ice water bath. Further digestion of viral proteins was inhibited by the addition of phenylmethylsulfonylfluoride (PMSF; Sigma-Aldrich Co., Saint Louis, MO, USA) to a final concentration of 5 mM. Subsequently, these particles were separated into two different tubes; one for structural analysis and the other for functional analysis. The first was boiled for 5 minutes at 95°C in a one-quarter volume of $5 \times$ electrophoresis sample buffer (ESB; 250 mM Tris [pH 6.8], 10% SDS, 0.5% bromophenol blue, 50% glycerol, 500 mM β-mercaptoethanol) and briefly centrifuged for 3 minutes at $21,000 \times g$ (IEC Micromax RF refrigerated centrifuge; Thermo Electron Co., Milford, MA, USA). The supernatant was then resolved by sodium dodecyl sulfate polyacrylamide

gel electrophoresis (SDS-PAGE) to confirm the particle formation (i.e. outer proteins digested). For the second tube, virus particles were used to infect cells at MOI of 2 PFU/cell, thus, testing the particle's infectivity (also described as functional analysis).

2.2.5.2. ISVPs and Cores

To obtain T1L ISVPs, the same protocol described in 2.2.5.1. was followed except that digestions were made in the absence of detergent and virions were treated for 1 hour at 37°C with 200 µg/ml of CHT. To obtain cores, virions were adjusted to 6.5×10^{13} particles/ml and treated with 200 µg/ml of CHT for 3 hours at 37°C. Immediately after time lapsed, samples were chilled on ice and reactions were stopped by the addition of 5mM final concentration of PMSF. The production of ISVPs and cores were confirmed via SDS-PAGE. The viability of ISVPs was verified by functional analysis and/or plaque assay.

2.3. Structural Analysis

Every sample submitted to CHT digestion was subsequently resolved in SDS-PAGE to visualize the σ3- and µ1-derived proteolytic fragments. After electrophoresis and staining of the polyacrylamide gel, proteins were photographed and subjected to densitometric analysis.

2.3.1. SDS-PAGE

Samples to be analysed by SDS-PAGE were diluted 4:1 with 5 × ESB and heated for 5 minutes at 95°C. Twelve percent linear or 5 − 15% gradient polyacrylamide gels

(8.6W × 6.8L × 0.15T cm) were used for protein separation. Equal amounts of virus particles were loaded per well and resolved for 1½ hour at 30 mA of constant current (Power Pac 200 unit, Bio-Rad Laboratories Inc., Hercules, CA, USA). Virus-derived proteins were stained by a Coomassie-like stain solution (GelCode Blue Stain Reagent; Thermo Scientific Inc., Waltham, MA, USA) and imaged with a Fluor Chem Q Multi Image III (Alpha Innotech Co., San Leandro, CA, USA) for densitometric analysis of the fragments.

2.3.1.1. Densitometric analysis of reovirus outer-capsid proteins

Stained gels containing reovirus digested proteins were exposed to an imaging surface and photographed. The integrated measure of the intensity and size of each band (i.e. absolute intensity) was carried out from Adobe Photoshop 7.0 (Adobe Systems Inc., San Jose, CA, USA). Core protein λ was used as a standard control to compare the amount of σ3 left during protease treatment. For each lane, mean densities were determined for bands corresponding to the reovirus λ and σ3 proteins. The ratio was calculated by dividing the absolute intensities of bands corresponding to σ3 by those corresponding to λ. Statistics were calculated using GraphPad Instat 3.05 (GraphPad Software Inc., San Diego, CA, USA) and means were plotted by SigmaPlot 10.0 (Systat Software Inc., Chicago, IL, USA).

2.4. Functional Analysis

Purified reovirus virions at a concentration of 1×10^{13} particles/ml in D-buffer were treated by CHT either at 10 µg/ml (for transitional particles) or 200 µg/ml (for ISVPs) at

32°C (for various times) or at 37°C (for one hour), respectively. Samples were then chilled on ice and the reactions were further stopped by the addition of 5mM PMSF. Samples were kept on ice until they were used for infection. Monolayers of L cells (5×10^5) in 24-well plates (Corning Inc., Corning, NY, USA) were preincubated for 1 hour at 37°C in medium supplemented with selected antiviral drugs. The medium was removed, and cells were adsorbed with different reoviral particles (e.g. intact virion, virus-to-ISVP transitional particles, and ISVPs) at a MOI of 2 PFU/cell in $1 \times$ PBS. After one hour incubation at room temperature, the inoculum was aspirated and 0.5 ml of fresh medium containing an appropriate concentration of acidification inhibitors, or cysteine protease inhibitor, or clathrin-, or caveolae-mediated endocytosis inhibitors, was added to the wells. After incubation at 37°C for 24 hours, cells were frozen and thawed twice, then subjected to sonication at mid-range for 10 seconds (Vibra-Cell sonicator; Sonics & Materials Inc., Danbury, CT, USA). Viral titers in cell lysates were consequently determined via plaque assay. Each infected monolayer (from the 24-well plate) was twice titrated. Statistics of at least three independent experiments were calculated using GraphPad Instat 3.05 (GraphPad Software Inc., San Diego, CA, USA). The significance of group bars was verified by one-way ANOVA followed by Tukey's test. Means and error bars were plotted by SigmaPlot 10.0 (Systat Software Inc., Chicago, IL, USA).

2.4.1. Pharmacological Inhibitors

To test whether the particles produced by the *in vitro* proteolysis were as infectious as intact virions, a series of entry blocker drugs were selected depending upon their targets and effects inside the cells. Ammonium chloride (NH_4Cl) and chloroquine

(Sigma-Aldrich Co., Saint Louis, MO, USA) are weak bases which inhibit the activity of acid-dependant proteases and the virus release from endosome. E-64 (Calbiochem, San Diego, CA, USA) is an irreversible and highly selective cysteine protease blocker. It stops the proteolysis reaction and virus is consequently paralyzed within lysosome. The administration of chlorpromazine and methyl-β-cyclodextrin (MβCD; Sigma-Aldrich Co., Saint Louis, MO, USA) causes an inhibitory effect over the cell membrane. The first inhibits clathrin-mediated-endocytosis and the second blocks caveolae-mediated-endocytosis. As a treatment result, the virus uptake into L929 cells is compromised. All stocks were initially prepared by dissolving the proper amount of drug in distilled water. The greatest concentration of inhibitor was chosen regarding its effect on both virus entry and cell viability. To test that, NH_4Cl (10 mM, 20 mM, and 40 mM), chloroquine (50 µM, 100 µM, 150 µM and 200 µM), E-64 (200 µM), chlorpromazine (5 µg/ml, 7.5 µg/ml, 10 µg/ml, 12.5 µg/ml, 15 µg/ml, 20 µg/ml), and MβCD (2.5 mM, 3.5 mM, 5 mM, 6 mM, 7 mM, 8 mM) were freshly prepared from stocks and the final dosages were administrated to cells according to section 2.4. As a control, cells were also mock treated with only MEM for 1 hour at 37°C. All drug solutions were maintained at room temperature, except for E-64 and MβCD, which were stored at -20°C.

2.5. Cell Viability

Monolayers treated with pharmacological inhibitors were microscopically inspected to determine the overall status of the cells post-treatment. L cells (5×10^5) in 24-well plates (Corning Inc., Corning, NY, USA) were incubated for 1 hour at 37°C with MEM only or supplemented to contain 20 mM NH_4Cl, or 100 µM chloroquine, or 200 µM E-

64, or 10 µg/ml chlorpromazine, or 5 mM MβCD. Following incubation time, the medium was removed and a fresh dose of each treatment was administrated to the cells. After leaving the plates at 37°C in 5% CO_2 atmosphere for 24 hours, the medium was collected from the wells to remove cells undergoing CPE and cells that were still on the monolayer were harvested by low concentration of trypsin - EDTA treatment. The apparently viable cells were microscopically counted using a haemocytometer and the final result was taken by comparing the percentage of cells counted on the control well with those counted on the drug-treated wells. Statistics were calculated using GraphPad Instat 3.05 (GraphPad Software Inc., San Diego, CA, USA) and the standard error of means were plotted by SigmaPlot 10.0 (Systat Software Inc., Chicago, IL, USA).

2.6. Fluorescence Analysis

Fluorescence analysis of intact and digested particles was performed by labelling amino groups (i.e. arginine and lysine) of virions with Alexa Fluor 488 carboxylic acid, succinimidyl ester (Molecular Probes Inc., Eugene, OR, USA). The staining compound was first dissolved in N,N-dimethylformamide (Sigma-Aldrich Co., Saint Louis, MO, USA) to a final stock concentration of 15.54 mM and stored at -20°C until use. Purified virions (1×10^{13} particles/ml) were diluted into 0.05 M sodium bicarbonate (Sigma-Aldrich Co., Saint Louis, MO, USA), pH 8.5, and incubated with 100 µM Alexa Fluor 488. Incubation was held in the dark and with continuous stirring for 90 minutes at room temperature. After staining, particles were dialyzed against 1000 ml of PBS for 4×30 minutes and later transferred to appropriate vessels. Labelled virions at 1×10^{13}/ml were then placed on ice and subjected to a digestion assay according to the protocol described

in section 2.2.5.1. Titration assay was performed as described in section 2.2.2. to test the infectivity of the labelled virus.

2.6.1. Anti-reovirus monoclonal antibody

The 4F2 reovirus-specific monoclonal antibody (mAb) was selected based on previous findings related to recognition of the virus σ3 protein by Western-blot. Nonetheless, the same study has reported that 4F2 mAb bound T3D extensively better than T1L, which imply that 4F2 is a σ3-T3D-specific mAb (Virgin et al, 1991). Despite that, this antibody was applied to this research due to the lack of options to test T1L σ3 recognition by Western-Blot. However, in this study 4F2 behaved as T1L-μ1-specfic. Spleen cells from mice immunized against T1L were previously harvested and the fused 4F2 hybridoma cells were cryopreserved at -130°C as laboratory's stocks. After thawing the cells at 37°C, hybridomas were transferred to a conical tube containing 10 ml of warm Gibco RPMI 1640 medium (Molecular Probes Inc., Eugene, OR, USA) plus 10% FCS. The tube was centrifuged at $340 \times g$ for 5 minutes (IEC Centra GP8 Centrifuge; Thermo Electron Co., Milford, MA, USA) to remove any remaining dimethyl sulfoxide used in cryopreservation. Cells were resuspended in 10 ml of fresh completed medium and the total volume was divided into two T25 flasks (Corning Inc., Corning, NY, USA). These were then transferred to a 37°C incubator with 5% CO_2 in air. On the recovering days, cells were inspected, fed, and split (if necessary) to maintain the best growth at $2 \times 10^5 - 7 \times 10^5$ viable cells/ml. After a week of incubation the cultures growing in serum supplemented medium were transferred to a pre-warmed (37°C) serum-free medium (Gibco Hybridoma-SFM; Molecular Probes Inc., Eugene, OR, USA), placed into $4 \times$

40

T225 flasks (Corning Inc., Corning, NY, USA), and incubated at 37°C with 5% CO_2 atmosphere. Conditions to encourage the release of 4F2 antibodies from the hybridoma cells were established for two weeks, when no media was replaced and the cell death therefore promoted. To collect antibodies, dead cells were separated from the supernatant by centrifugation at 830 × g for 2 minutes (IEC Centra GP8 Centrifuge; Thermo Electron Co., Milford, MA, USA). The supernatant was collected, filtered through a 0.22 μm stericup filter unit (Millipore Co., Billerica, MA, USA), and purified slowly through a protein G sepharose 4 fast flow column (GE Healthcare Bio-Sciences Co., Piscataway, NJ, USA). After adsorbing antibodies overnight at 4°C, the column was rinsed five times with PBS to eliminate nonspecific proteins. The antibodies were finally eluted by 0.1 M Glycine-HCl, pH 2.8, in twelve tubes containing 100 μl of 1M Tris, pH 8.8. The fractions which provided the highest absorbance were pooled and subjected to dialysis for 2 × 24 hours against 4 liters of PBS. After dialysis, antibodies were transferred to a conical tube and filter-sterilized by a 0.22 μm filter connected to a syringe. Antibodies were collected in appropriate vessels and stored at 4°C or frozen with 50% glycerol at -80°C. To remove the remaining glycine, beads were submitted to a final wash with PBS and stored with 0.02% sodium azide in PBS at 4°C. The concentration of 4F2 monoclonal antibodies was finally determined by protein assay via BSA standard curve.

2.6.2. SDS-PAGE and immunoblotting

Samples which were previously labelled with Alexa Fluor 488 were subjected to proteolysis with either 10 μg/ml or 200 μg/ml of CHT to promote the formation of virion-to-ISVP transition particles or ISVPs, respectively. Every product of digestion as well as

intact virions were processed in 5 – 15% gradient gels to confirm particle formation. Proteins were diluted as described in section 2.3.1. but resolved by SDS-PAGE in the dark. Gel was disconnected from the power supply (PowerPac 200, Bio-Rad Laboratories, Hercules, CA, USA) after resolving for approximately 1½ hour at a current of 30 mA. Alexa-labelled proteins were immediately excited (475 nm peak wavelength) and photographed by a fluorescence imager (Fluor Chem Q Multi Image III; Alpha Innotech Co., San Leandro, CA, USA). Gels were subsequently stained with GelCode Blue Stain Reagent (Thermo Scientific Inc., Waltham, MA, USA) and photographed under trans white light to observe all proteins in gel. For immunoblots, protein samples were resolved by SDS-PAGE and transferred to a polyvinylidene fluoride (PVDF) membrane at 100 V for 1 hour (Bio-Rad transblot cell; Bio-Rad, Hercules, CA, USA) at 4°C in the presence of transfer buffer (25 mM Tris, 192 mM glycine, 20% methanol [pH 8.3]). The membrane was incubated overnight with the reovirus T1L-µ1-specific monoclonal antibody (4F2; at final concentration of 10 µg/ml) after blocking it for 2 hours at room temperature. The antibody detection was achieved by using 1:200 goat anti-mouse IgG conjugated to horseradish peroxidase. Finally, the immune complexes were revealed by the enhanced chemiluminescence system (ECL; GE Healthcare Bio-Sciences Co., Piscataway, NJ, USA) in accordance with the manufacturer's instructions.

2.6.3. Flow Cytometry and Fluorescence Focus Assay

All samples which were previously submitted to CHT treatment were analysed by flow cytometry not only to assess the digestion of single particles but also to unveil the distribution of proteins and particles along the *in vitro* proteolysis pathway. Virions,

virion-to-ISVP transition, and ISVP particles were incubated with a monoclonal antibody to the type 1 μ1 protein, 4F2, in PBS containing 1.5% BSA and 0.05% Tween-20 (Acros Organics, Geel, Belgium). The reactions were carried out in the dark with continuous rocking overnight at 4°C. On the following day, the polycarbonate tubes were centrifuged in a pre-chilled TLA 100.3 rotor at 30,000 rpm (48,600 × g) for 30 minutes at 4°C (Optima-Max ultracentrifuge; Beckman Coulter, Brea, CA, USA). Supernatants were carefully aspirated and the pellets were resuspended in fresh PBS. To remove the unbound antibodies, samples were subsequently washed by centrifugation using the same conditions as before. After removing the supernatant, pellets were resuspended in a 1:100 dilution of Alexa Fluor 405 goat anti-mouse IgG antibody (Molecular Probes Inc., Eugene, OR, USA) in PBS. The secondary antibody was incubated with a constant and gentle spinning in the dark for 1 hour at room temperature. After incubation time, samples were pelleted and subsequently washed with PBS to remove any unbound antibody. The remaining complexes formed by Alexa Fluor 488 labelled virus, 4F2 monoclonal antibody, and Alexa Fluor 405 goat anti-mouse IgG antibody, were finally detected via flow cytometry. At least 10,000 events were acquired per sample on a LSRII flow cytometer (Becton Dickinson & Co., Franklin Lakes, NJ, USA) and analysed with the FACSDiva software (version 6.1.2; Becton Dickinson & Co., Franklin Lakes, NJ, USA). Green fluorescent polystyrene microspheres (0.088 μm in diameter; Thermo Scientific Inc., Waltham, MA, USA) were acquired separately as a reference to the samples. For fluorescence focus assay, the same protocol described above was adopted. The difference was that following the incubation with secondary anti-mouse antibody, samples were centrifuged and slightly resuspended in PBS to maintain pellets still

43

detectable for fluorescence microscopy. Samples were transferred to an 18-well slide, imaged by a laser inverted microscope (Axio Observer Z1; Carl Zeiss MicroImaging GmbH, Jena, Germany) and processed with the AxioVision software (version 4.8.1).

3. RESULTS

3.1. Virion proteolysis generates ISVPs in the presence of α-chymotrypsin.

Under normal conditions, ISVPs differ from virions in numerous biochemical characteristics, including the removal of σ3, the cleavage of µ1/µ1C into fragments δ and φ, and the apparent modification in σ1 conformation (Dryden et al, 1993). To detect any difference in the infectivity of virions or ISVPs, the *in vitro* production of both is essential. Thus, virus stock T1L was amplified and purified as described in sections 2.2.3 and 2.2.4 in Materials and Methods (M&M) to generate intact full virions. α-chymotrypsin was diluted in D-buffer to 500 µg/ml as stock, and purified virions to 1×10^{13} particles per ml in PBS. Intact virus particles were then submitted to proteolysis for 1 hour at 37°C with 200 µg/ml of enzyme to generate ISVPs as per standard procedures (Vigin et al, 1991; Jané-Valbuena et al, 1999; section 2.2.5.2 in M&M). After 1 hour, reactions were quenched by submersion of tubes in an ice water bath followed by the addition of 5 mM final concentration of PMSF. About 2.5×10^{11} particles were then taken from each digested tube and loaded in the stacking gel for SDS-PAGE analysis. This demonstrated a clear and expected difference in protein composition between the virion and the ISVP band (Figure 4). As noted, outer capsid σ3 has been completely cleaved after one hour of digestion and µ1/µ1C protein was cleaved in a more limited fashion to yield the stable fragments µ1δ/δ (63/59 kDa; N-terminal portion of µ1/µ1C) and φ (13 kDa; C-terminal portion of µ1/µ1C, not resolved by the dye) (Figure 4). As expected, the T1L σ1 protein and other proteins associated with the core were not cleaved by the treatment with CHT. These initial results confirm numerous prior observations
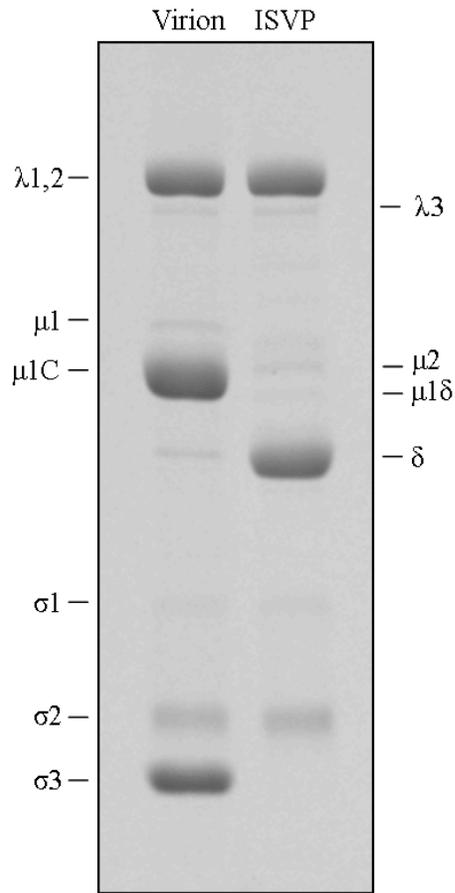
Figure 4. Virion proteolysis generates ISVP in the presence of α-chymotrypsin. Purified T1L virions (1×10^{13} particles/ml) were treated with 200 μg/ml of CHT enzyme for 1 hour at 37°C. Digestion was quenched by cooling the samples in an ice water bath followed by the addition of PMSF. Approximately 2.5×10^{11} generated particles were resolved in a 5 – 15% gradient polyacrylamide gel for 1½ hour at 30 mA of constant current. Gel was stained by a coomassie-like stain solution and the viral proteins were then imaged. A reference lane was loaded with untreated virions (virion).

regarding ISVP production in the presence of α-chymotrypsin (Joklik, 1972; Borsa et al, 1973; Chandran & Nibert, 1998; Hadžisejdić et al, 2006; Schiff et al, 2007).

3.2. ISVPs retain infectivity in the presence of viral entry blockers.

Another property in which virions differ from ISVPs is that ISVPs are able to bypass the activity of entry blockers such as NH_4Cl and E-64, and generate progeny while virions can not (Sturzenbecker et al, 1987; Chandran & Nibert, 1998; Ebert et al, 2001). The evidence indicates that these agents block the infectivity of virions by inhibiting cleavage of outer capsid proteins. Conversely, these agents have no effect against the infectivity of ISVPs since cleavage of outer capsid proteins have already occurred extracellularly. The fact that σ3 protein needs to be cleaved as a first step to produce infection and that viral entry inhibitors may stop this reaction, correlates with the sensitivity of virions to these compounds (Sturzenbecker et al, 1987; Nibert et al, 1991a). To determine whether ISVPs produced in this study would be useful for testing the mechanism of viral entry, the infectivity of virions and ISVPs in the presence or absence of different concentrations of blockers were assessed. The concentration that produced the largest difference between virion and ISVP plaque titers was then considered optimal to test subsequent samples in this study. The final concentrations selected as standards for each drug were therefore: 20 mM NH_4Cl, 100 μM chloroquine, 10 μg/ml chlorpromazine, 5 mM MβCD, and 200 μM E-64 (Figure 5A-E). As expected, the results confirmed the effects of all dugs tested on infections by virions or ISVPs, and also demonstrated that in opposition to the first, the latter retain full infectivity in presence of these pharmacological compounds. For instance, a ≥ 2 $\log_{10}$ difference in titer was

demonstrated between the virion and ISVP after treatment with the acidification inhibitors NH$_4$Cl (20 mM) or chloroquine (100 μM) (Figure 5A-B). In the presence of endocytosis inhibitors, a $\geq$ 1.5 log$_{10}$ difference in titer was described between virion and ISVP treated with chlorpromazine (10 μg/ml) or MβCD (5 mM). However, the highest difference between virion and ISVP titers after treatment was verified with the protease inhibitor E-64 (200 μM), which showed a minimum of 3 log$_{10}$ difference in titer from the intact to the digested particle (Figure 5E). The considerable difference in titer presented by virion and ISVP was expected and demonstrated that virions are blocked by inhibitory drugs whereas ISVP remains fully infectious, presumably by selecting another pathway for entry. Since the endocytosis pathway is not needed, ISVP could bypass the cell membrane and release the transcriptionally activated core particle within cell cytoplasm for genome transcription, translation and the consequent generation of progeny.

3.3. Certain biochemical inhibitors of reovirus entry are toxic to murine cells.

Since several viruses are dependent on the cell machinery to produce a successful infection, a non-toxic environment with good cell condition is therefore essential to these microorganisms. Like hormones, proteins, lipoproteins and toxins, many non-enveloped viruses such as reovirus first access the cell and traffic to its interior via a process known as endocytosis (Maratos-Flier et al, 1986; Nagafuku et al, 2003). For that reason the endocytosis pathway has been chosen as favourite targets for antiviral agents (Patick & Potts, 1998; Nagafuku et al, 2003). In this study, the cytopathic effects of each antiviral drug were first assessed to determine whether the cell condition would affect the infectivity of reovirus. The chosen compounds, 20 mM NH$_4$Cl, or 100 μM chloroquine,

A. Concentration of Ammonium Chloride Treatment

B. Concentration of Chloroquine Treatment

C. Concentration of Chlorpromazine Treatment

D. Concentration of MβCD Treatment

E. Concentration of E-64 Treatment
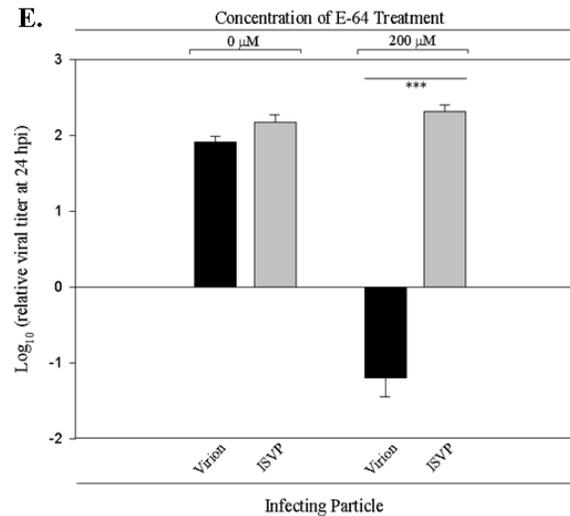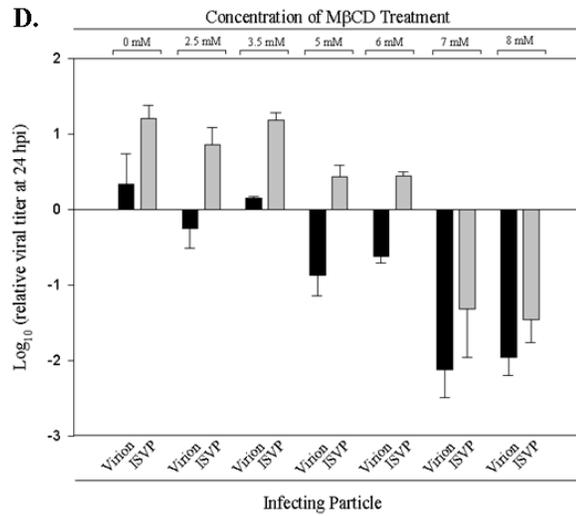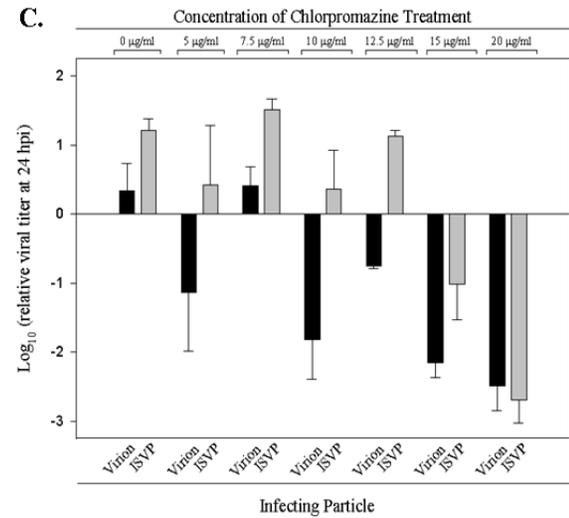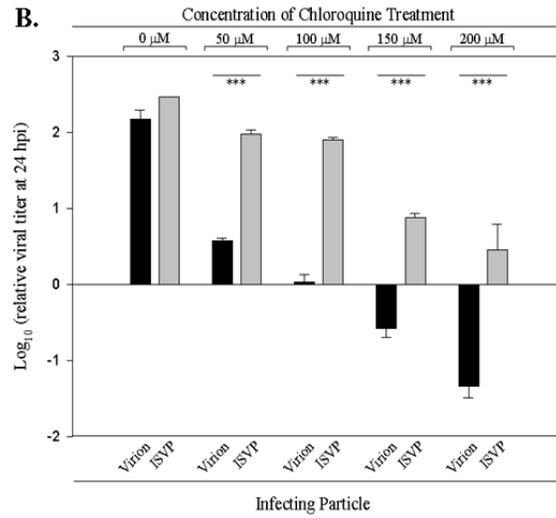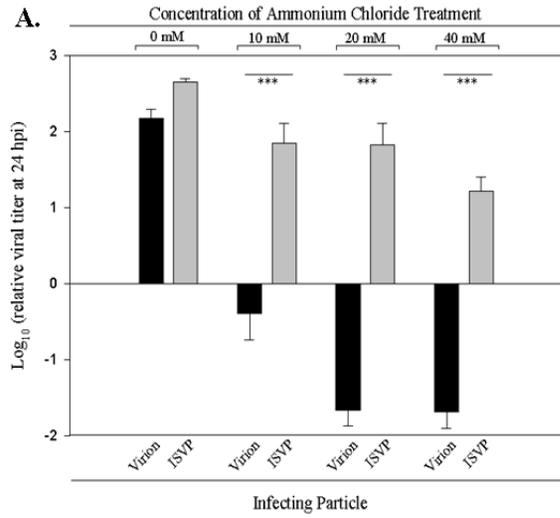
Figure 5. Infectivity of T1L virions and ISVPs in the absence and presence of viral entry blockers. A – E. Purified T1L virions and ISVPs were used to infect L929 cells at a MOI of 2 PFU/cell in the absence or presence of different concentrations of virus inhibitors such as the acidification inhibitors, ammonium chloride (A) and chloroquine (B); the clathrin-mediated endocytosis inhibitor, chlorpromazine (C); the caveolae-mediated endocytosis inhibitor, MβCD (D); and the cysteine protease inhibitor, E-64 (E). E-64 was tested at 200 μM in accordance to the concentration applied in comparable studies. Samples were harvested at 24 hours postinfection (hpi), and titers were determined via plaque assay. Each bar represents the mean $\log_{10}$ PFU/ml derived from at least three independent experiments. Data expressed was relative to starting infectious material. Error bars indicate the standard error of the means (SEM). *** = P < 0.001 was considered an extremely significant difference, as determined by Tukey's test.

or 10 µg/ml chlorpromazine, or 5 mM MβCD, or 200 µM E-64, were incubated with L cells at 37°C as for infection procedures, however, without the presence of virus particles in the growth medium. After 24 hours of incubation, cell's morphologies were visualized in microscope and only the apparently viable cells were counted. The results showed that NH$_4$Cl and E-64 were the least cytopathic agents used in this study. These drugs caused no change in the appearance or rate of growth of the subconfluent cultures and cells remained about 100% viable. In contrast, the chosen concentrations of chlorpromazine, chloroquine and MβCD caused different levels of cytotoxicity; viable cells were reduced to less than 50% by chloroquine and chlorpromazine; and even less (20%) by MβCD treatment (Figure 6). Although we used the latter compound at a concentration lower than what was used in previous studies (Rodal et al, 1999; Sieczkarski et al, 2002; Hadžisejdić, 2005), MβCD caused a profound change in the morphology of the cells. Thus, this toxic effect might be related to the amount of virus titer recovered by plaque assay after infecting cells in the presence of the last three cytotoxic drugs (Figure 5).

3.4. Sodium tetradecyl sulphate combined with α-chymotrypsin segregates cleavage of reovirus outer proteins σ3 and µ1.

Previous studies have shown the importance of outer protein cleavage σ3 and µ1 during reovirus infection. Virions treated with trypsin or α-chymotrypsin have been shown to undergo proteolysis that rapidly generates ISVPs; a more infectious particle (Joklik, 1972; Coombs, 1998). ISVPs are characterized by the absence of σ3 and cleavage of µ1 into smaller fragments (δ/ϕ). For that reason, it was first thought that infectivity of ISVPs was probably related to the cleavage of µ1. However, Chandran and
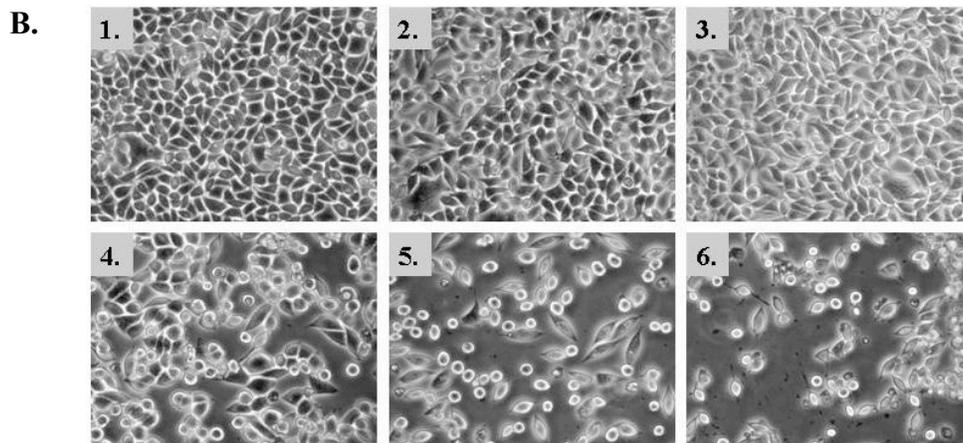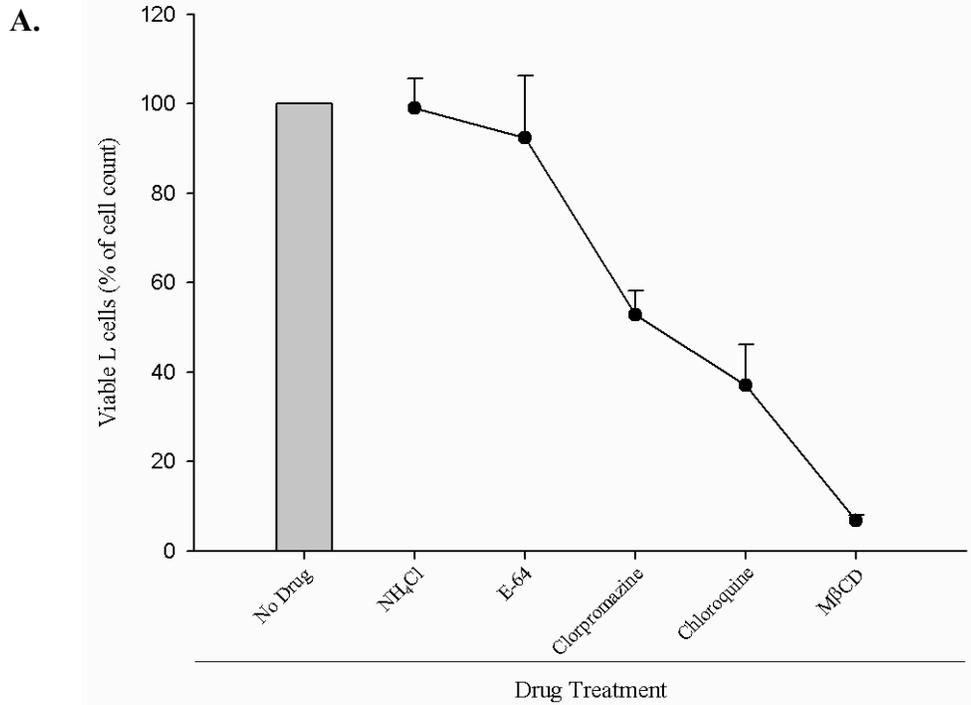
Figure 6. Cytotoxic effect of antiviral drugs on L929 cells after 24 h incubation. A. Monolayers of L929 cells were treated for 1 hour with the selected antiviral drugs: NH_4Cl (20 mM), E-64 (200 μM), chlorpromazine (10 μg/ml), chloroquine (100 μM), and MβCD (5mM). After 1 h, fresh medium supplemented with drugs was replaced and incubated at 37°C for additional 24 h. Cell's morphologies were microscopically counted to identify the percentage of viable cells after treatments. Effect of each drug concentration is shown as average of cell viability collected from three independent experiments. Error bars indicate the standard error of the means. **B.** Cytopathic effect of viral entry blockers on established L929 cells at 24 h post incubation. Cell monolayers were treated as described in A with: NH_4Cl (2), E-64 (3), chlorpromazine (4), chloroquine (5), MβCD (6), or left untreated (1). Photomicrographs (100× magnification) were taken at 24 h post incubation in the presence of these drugs.

Nibert (1998) have shown that cleavage of µ1/µ1C is dispensable for reovirus entry after testing the protein digestion in the presence of sodium tetradecyl sulphate (14SO$_4$), which protects the penetration protein from cleavage (Chandran & Nibert, 1998). Thereafter, Hadžisejdić (2006) confirmed this protection effect and described that in the presence of 14SO$_4$, once σ3 has been removed, µ1 digestion was more rapid and complete. Due to the significance of proteolysis in reovirus infection, this study was designed to understand the cleavage consequence of both σ3 and µ1 prior to ISVP formation (i.e. the transition pathway). In order to investigate this, it was important to separate σ3 digestion from δ generation and µ1/µ1C proteolysis. Consequently, this would make it possible to demonstrate if σ3 is a determinant in reovirus infection. To test this, purified virions were digested from between seconds to minutes to establish *in vitro* what here is called the "transition pathway". Samples resolved by SDS-PAGE showed that while σ3 was progressively removed, there was no detectable µ1/µ1C cleavage until 3 − 5 minutes of treatment with 1mM of 14SO$_4$ plus 10 μg/ml of CHT (Figure 7A). However, digestion of µ1 happened much faster after most of its "protective" σ3 has been cleaved (note; there is still some σ3 left after 7 − 10 minutes but no δ formation in the time point digestion). This result is consistent with and confirms previous results described in Coomb's group. Also, it has demonstrated that digestion of σ3 can be segregated from µ1 digestion (Figure 7A) (Mendez et al, 2003; Hadžisejdić et al, 2006).

3.5. Stoichiometry reveals the percentage of σ3 still present at moment of µ1 cleavage.

Densities of σ3 and λ protein bands were quantified after electrophoretic analysis of reoviral particles generated in the presence of CHT and 14SO$_4$. Core protein λ was used

as a standard to compare the amount of σ3 left during protease treatment. The ratio σ3/λ was determined for each lane by measuring the mean densities of both proteins individually. Analysis of the ratio demonstrated that about 25% of σ3 is still present at 5 – 7 minutes of digestion (Figure 7B). Compared with the previous section, 7 minutes was exactly when μ1 protein started to be progressively removed (compare with μ1 band at 10 minutes). The fact that about 75% of σ3 has been cleaved before CHT exerted a substantial effect on the μ1 protein might have some consequence on virus' infectivity. Since outer capsid proteins are believed to play a role in the early steps of virus infection, treating the particles generated by this method with antiviral agents may provide more information about the functionality of σ3 in particle's infectivity.

3.6. Detergent plus protease treatment generated a particle that has incomplete σ3 digestion but bypasses entry blockers like ISVPs.

Entry of reovirus into cells has been related to alterations in the virus outer capsid layer, which generates a more infectious particle called ISVP (Hadžisejdić et al, 2006). A protocol that generates particles with σ3 and μ1 still present in the virus structure (verified under SDS-PAGE conditions) was tested in the present study. Infectivity of these particles was determined in the presence or absence of entry inhibitors to determine whether or not the presence of intact σ3 is necessary for viral entry. To test this, purified virions were digested with a low concentration of CHT in the presence of $14SO_4$ from seconds to minutes at 32°C. ISVPs were also generated, but using a higher concentration of CHT, in the absence of $14SO_4$, and for 1 h at 37°C. An aliquot of each digested tube was taken for SDS-PAGE structural analysis and the remainder was used for infectivity
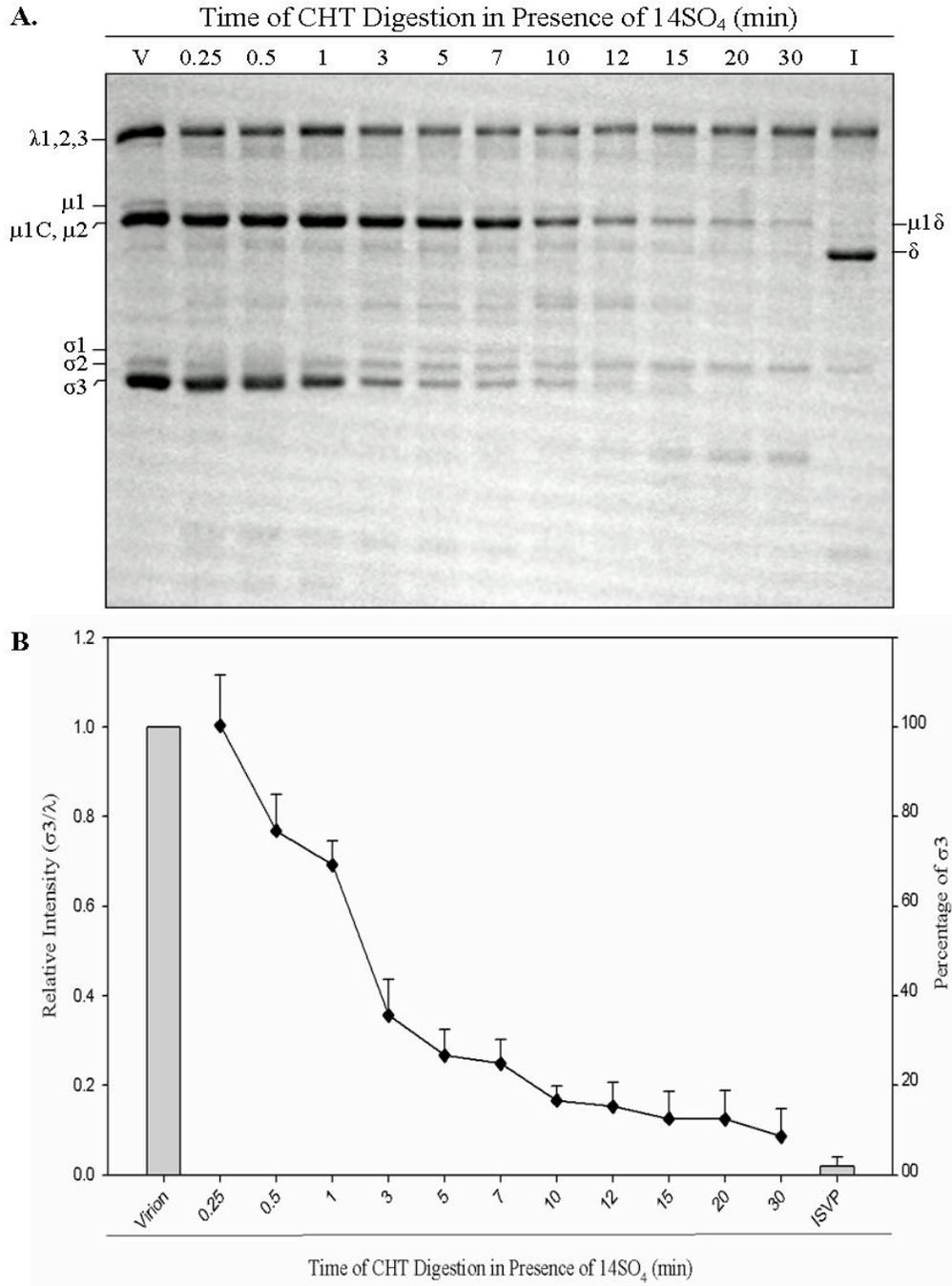
Figure 7. Cleavage of outer proteins σ3 and µ1 is demonstrated by stoichiometry. A. Detergent 14SO$_4$ was combined with CHT to generate particles along the transition pathway and segregate cleavage of proteins σ3 and µ1, concomitantly. **B.** Stoichiometry reveals that approximately 75% of σ3 needs to be removed from the outer capsid of virions to allow µ1 exposure and proteolysis with CHT. Each time point represented in B illustrates means from three independent experiments. Error bars indicate the standard error of the means.

analyses. L929 cells were pre-treated for 1 hour in the presence or absence of 20 mM NH$_4$Cl (acidification inhibitor), 100 μM chloroquine (acidification inhibitor), 10 μg/ml chlorpromazine (clathrin-mediated endocytosis inhibitor), 5 mM MβCD (caveolae-mediated endocytosis inhibitor), and 200 μM E-64 (cysteine protease inhibitor). Subsequently, cells were infected with purified undigested virions, various 14SO$_4^-$ digested particles, and ISVPs at a MOI of 2 PFU/cell. After 1 hour of adsorption medium supplemented with appropriate drugs was replaced and plates were incubated at 37°C for 24 hours. The amount of progeny virion production was afterwards determined by plaque assay. SDS-PAGE analysis showed that particles digested for less than five minutes contained considerable amounts of σ3 protein (Figure 7); however, when placed in the presence of entry blockers (NH$_4$Cl, chloroquine, chlorpromazine, MβCD, or E-64), particles behaved essentially like virions: progeny was inhibited (Figure 8). Particles digested for five-to-seven minutes still contained small amounts of σ3 (Figure 7); however, their infectivity resembled authentic ISVPs: progeny production was not inhibited by any chosen inhibitor (Figure 8). For instance, in the presence of acidification inhibitors (NH$_4$Cl and chloroquine), ISVP has an infectivity that was 100-fold higher than virions treated under the same conditions. Also, particles in the transition pathway achieved by digestion of intact virions had an infectivity that was at least 10-fold higher than virions, suggesting that these particles contain some structural modification that converts them into a more infectious particle, like ISVPs. Similarly, when treated with a cysteine protease inhibitor (E-64), ISVPs and particles digested for about 5 to 7 minutes had an increase of 1.5 log$_{10}$ in titer in comparison to intact virions. Even in harsh cell condition due to drug toxicity, endocytosis-mediated inhibitors (chlorpromazine and

MβCD) have demonstrated that, with a 10-fold increase in titer, ISVP is in fact more infectious than intact virions. At same drug treatment, particles in the transition pathway had about a half $\log_{10}$ change in titer when compared to intact virions. The infectivity of both ISVP and particles in the presence of endocytosis blocker agents was lower than the infectivity of samples treated with other antiviral agents. The fact that chlorpromazine and MβCD are highly toxic to L cells in comparison to other chosen inhibitors (e.g. NH_4Cl and E-64) may explain the difference in titer results, which is most likely caused by the lack of cell viability. In general, when the titers of treated vs. untreated particles were compared within all drug trials, particles displayed an infectivity that was comparable to ISVPs mostly after 7 minutes of digestion (Figure 8H). These results indicate that it is not the cleavage of μ1, but rather the proteolytic digestion σ3, that is a crucial factor in particle internalization (see gel band for 7 minutes in Figure 7A and compare its infectivity in Figure 8). Also, these results support that not all σ3 needs to be proteolytically digested for the particle to behave as ISVPs. The fact that the intermediate particles are more infectious than virions may describe some structural similarity with ISVP forms. Nevertheless, the detailed composition of these populations in the transition pathway remains to be explained. Therefore, a better understanding of both transitional particles and ISVPs would clarify doubts regarding the real identity of particles present during cell entry.

3.7. Fluorescence techniques confirmed CHT proteolysis on the reovirus labelled particles.

One of the questions raised about the digestion effect of CHT on the reovirus outer

G.

H.

I.

J.

K.
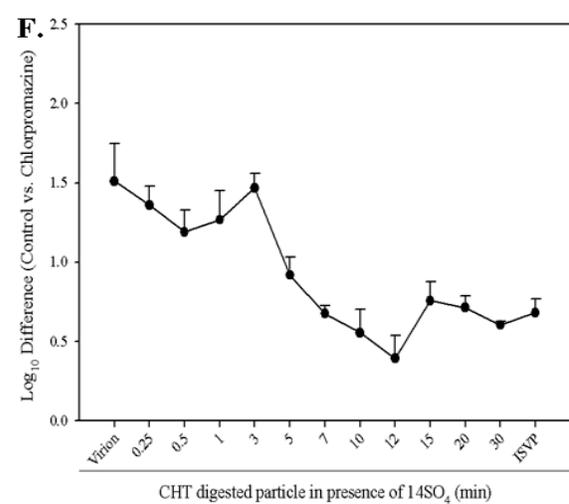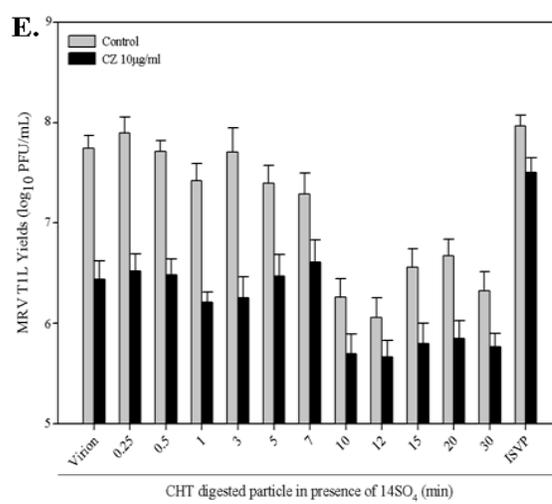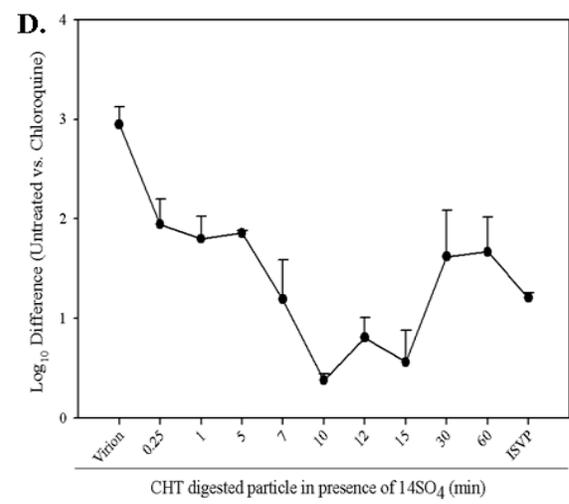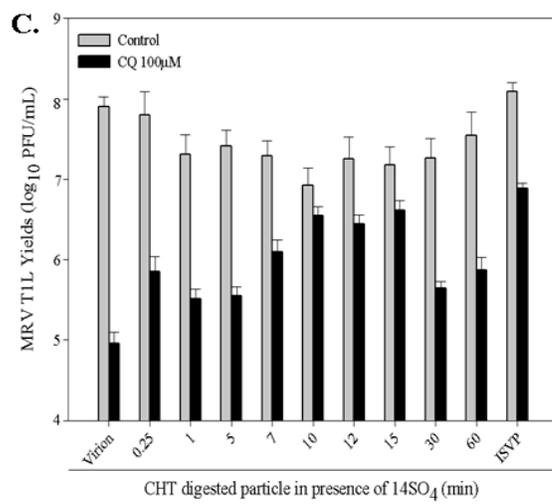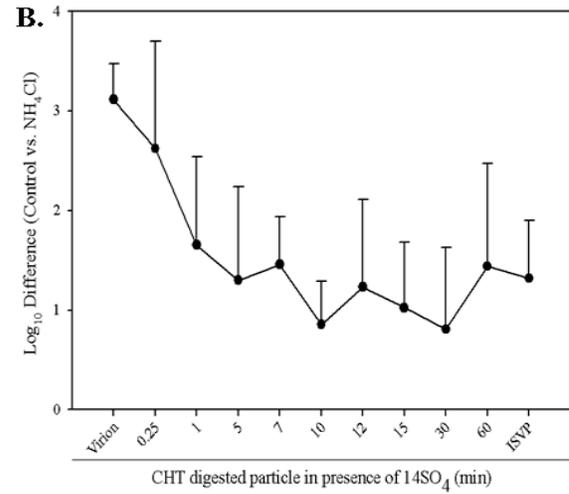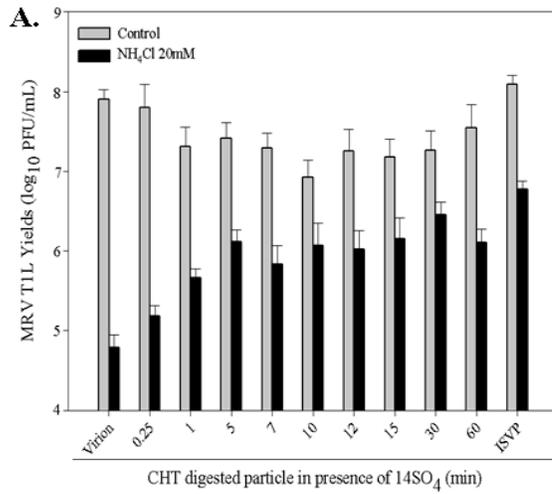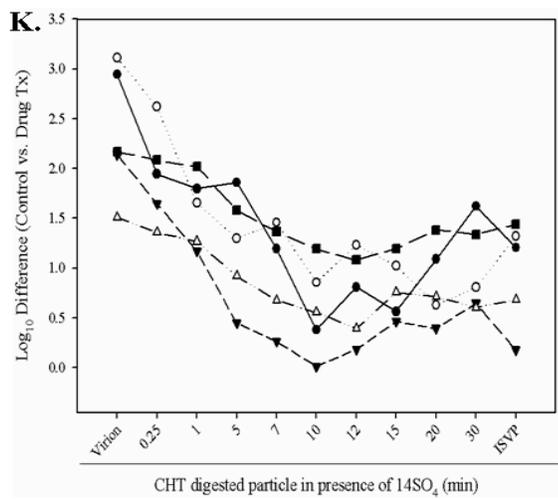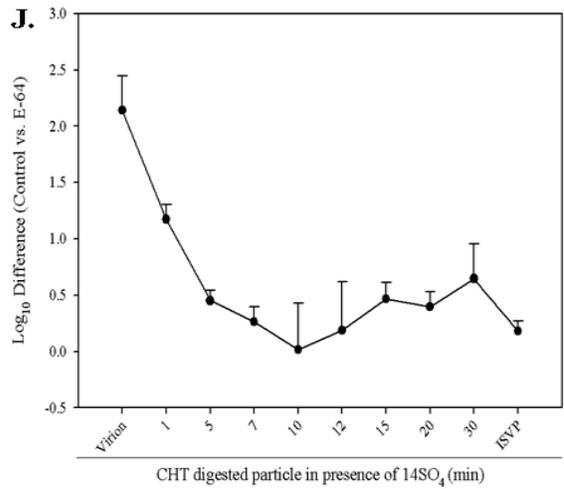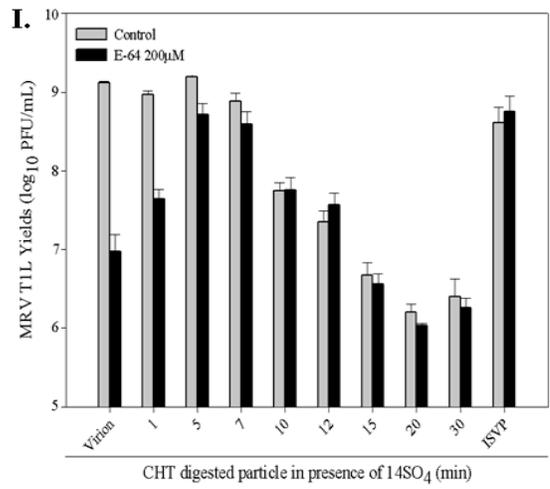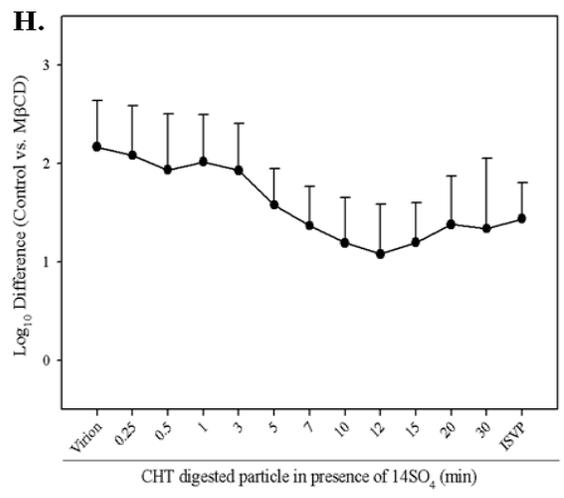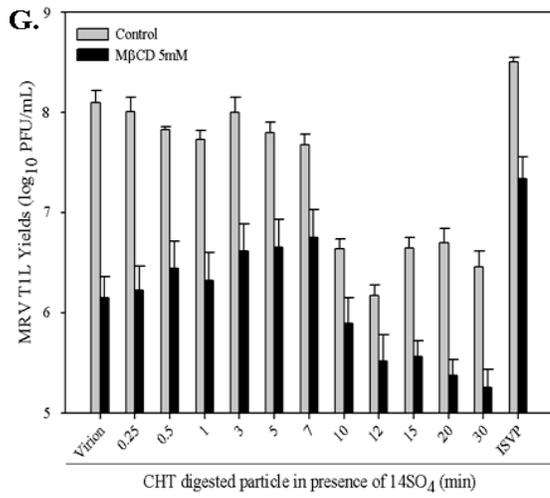
Figure 8. Infectivity of digested particles in the presence of viral entry blockers. Purified T1L virions were digested for specified periods of time with 10 μg/ml CHT in the presence of 1 mM $14SO_4$. Undigested virions, digested particles and ISVPs were tested in the presence and absence (control) of viral inhibitors. After 24 h of viral growth, titers were determined as PFU/ml. The $\log_{10}$ difference in titer described by each treated vs. untreated particle was subsequently plotted. **A-B.** Infectivity and $\log_{10}$ difference in titer of particle growth in the presence of 20 mM NH_4Cl. **C-D.** Infectivity and $\log_{10}$ difference in titer of particle growth in the presence of 100 μM chloroquine (CQ). **E-F.** Infectivity and $\log_{10}$ difference in titer of particle growth in the presence of 10 μg/ml chlorpromazine (CZ). **G-H.** Infectivity and $\log_{10}$ difference in titer of particle growth in the presence of 5 mM MβCD. **I-J.** Infectivity and $\log_{10}$ difference in titer of particle growth in the presence of 200 μM E-64. **K.** Combined $\log_{10}$ difference in titer of all pharmacological agents to describe the particle-to-ISVP similarity in growth for panels B (○), D (●), F (△), H (■), and J (▼). Error bars in A-J indicate the standard error of the means collected from at least three independent experiments.

proteins is related to the types of particles formed by digestion. There is also a possibility that some ISVPs have been formed during the brief viral proteolysis in presence of 14SO$_4$, which could explain the increased titer of particles digested for about 7 minutes. An ISVP subpopulation might not be detected when tested by SDS-PAGE. Therefore, a novel protocol was developed to determine if the population of particles produced by digestion in presence of 14SO$_4$ was homogenous or heterogeneous. Fluorescent dyes such as fluorescein isothiocyanate (FITC), Alexa Fluor, SYBR Green, SYBR Gold, 4'6-diamidino-2-phenylindole (DAPI) and many others have been described in the literature as an invaluable tool for both qualitative and quantitative analyses of viruses. Viruses from several families (Baculoviridae, Herpesviridae, Myoviridae, Phycodnaviridae, Picornaviridae, Podoviridae, Retroviridae, Siphoviridae, Orthomyxoviridae, Reoviridae, etc.) have been detected after staining with these fluorescent agents (Georgi et al, 1990; Brussaard et al, 2000; Huang et al, 2004; Fecek et al, 2006; Xie, 2009). Detection of individual fluorescently labelled reovirions in living cells was described by Field's group in 1990 with a study about virus-host interactions using rhodamine B and FITC (Georgi et al, 1990). More recently a new generation of fluorescent dye, Alexa Fluor 488 (AF488), was effectively used to test the ability of reovirus labelled particles to infect host cells and cause pathogenesis (Fecek et al, 2006). The same study applied matrix-assisted laser desorption/ionization time of light (MALDI-TOF) and the results show that AF488 labelled the external proteins whereas inner capsid proteins appeared to remain non-labelled or labelled at levels below the detection limits (Fecek et al, 2006). Therefore, three major approaches were used in this research to discriminate and characterize the CHT digested particles. First, virions were labelled with Alexa Fluor 488

and resolved by SDS-PAGE as a confirmatory test. Second, labelled virions were digested and major time points were used for infectivity analysis. Third, the product of digestion was also analysed by flow cytometry (FCM), a sensitive detection device for discrimination of labelled particles. To perform the first approach, T1L fluorescently labelled particles were produced and digested under same conditions as unlabelled viruses. Samples were resolved by SDS-PAGE to determine whether or not reovirus outer proteins could be labelled. Alexa succinimidyl esters are specific for amino groups, thus, the potential targets in a protein are primarily arginine and lysine (Huang et al, 2004). As expected, the only proteins labelled by AF488 were located on the outer most part of the capsid, that is; σ3, µ1, and λ (Figure 9A). The results indicated that fluorescently labelled virions were digested by CHT in a similar manner to unlabelled particles (Figure 7 A-B and 9 A-C). Additionally, digestion of µ1 also initiated only after most of σ3 was removed from the outer capsid (note an initial δ band formation at approximately 5 minutes of digestion in Figure 9B). Since µ1 was labelled by AF488, the product of its cleavage (δ) was also detected in the gel (note a light band at δ region in Figure 9A). When comparing the level of staining of the standard Gel Code Blue solution versus AF488, densitometric analysis data described that AF488 did not enhance the intensity of bands expressed by the excitation and emission of the dye (Figure 9C, curves A [◆] and B [◆]). In fact, the levels of proteins presented in all gels were quite similar after three minutes of digestion (Figure 9C). Data indicated that virions stained with Alexa Fluor 488 can represent a good model not only for detection of viral proteins but also to describe the enzymatic effect of CHT on these proteins. Whether the staining has any effect on reovirus infectivity was checked in the following section.
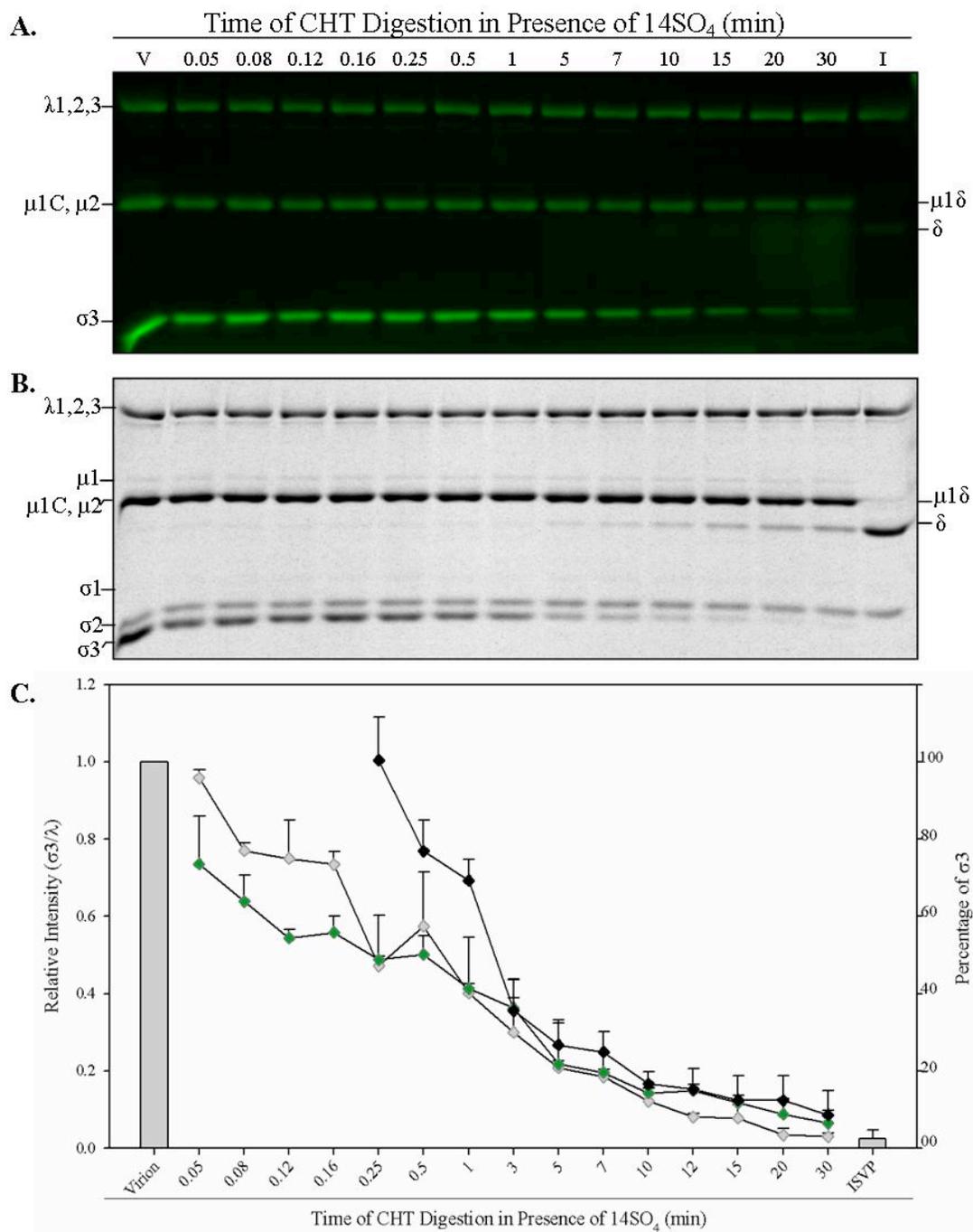
Figure 9. Fluorescence techniques confirmed CHT proteolysis on the reovirus labelled particles. A. T1L virions were labelled by AF488 and digested in line with selected time points. Each sample was resolved by SDS-PAGE and bands were photographed by excitation of dye (475 nm) on a fluorescent imager. **B.** Gel in A was subsequently stained with a coomassie-like solution and photographed under trans white light. **C.** Integrated measure of intensity and size of σ3 and λ bands on A (◆), B (◆), and Figure 7A (◆) were determined for densitometry purposes. Error bars indicate the standard error of the means for at least two independent experiments.

3.8. Labelled reoviruses retain infectivity.

As previously demonstrated Alexa Fluor 488 labelled the outer capsid proteins of reovirus and the labelled proteins were digested by CHT under same manner as unlabelled virions. Therefore I next tested if the infectivity of these particles would change due to the binding dye. When heavily labelled virus was used to infect L929 cells in a normal plaque assay, results indicated that particles were capable of infection and plaque formation. AF488 labelling increased the particle to PFU ratio of virions from 35 (unlabelled) to 106 (labelled); however, this result was not considered significant as the difference in titer was less than ½ $\log_{10}$. To determine if labelled particles would behave similarly in the presence of antiviral drugs as unlabelled particles, infectivity analysis was also tested after labelling and digestion of reovirions. NH_4Cl and E-64 were the only drugs evaluated because they showed less toxicity to the cells and have been more represented in the reovirus literature. There was no relevant difference between progeny production from stained intact virions and stained particles digested for 5 or 7 minutes (Figure 10). Even though infectivity in the presence of drugs of labelled ISVPs was lower than unlabelled ISVPs, these particles still remained slightly (but insignificantly) more infectious than the others (compare Figures 8A and 8I with Figure 10). In agreement with Fecek and colleagues (2006), these results indicate that Alexa Fluor 488 did not alter the ability of virions to bind and produce infection under normal conditions (ratio particle/PFU data described above). However, in the presence of entry blocker agents, the infectivity effect was altered a minimum of 10-fold (compare NH_4Cl virion bars in Figure 8A to Figure 10) to a maximum of 1000-fold (see ISVP bars in Figure 8I and Figure 10).
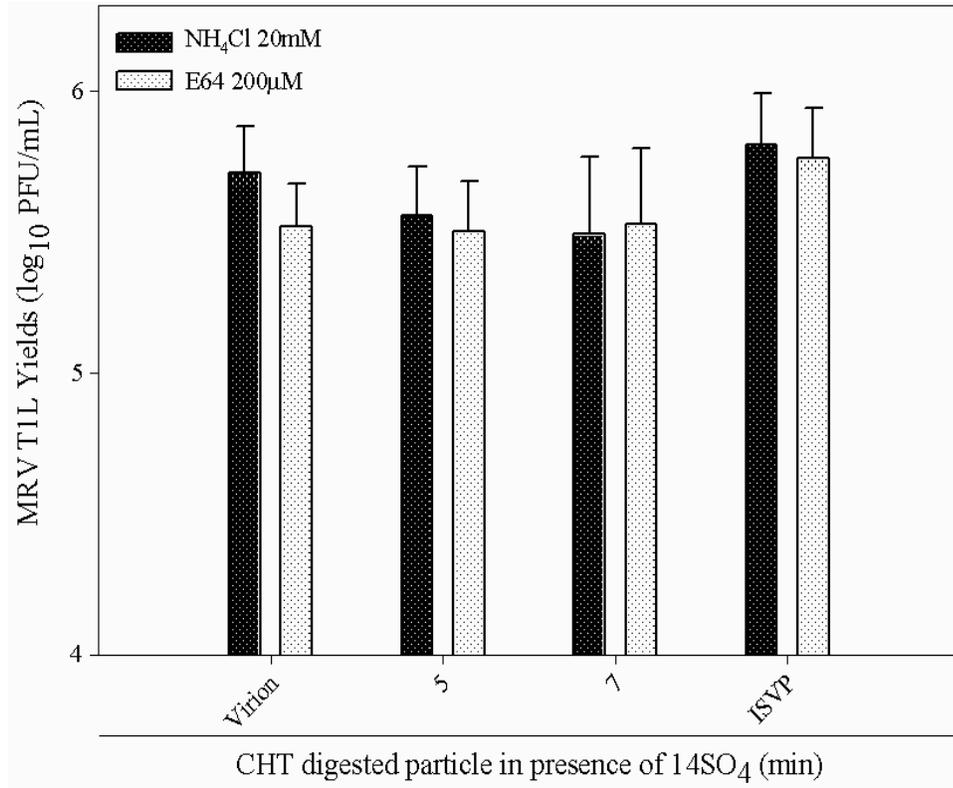
Figure 10. Digested particles lost the ability to bypass antiviral effect when linked to a fluorescent dye. T1L virions were stained with Alexa Fluor 488, digested with CHT in the presence or absence (ISVP) of $14SO_4$ and tested for infectivity in the presence of antivirals NH4Cl, an acidification inhibitor, and E-64, a protease inhibitor. Bars indicate a minor change in titers of virions, transition particles and even ISVPs. A chemical reaction of virus outer proteins and dye was believed to be the cause of low titers for transition particles and ISVPs. Each bar represents the means from three independent experiments. Error bars indicate the standard error of the means.

Also the $\log_{10}$ difference in titers of treated virions versus treated ISVPs shifted from about 3.11 to 0.06 for NH_4Cl, and from 2.0 to 0.17 for E-64. These may explain the importance of σ3 cleavage and μ1 accessibility during virus-to-cell interactions. Since about 80% of σ3 was removed, μ1 became almost completely exposed on the viral surface. Once again, this indicates that σ3 release is probably involved in the binding and internalization of virus via receptor-mediated endocytosis, while μ1 is involved in the penetration as described by Nibert's group (Zhang et al, 2006). Presumably, some μ1C was cleaved at its N-terminal when ISVPs were produced *in vitro* but not within the cell endosome. Fecek et al. (2006) has described that labelling could affect the capacity of σ1 to interact with the host cell membrane. However, the fact that Alexa Fluor targets amino groups and presumably antagonizes the cleavage of μ1 (to release μ1N necessary for penetration) within the endosome may explain the lower progeny production for the labelled digested particles, which have not been affected in the absence of drugs or in section 3.6 (Figure 8 and 10). Virgin et al. (1994) have described a similar inhibitory effect when monoclonal antibodies against reovirus outer proteins blocked the virus proteolysis and infectivity in the presence of NH_4Cl. Why are unlabelled viruses digested for 5 or 7 minutes and ISVPs able to bypass the antiviral effects whereas labelled viruses do not? Developing a method to analyse single particles in a total population was therefore crucial to understand the nature of every generated reovirus particle.

3.9. Alexa Fluor 488 along with monoclonal antibody specific to outer capsid proteins permits detection of reovirus via fluorescent techniques.

Monoclonal antibodies (mAbs) have been used in reovirus research to investigate proteins that are exposed on the surface of the virion particle and also to describe the relationship among them (Hayes et al, 1981; Virgin et al, 1991; Virgin et al, 1994) In order to address the possibility of having a subpopulation of ISVPs in the T1L virion digestions with CHT in the presence of $14SO_4$, a monoclonal antibody specific to reovirus was analysed by fluorescence focus assay and further via flow cytometry. 4F2 was the monoclonal antibody chosen to describe the similarities and differences of the particles tested in this study. Since this antibody has been described to bind specifically to σ3 protein in reovirus T3D, the expectation was that in the presence of T1L the recognition would be quite similar (Virgin et al, 1994), because the σ3 proteins of T3D and T1L have 97% identity, differing only in 11 amino acids (Giantini et al, 1984; Atwater et al, 1986). However, when 4F2 mAb was applied to membranes of western blots containing proteins of both reovirus strains, the luminescence of σ3 band was noticeably brighter in T3D than in T1L (see white arrows in Figure 11B). Surprisingly, the brighter T1L band was located at the same position as µ1. Additionally, when T1L ISVPs were tested for 4F2 mAb binding, the luminescence was detected at the δ position (cleavage of µ1) (Figure 11B). To discard any possibility of contamination three different antibody amplifications were tested. Two are represented in Figure 11B where 4F2 bound to T1L µ1 and T3D σ3. Because no other reovirus σ3-specific antibody has become available for analysis via western blot and also because the goal was the detection of σ3 or µ1 present on the viral structure, further fluorescence techniques were performed using the 4F2 mAb. To assess the binding of the untagged primary monoclonal antibody (4F2), a secondary goat anti-mouse IgG (Alexa Fluor 405 [AF405]) was needed. Therefore,
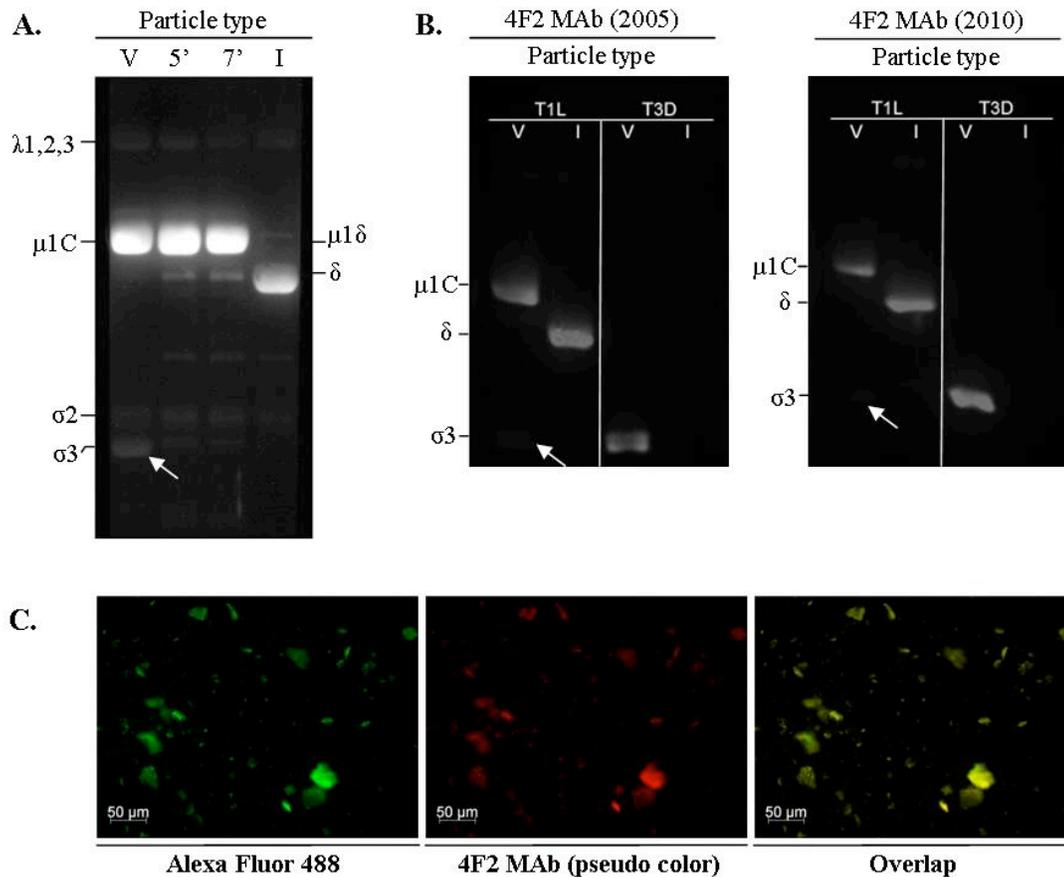
Figure 11. Assessment of mAb 4F2 binding to reovirus via western blot and fluorescence microscopy.
A. A membrane containing reovirus proteins transferred from a common SDS-PAGE was placed in the presence of 4F2 antibody. Binding of antibody to µ1 protein of reovirus T1L was detected via ECL luminescence. **B.** The same procedure described in A was performed in B but using both reovirus strains; T1L and T3D. Western blot showed that 4F2 antibody bound more efficiently to µ1 than σ3 protein on reovirus T1L (faint band at white arrow). Conversely, 4F2 bound uniquely to σ3 protein when tested with proteins resolved from T3D strain. Virus (V), 5 or 7 minutes of digestion in presence of detergent and CHT (5') or (7'), ISVP (I). **C.** Fluorescence image taken from reovirus T1L stained with AF488 and target by 4F2 mAb plus AF405 secondary antibody. A pseudo color was used for better visualization of co-expression of fluorescence at channel overlap.

intact virions were primarily labelled with AF488 then incubated with 4F2 mAb and subsequently with AF405-labelled secondary antibody. The complex was centrifuged to create big pellets for analysis via fluorescence microscopy; otherwise the visualization of virus-sized particles would be expected to be extremely difficult, or impossible. Pellets were slightly resuspended and the excited fluorescent proteins were photographed soon after detection (Figure 11B). Particles were first inspected for AF488; representative of the total virus outer proteins stained (described by green colour). Then, AF405 emission was detected (described in red as pseudo colour for blue at AF405 channel). The overlap of both channels indicated the detection of both, virus and antibody linked to µ1 protein, via a fluorescence focus technique. Consequently, this complex should also be detected in the subsequent flow cytometry analysis.

3.10. Alexa labelled particles combined with µ1-specific antibody allowed the discrimination of single T1L viruses within CHT digested population via flow cytometry.

Flow cytometry was primarily established as an automated method to determine the optical and fluorescence features of cells (Wedemeyer & Pötter, 2001). These cell sorters have become more rapid and more sensitive allowing broader applicability in medical diagnostics (McSharry et al, 1990; Wedemeyer & Pötter, 2001; Janossy & Shapiro, 2008; She et al, 2009). For instance, this tool has been used for virus detection (e.g. vaccinia, dengue, rabies, adenovirus, herpes, HIV, rotavirus, reovirus, etc), titration (e.g. dengue, adenovirus), and infection monitoring (e.g. binding/internalization of influenza virus) (McSharry et al, 1990; Nichols et al, 1993; Domínguez et al, 1998; Barardi et al, 1999; Brussaard et al, 2000; Hitt et al, 2000; Kao et al, 2001; Bordignon et al, 2002a;

Bordignon et al, 2002b; Lambeth et al, 2005; Bottley et al, 2007). In 1979, flow cytometry was successfully used to describe the detection of reovirus particles (Hercher et al, 1979). Years later, Fecek and colleagues (2006) detected fluorescently labelled reovirus particles in a more sensitive flow cytometry approach. However, discrimination of different populations of reovirus particles by mAbs and fluorescent techniques like flow cytometry has not yet been reported. As demonstrated in Figure 12A-C, both unlabelled and labelled (green stained AF488 particle or mAb labelled AF405) intact reovirions could be detected via flow cytometry. In agreement with Hercher et al (1979), the plot indicating unlabelled reovirus count versus side scatter (SSC) was well represented by a half curve located at the very left side of this plot (Figure 12A). Additionally, viruses that were labelled with the green fluorescent dye were detected under the "dim" area created specifically to identify the presence or detection of green fluorescently labelled viruses. Moreover, viruses that were incubated only with the murine mAb 4F2 and AF405-labelled goat anti-mouse secondary were also detected by flow cytometry. Note the difference in detection between unlabelled or labelled AF488 and AF405, indicating that antibody has bound to the reovirus µ1 capsid protein (as described by the count versus AF405 curve in Figure 12C, bottom right plot). Consequently, all three tested samples (i.e. unlabelled virion, AF488 labelled virion, and mAb 4F2-AF405 labelled virion) were used as controls to test all other particles by the same technique. For the normal forward scatter (FSC) vs. SSC plot, the resolution of BD LSR II cytometer is about 0.5 – 1.0 µm. Since it was possible to detect reoviruses via a fluorescent dye and/or a labelled antibody, the idea of characterizing and discriminating these particles using a two colour approach appeared quite tempting. The dye would be
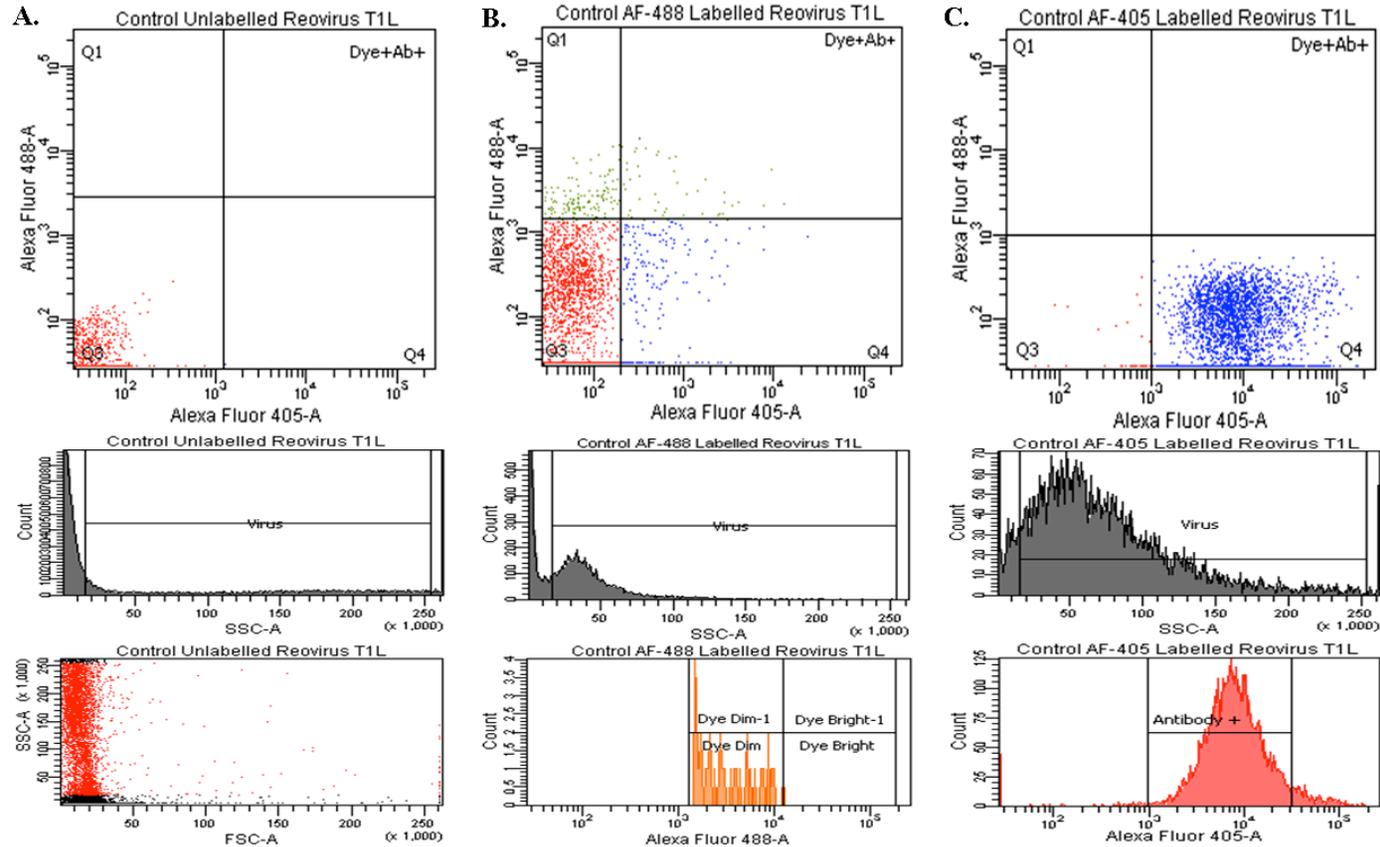
Figure 12. Analysis of unlabelled or labelled reovirion particles via flow cytometry. Laser excitation and fluorescence emission of Alexa Fluor 488- vs. Alexa Fluor 405-labelled particles were measured. Fluorescence signals related to single events are described in the top panels (A-C). Count vs. side scatter (SSC) middle panels illustrate the selected events (A-C). **A.** Unlabelled reovirions. SSC vs. forward scatter (FSC) bottom panel represents the identified events. **B.** AF488 labelled reovirions. Count vs. Alexa Fluor 488 bottom panel describes the dye intensity in "bright" or "dim" fields. A dim colour of the dye could be detected. **C.** Unlabelled reovirus reacted with mAbs tagged to AF405 and were identified as antibody positive. The effect demonstrated that antibody bound reovirions as clearly illustrated by the curve in the bottom panel count vs. Alexa Fluor 405.

used to characterize the presence of virus particles, with all the outer capsid proteins labelled (λ, μ1, σ3). Whereas the labelled mAb would be used to discriminate these particles, with the differences on the presence or absence of μ1 protein specifically positioning the particle form along the antibody axis on the dot plot. However, as the addition of the primary antibody followed by secondary antibody involved washing plus centrifugation of the samples, the possibility of having virus aggregates in the final analyte should be considered. Therefore, aliquots of samples were analysed in a low flow velocity, meaning that the flow stream would be narrowed to decrease the number of event rates (i.e. viruses) passing through the laser beam. The standard low flow rate of the BD LSR II is 240 events per second. The average flow rate taken from a total of at least 10,000 events was determined as 241 events per second for the three main particles tested in this study (i.e. virus, 7 minute-digested, and ISVP). Although there was similarity in results with the cytometer standard, one other aspect that should be considered is the size of the virus. Even though the cytometer stream was narrowed, several $\leq$ 85 nm particles could conceivably pass through the laser as either singlet or doublets. Since events with high width could correspond to aggregates (Figure 13A), by measuring the width parameter vs. the area of each sample it was possible to confirm that particles analysed in this study were not part of a doublet discrimination (Figure 13B-D). Based on this, samples of virion, 7 minute-digested and ISVP were inspected in the flow cytometer to determine the content of each population; whether homogenous or heterogeneous. Results demonstrated plots that were nicely distinguishable from each other. As every experiment began with the intact virion particles, it was expected that these particles would have the highest intensity of antibody and a linear intensity of dye detected in the
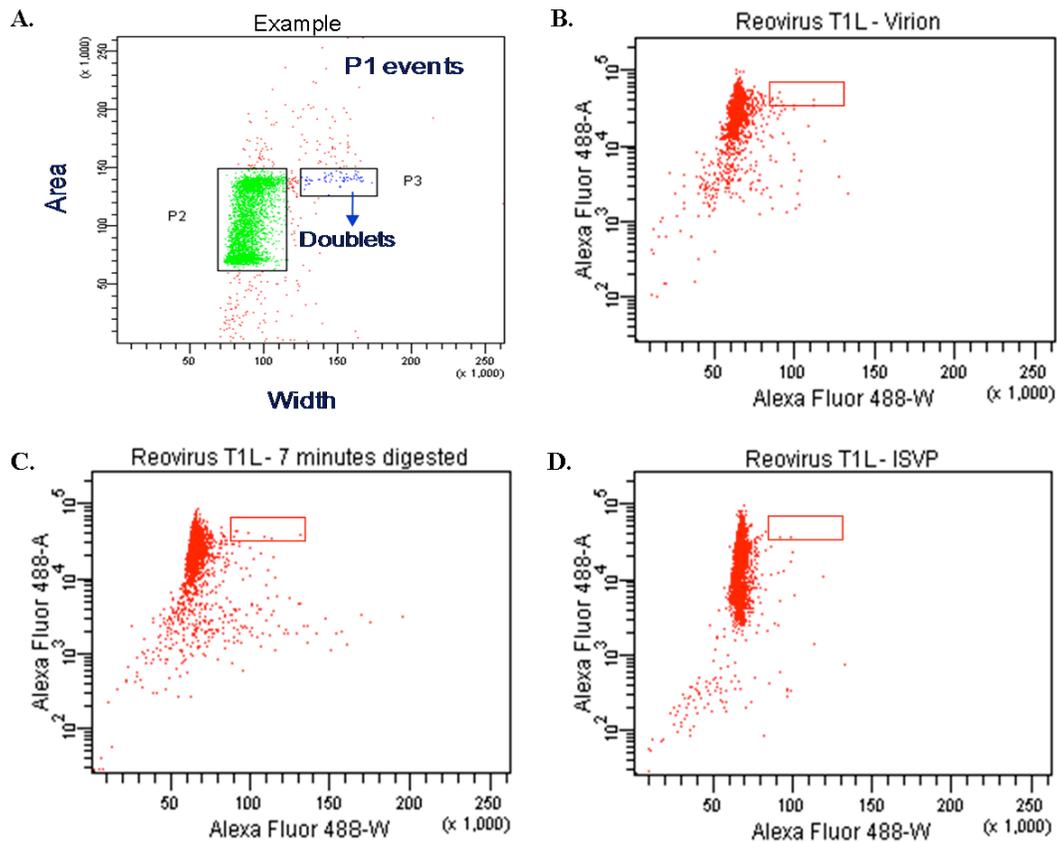
Figure 13. Area versus width distinguished reovirus analytes as non aggregates.
A. Example that may distinguish singlet from doublet particles passing through the laser beam of a flow cytometer. The higher is the width the bigger is the particle, which in here determines presence of aggregates. **B.** Analysis of area vs. width for an intact labelled virion particle. **C.** Analysis of area vs. width for a labelled particle digested for 7 minutes in the presence of $14SO_4$ and CHT. **D.** Analysis of area vs. width for a labelled particle digested by CHT to form ISVP particles. Red boxes were drawn to establish the position of possible doublets. The vast majority of the particles were present within singlet regions and very few were found in the doublet discrimination box. Example adapted from (http://www.bd.com/videos/bdb/dna_canto2_course/M3/index.htm)

laser beam (see plots in Figure 14 and statistics in Table 2). Plots have demonstrated that

virions were more positive to antibody bound (note count vs. antibody AF405 chart in

Figure 14A) than other particles. Regarding the dye emission, data demonstrated that

particles could be stained "bright" and "dim" presumably describing the level of

proteolysis of the particle-associated dye (note Figure 14A, and count vs. dye AF488

chart). By the time that virions were digested for 7 minutes with CHT in the presence of

$14SO_4$, a small population was shifted from the "virion bright" and "virion dim" gates to

the "P2" and "ISVP" gates (Figure 14B). This shift indicates that particles were not

losing a large amount of fluorescence (Figure 14B - count vs. dye AF488), consequently,

this shift was determined by the presence of antibody (Figure 14B – count vs. antibody

AF405). Statistics confirmed that antibody was discriminating the digestion along the

virus-to-ISVP transition pathway (Table 2). For instance, the plot related to ISVP

described the digestion of µ1 protein as expected (Figure 14C). Because ISVP are

characterized by the absence of σ3 and cleavage of µ1 into its fragments δ and ϕ, I

expected a particle not as bright as virions and 7 minutes-digested, which could be

distinguishable by the lack of antibody. Although µ1 was cleaved, both the antibody and

the dye could detect δ protein present on the ISVP structure (Figure 9A, see faint band

related to ISVP δ coming from the cleavage of stained µ1 protein; Figure 11A-B, note the

δ detection by the 4F2 antibody on western blot analysis). Therefore, flow cytometry

confirmed SDS-PAGE and Western Blot results about the digestion to ISVP. The dots

presented in "virus bright" and "virus dim" gates were shifted to "ISVP" and "P1" gates

when ISVPs were passing through the laser (Figure 14A-C). This effect described

particles that were still positive for antibody and dye in the "ISVP" gate but negative for

A.

Reovirus T1L - Virion

Dye+Ab+

Q1
P1
ISVP
P2
Virus Bright
Virus Dim
Q3
Q4

Dye Alexa Fluor 488-A

Antibody Alexa Fluor 405-A

B.

Reovirus T1L digested - 7 minutes

Dye+Ab+

Q1
P1
ISVP
P2
Virus Bright
Virus Dim
Q3
Q4

Dye Alexa Fluor 488-A

Antibody Alexa Fluor 405-A

Reovirus T1L - Virion

Count

Dye Dim-1
Dye Bright-1
Dye Dim
Dye Bright

Dye Alexa Fluor 488-A

Reovirus T1L digested - 7 minutes

Count

Dye Dim-1
Dye Bright-1
Dye Dim
Dye Bright

Dye Alexa Fluor 488-A

Reovirus T1L - Virion

Count

Antibody +

Antibody Alexa Fluor 405-A

Reovirus T1L digested - 7 minutes

Count

Antibody +

Antibody Alexa Fluor 405-A

75

Figure 14. Flow cytometry discriminated reovirus population. Reovirions were fluorescently green labelled with Alexa Fluor 488, digested with CHT in the presence of $14SO_4$ for 7 minutes or in the absence of $14SO_4$ for 1 hour to generate ISVPs. Thereafter, each particle was incubated with 4F2 murine antibody and labelled with a secondary anti-mouse antibody tagged to Alexa Fluor 405 (blue). Particles were then inspected by the BD LSR II cytometer. **A.** Intact reovirion particles non-digested by CHT. **B.** Particles digested for 7 minutes at 32°C with CHT in the presence of $14SO_4$ detergent. **C.** Particles digested with CHT for 1 hour at 37°C to form ISVPs. **D.** Core particles. Cores were generated by digestion of unlabelled virions with CHT for 3 hours at 37°C, and further labelled with Alexa Fluor 488 (Un Core 488), 4F2 murine antibody and Alexa Fluor 405. Panels describe populations according to the presence of dye (in detail at second panel) and antibody (in detail at third panel). Experiment was performed in at least three independent analyses that yielded similar results.

Table 2. Statistical differences of reovirus particles detected via flow cytometry.

Population	# Events	Percentage	Dye MFI[*]	Antibody MFI[*]
Virion				
Dye +ve	10,434	44.0	19,877	1,868
└ Dye Bright	8,002	76.7	24,461	2,305
└ Dye Dim	2,185	20.9	5,365	475
Antibody +ve	7,987	76.5	24,274	2,311
Gate Virus Bright	7,728	74.1	24,455	2,329
Gate Virus Dim	1,214	11.6	5,869	507
Gate P2	40	0.4	32,176	1,292
Gate ISVP	197	1.9	14,001	511
Gate P1	186	1.8	3,394	93
7 minutes digested				
Dye +ve	10,379	45.5	17,464	1,232
└ Dye Bright	8,546	82.3	19,376	1,357
└ Dye Dim	1,792	17.3	8,756	663
Antibody +ve	6,381	61.5	19,730	1,633
Gate Virus Bright	5,801	55.9	19,589	1,653
Gate Virus Dim	857	8.3	8,502	696
Gate P2	219	2.1	30,149	1,179
Gate ISVP	2,178	21.0	16,489	565
Gate P1	175	1.7	12,033	101
ISVP				
Dye +ve	10,263	43.9	10,662	254
└ Dye Bright	3,966	38.6	15,927	347
└ Dye Dim	6,188	60.3	7,473	199
Antibody +ve	115	1.1	15,247	1,849
Gate Virus Bright	80	0.8	17,327	1,333
Gate Virus Dim	230	2.2	5,625	392
Gate P2	3	0.0	33,087	1,004
Gate ISVP	4,099	39.9	12,898	355
Gate P1	3,883	37.8	9,826	87

[*]**MFI:** Mean Fluorescence Intensity.

the antibody in the "P1" gate. As Alexa Fluor 488 labelled particles by staining σ3, μ1, and λ proteins, the digestion effect of CHT would finish with only λ proteins positively labelled for the dye on the surface of the particle. Conversely, as antibodies were specific to μ1 protein but were also able to recognize δ, particles that lack both of these proteins would be negative for the antibody. Therefore, gates indicated that virions were mostly contained at "virion bright" and "virion dim" areas, consequently, positive for both the dye and the antibody. Particles digested for 7 minutes were mostly located at "virus" gates, "P2" gate (positive for the dye and less positive to μ1 bound antibody), "ISVP" gate (positive for the dye and antibody to δ), and some presence at "P1" gate. Particles digested to ISVP were mostly present in "ISVP" and "P1" gates, with some small presence in "virus" gates. The "P1" gate was understood to relate to particles that were presumably positive for the dye (λ) but negative for the antibody. The analysis of the reovirus inner capsids (that contain only λ protein on the virus surface) confirmed the identity of this P1 population as core particles (Figure 14D). To conclude this study, an average of all titers achieved by virions, 7 minute-digested, and ISVP in the presence of the five tested entry blockers (i.e. NH_4Cl, chloroquine, chlorpromazine, MβCD, and E-64) were taken into consideration to compare with the flow cytometry results. The idea was to describe if infectiousness of the virus was related to the particles detected within the "ISVP" gate. Surprisingly, the resultant chart demonstrated that presence of ISVP was a determinant in virus resistance to drugs. The more ISVP is formed the more resistant is the "mixture of virus particles". Consequently, the presence of a subpopulation of ISVPs was the reason for the increased titers for the 7 minute-digested particle. The ability of

digested particles to bypass entry blockers is therefore determined by the formation of ISVPs in the virus population (Figure 15).
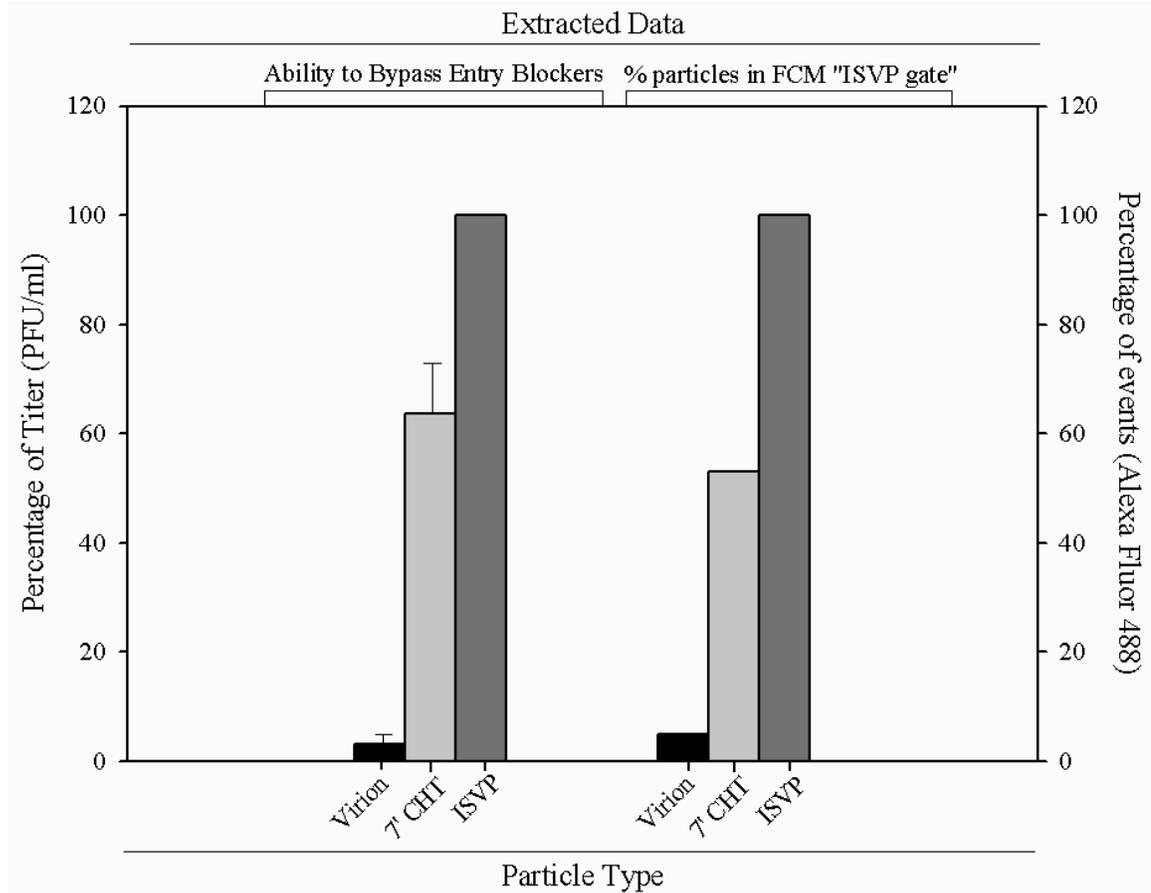
Figure 15. Presence or absence of ISVPs determined virus resistance to entry inhibitors. Particles were digested with CHT for 7 minutes in the presence of 14SO$_4$ (7' CHT), or for 1 hour to form ISVPs. Their infectivity was tested in the presence of pharmaceutical agents such as acidification inhibitors, endocytosis inhibitors, and protease inhibitor that would block the virus entry into cell. As ISVPs demonstrated the highest titer and were considered the more infectious particle, its titer was accepted as indicative of virus 100% capacity to bypass entry blockers. Therefore, titers achieved with intact virions and 7 minutes digested particles were proportionally converted to percentages according to ISVP's titer. In flow cytometry (FCM), the number of events within the "ISVP" gate was recorded for each inspected particle. As ISVP particle demonstrated the highest number of events in this gate, it was considered 100%. The other two particles were proportionally converted in percentage according to the events registered for ISVP.

4. DISCUSSION

The existence of three main particles (virion, ISVP and core) has been known for a long time in the reovirus field. The big question is related to the proteomic changes in the transitional course, mainly along the virus to ISVP pathway. The main proteins affected during this transition are the outer capsid proteins; σ3, μ1 and σ1. In fact, intact reovirions need to be proteolytically digested in order to infect cells, replicate and release progeny. During this process σ3 is removed from virions, μ1 is cleaved and σ1 becomes extended to characterize the ISVP particle. The same process can be achieved *in vitro* by using low concentrations of enzyme such as α-chymotrypsin. Data in this study have demonstrated that in fact, digestion of virions to ISVP can be performed *in vitro*, and even more, tracking of the intermediary steps can also be achieved by using time point digestions during the virion to ISVP pathway (Figure 4 and Figure 7). Because ISVP is an obligate intermediary particle in reovirus disassembly, the capture of intermediate particles that lie within virus-to-ISVP pathway was possible by proteolysis of T1L with an enzyme. A former student from Dr. Coombs group has shown that cleavage of the outer proteins could be controlled by using low concentrations of CHT combined with $14SO_4$ detergent in the digestions (Hadžisejdić et al, 2006). The effect was indeed achieved in the time point digested samples of this study, and the demonstration that cleavage of σ3 could be segregated from μ1 was also confirmed. According to SDS-PAGE data, approximately 75% of σ3 need to be removed for an initial demonstration of μ1 cleavage (Figure 7A). This is in agreement with previous publications which indicate that σ3 acts as a protector of μ1 protein (Liemann et al, 2002; Schiff et al, 2007).

Therefore, any µ1-dependent virus effect (i.e. membrane penetration) is presumably also dependent on σ3 proteolysis. Further analyses of these time point digested samples have described particles that interestingly behaved like ISVPs. This fact occurred when virions, particles digested for brief periods of time (i.e. minute-digested particles), and ISVPs were used to infect cells in the presence of entry blocker agents (Figure 8). Acidification inhibitors such as chloroquine and ammonium chloride were used to block the particles within the vesicle. The expectation was that infecting virions would not be converted into ISVPs and therefore, progeny release would be significantly less in comparison to the *in vitro* pre-formed ISVPs, which could directly penetrate membrane and produce progeny. In fact, data showed lower levels of virion progeny production in the presence of acidification inhibitors (Figure 5A-B and Figure 8A-D). However, the 7 minute-digested particles started to ignore the blocking effect and progeny titers were increased (Figure 8A-D). Thus, important changes occurred during the first 7 minutes of digestion and allowed the particle to behave like the more infectious ISVP (Figure 8B, 8D and 8K). The same effect was achieved when particles were treated with the cysteine protease inhibitor, E-64; with the clathrin-mediated endocytosis inhibitor, chlorpromazine; and with the caveolae mediated endocytosis inhibitor, MβCD. It is believed that reovirions enter susceptible cells via endocytosis (presumably via clathrin mediated-endocytosis), and ISVPs are able to enter cells either by endocytosis or directly via membrane penetration (Sturzenbecker et al, 1987; Schiff et al, 2007). Besides NH_4Cl and chloroquine; E-64, chlorpromazine and MβCD were also tested in this study to evaluate virus' infectivity. Data collected from these trials were in agreement with the data collected with acidification inhibitors. Particles digested for less than 7 minutes

contained significant amounts of non-cleaved σ3 (as seen in SDS-PAGE) and therefore, were not able to bypass entry blockers. Particles digested for more than 7 minutes contained approximately 25% of σ3 left; however, infectivity was not inhibited by any chosen inhibitor (Figure 7 and Figure8). Surprisingly, after 7 minutes of digestion and in the presence of E-64, chlorpromazine and MβCD, particles had a great decrease in titer, which suggests the formation of cores within the digested population (Figure 7 and Figure8). According to these data, 75% of σ3 needs to be removed from the virus surface to allow particle penetration. Consequently, it is reasonable to suggest that not all σ3 needs to be digested in order for virus to gain entry into the cells and produce progeny. Although particles used in this infectivity experiment were proteolytically digested in the presence of $14SO_4$, which prevents μ1 cleavage and ISVP formation, there is still a possibility that detergent did not efficiently block the proteolysis of all particles. Moreover, the analysis of particles in SDS-PAGE determines the content of an entire population but does not differentiate between particles. Therefore, the infectivity effect of 7 minute-digested particles could be either related to an ISVP subpopulation or a result from a real intermediate particle. To distinguish between those two possible outcomes, virions were labelled by a fluorescent agent and analysed via fluorescence techniques. The gel analysis result achieved from these particles was comparable to data from unlabelled particles; 20% of σ3 was still present on the labelled particles after 7 minutes of digestion (Figure 7A-B and Figure 9A-C). However, the infectivity analyses of these particles have demonstrated that they were not able to bypass entry blockers like unlabelled particles (Figure 10). An explanation could be that Alexa Fluor labels and antagonizes the proteins' amino groups which are necessary during virus penetration.

Therefore, progeny release was not as high as demonstrated by unlabelled particles because μ1 was not freely available on the surface of the particle to promote the necessary structural modifications that precede virus internalization. The same labelled particles were subsequently analysed via flow cytometry in order to describe the real content of the 7 minute-digested material. Particles inspected in flow cytometry were distinguished by the amount of AF488 (dye) and AF405 (antibody) detected through the laser beam. The fact that 7 minute-digested particles have μ1 still present and σ3 not completely removed from the virus surface was not in total agreement with the data represented by the cytometer (Figure 9 and Figure 14). As demonstrated in section 3.10, antibody was able to bind and select these particles to the "virus bright" gates, which were set to indicate full particles. Also, a "P2" population was described presumably to demonstrate the transition particle that has σ3 present (dye positive) and μ1 minimally cleaved (antibody shifted), which is consistent with previous peptides findings using MALDI-TOF (Mendez et al, 2003). Moreover, "ISVP" gates were filled in the analysis of this particle, demonstrating particles that lack both μ1 and σ3 but were positive for δ. Consequently, the band demonstrated for 7 minute-digested particle in SDS-PAGE comes from a mixture of reovirus forms. This means that some virions are still present in the aliquot and represent the 20-25% of σ3 protein described in gel analysis (Figure 7B and 9C). The presence of a faint δ band in gel analysis (Figure 9A-B and Figure 11A) can be related to ISVP been formed during the digestion within the 7 minutes, and this is consistent with the "ISVP" gate plotted on the cytometer analysis. ISVP particles have μ1 protein converted into δ, which has shown to fluoresce in SDS-PAGE (Figure 9A), bound to antibody in western-blot (Figure 11A-B) and be consisted in the ISVP gate of

cytometer analysis (Figure 14C). Overall, these results demonstrated a consistency among the three techniques used in this study to evaluate the reovirus particles. The SDS-PAGE was lacking in the demonstration of single particles but was effective in highlighting the CHT effect over the reovirus outer proteins. The western-blot was also effective in demonstrating the digestion effect and the recognition of µ1 and δ proteins by the 4F2 antibody. The real advance in this study was to demonstrate both SDS-PAGE and western-blot in one single experiment that was able to discriminate the particles produced along the transition pathway. As seen by the flow cytometer data, some events were present within the same gate areas in all samples analysed. Some more in "virus" gate and less in "ISVP" gate when virions "only" were detected; or the opposite when ISVPs were analysed. The fact that particles were co-expressed in different samples suggests that every population of reovirus tested in this study (i.e. virion, 7 minute-digested, ISVP and core) was composed of a mixture of forms, and therefore, resided within a heterogeneous population (made of virions, ISVPs, cores; and also by some transitional particles, which have a certain amount of σ3 present and a minimum cleavage on µ1 protein) and not in a homogenous population as previously considered. Consequently, the fact that particles digested for 7 minutes were more "resistant" to entry blockers is completely related to a subpopulation of ISVPs present in the samples. As described by the very last result of this study, ISVP is the particle determinant of reovirus infectiousness; any change in the presence of ISVPs would probably change the infectivity of the virus (Figure 15).

4.1. Future directions

As every study accomplished in research, this one was no different, and many more things can be done to take this study a step further. For instance, the use of fluorescently labelled particles could be microscopically analysed in a real time video as Georgi et al. (1990) have first demonstrated using rhodamine B or FITC (Georgi et al, 1990). The fact that labelled particles were not able to bypass entry blockers may be useful to unveil determinants in reovirus infection, such as; what happens to the viral proteins within vesicle? The same test could be done in the presence or absence of drugs. As predicted, drugs would block the particles and the fluorescence would be paralyzed within the vesicle, whereas, in the absence of drug the intensity would decrease by the time those proteins undergo processing (if the staining does not interfere in this pathway as speculated here in the infectivity analysis results). These could be used as determinants to understand the dynamics between cell compounds and virus particles. It was a pleasure to see that flow cytometer could discriminate reovirus particles within a population. Knowing that some cell sorters can separate particles into different tubes, applying it to this research could be very helpful for the analysis of these particles identity. One could sort these particles and test their identity on electron microscope, or test their infectivity to confirm if the very last plot of this study is consistent with the percentage of ISVPs present in the digested population. Also, because the antibody used in this study was recognizing both $\mu 1$ and δ, the differentiation of a third proposed particle, ISVP* (which differ from ISVP in the conformation of $\mu 1$ [$\mu 1$*] and by the absence of $\sigma 1$), was risky. A better discrimination of reovirus particles may be achieved if novel or multiple antibodies are elaborated to tag different reovirus capsid proteins. To conclude, as this research was

based on reovirus type 1 Lang, the use of reovirus T3D would be beneficial to fulfill the study of the *Reoviridae* family. Because T3D has shown some sensitivities to α-chymotrypsin that are reflected in the infectivity of the virus (due to the loss of σ1 attachment protein), the use of this strain can be slightly complicated. Therefore, a solution would be to use reassortants of T1L and T3D with most of the genes coming from T3D and the gene encoding for σ1 coming from T1L, for example. In this case, the 4F2 antibody would then bind to σ3 protein and therefore, particles would be discriminated by the presence or absence of this protein on their structure. Finally, experiments used in this study could be further applied as a model for studying other non-enveloped viruses, and consequently, understand the virus-to-host cell interactions that may be the hope for many lives (i.e. virus treatment - oncolytics).

5. REFERENCES

Aghi M & Martuza RL (2005) Oncolytic viral therapies - The clinical experience. *Oncogene* 24: 7802-7816

Agosto MA, Ivanovic T, & Nibert ML (2006) Mammalian reovirus, a nonfusogenic nonenveloped virus, forms size-selective pores in a model membrane. *Proc Natl Acad Sci U S A* 103: 16496-16501

Alain T, Hirasawa K, Pon KJ, Nishikawa SG, Urbanski SJ, Auer Y, Lulder J, Martin A, Johnston RN, Janowska-Wieczorek A, Lee PWK, & Kossakowska AE (2002) Reovirus therapy of lymphoid malignancies. *Blood* 100: 4146-4153

Amerongen HM, Wilson GAR, Fields BN, & Neutra MR (1994) Proteolytic processing of reovirus is required for adherence to intestinal M cells. *J Virol* 68: 8428-8432

Antar AAR, Konopka JL, Campbell JA, Henry RA, Perdigoto AL, Carter BD, Pozzi A, Abel TW, & Dermody TS (2009) Junctional adhesion molecule-A is required for hematogenous dissemination of reovirus. *Cell Host Microbe* 5: 59-71

Atwater JA, Munemitsu SM, & Samuel CE (1986) Biosynthesis of reovirus-specified polypeptides. Molecular cDNA cloning and nucleotide sequence of the reovirus serotype 1 Lang strain s4 mRNA which encodes the major capsid surface polypeptide σ3. *Biochem Biophys Res Commun* 136: 183-192

Baer GS & Dermody TS (1997) Mutations in reovirus outer-capsid protein σ3 selected during persistent infections of L cells confer resistance to protease inhibitor E64. *J Virol* 71: 4921-4928

Baer GS, Ebert DH, Chung CJ, Erickson AH, & Dermody TS (1999) Mutant cells selected during persistent reovirus infection do not express mature cathepsin L and do not support reovirus disassembly. *J Virol* 73: 9532-9543

Baker TS, Olson NH, & Fuller SD (1999) Adding the third dimension to virus life cycles: Three-dimensional reconstruction of icosahedral viruses from cryo-electron micrographs. *Microbiol Mol Biol Rev* 63: 862-922

Barardi CRM, Yip H, Emsile KR, Vesey G, Raj Shanker S, & Williams KL (1999) Flow cytometry and RT-PCR for rotavirus detection in artificially seeded oyster meat. *Int J Food Microbiol* 49: 9-18

Barton ES, Chappell JD, Connolly JL, Forrest JC, & Dermody TS (2001a) Reovirus receptors and apoptosis. *Virology* 290: 173-180

Barton ES, Connolly JL, Forrest JC, Chappell JD, & Dermody TS (2001b) Utilization of sialic acid as a coreceptor enhances reovirus attachment by multistep adhesion strengthening. *J Biol Chem* 276: 2200-2211

Barton ES, Forrest JC, Connolly JL, Chappell JD, Liu Y, Schnell FJ, Nusrat A, Parkos CA, & Dermody TS (2001c) Junction adhesion molecule is a receptor for reovirus. *Cell* 104: 441-451

Beattie E, Denzler KL, Tartaglia J, Perkus ME, Paoletti E, & Jacobs BL (1995) Reversal of the interferon-sensitive phenotype of a vaccinia virus lacking E3L by expression of the reovirus S4 gene. *J Virol* 69: 499-505

Berard A & Coombs KM (2009) Mammalian reoviruses: propagation, quantification, and storage. *Curr Protoc Microbiol*: 15C.1.1-15C.1.18

Berger EM, Cox G, Weber L, & Kenney JS (1981) Actin acetylation in drosophila tissue culture cells. *Biochem Genet* 19: 321-331

Bisaillon M, Bergeron J, & Lemay G (1997) Characterization of the nucleoside triphosphate phosphohydrolase and helicase activities of the reovirus λ1 protein. *J Biol Chem* 272: 18298-18303

Bisaillon M & Lemay G (1997) Molecular dissection of the reovirus λ 1 protein nucleic acids binding site. *Virus Res* 51: 231-237

Bodkin DK, Nibert ML, & Fields BN (1989) Proteolytic digestion of reovirus in the intestinal lumens of neonatal mice. *J Virol* 63: 4676-4681

Bordignon J, Comin F, Ferreira SCP, Caporale GMM, Lima Filho JHC, & Zanetti CR (2002a) Calculating rabies virus neutralizing antibodies titres by flow cytometry. *Rev Inst Med Trop Sao Paulo* 44: 151-154

Bordignon J, Pires Ferreira SC, Medeiros Caporale GM, Carrieri ML, Kotait I, Lima HC, & Zanetti CR (2002b) Flow cytometry assay for intracellular rabies virus detection. *J Virol Methods* 105: 181-186

Borsa J, Copps TP, & Sargent MD (1973) New intermediate subviral particles in the in vitro uncoating of reovirus virions by chymotrypsin. *J Virol* 11: 552-564

Borsa J, Morash BD, & Sargent MD (1979) Two modes of entry of reovirus particles into L cells. *J Gen Virol* 45: 161-170

Borsa J, Sargent MD, Lievaart PA, & Copps TP (1981) Reovirus: evidence for a second step in the intracellular uncoating and transcriptase activation process. *Virology* 111: 191-200

Bottley G, Holt JR, James NJ, & Blair GE (2007) Flow cytometric detection of adenoviruses and intracellular adenovirus proteins. *Methods Mol Med* 130: 205-213

Brussaard CPD, Marie D, & Bratbak G (2000) Flow cytometric detection of viruses. *J Virol Methods* 85: 175-182

Cashdollar LW, Chmelo RA, Wiener JR, & Joklik WK (1985) Sequences of the S1 genes of the three serotypes of reovirus. *Proc Natl Acad Sci U S A* 82: 24-28

Chandran K & Nibert ML (1998) Protease cleavage of reovirus capsid protein µ1/µ1C is blocked by alkyl sulfate detergents, yielding a new type of infectious subvirion particle. *J Virol* 72: 467-475

Chandran K, Zhang X, Olson NH, Walker SB, Chappell JD, Dermody TS, Baker TS, & Nibert ML (2001) Complete in vitro assembly of the reovirus outer capsid produces highly infectious particles suitable for genetic studies of the receptor-binding protein. *J Virol* 75: 5335-5342

Chandran K, Farsetta DL, & Nibert ML (2002) Strategy for nonenveloped virus entry: a hydrophobic conformer of the reovirus membrane penetration protein μ1 mediates membrane disruption. *J Virol* 76: 9920-9933

Chandran K, Parker JSL, Ehrlich M, Kirchhausen T, & Nibert ML (2003) The δ Region of Outer-Capsid Protein μ1 Undergoes Conformational Change and Release from Reovirus Particles during Cell Entry. *J Virol* 77: 13361-13375

Chappell JD, Gunn VL, Wetzel JD, Baer GS, & Dermody TS (1997) Mutations in type 3 reovirus that determine binding to sialic acid are contained in the fibrous tail domain of viral attachment protein σ1. *J Virol* 71: 1834-1841

Chappell JD, Prota AE, Dermody TS, & Stehle T (2002) Crystal structure of reovirus attachment protein σ1 reveals evolutionary relationship to adenovirus fiber. *EMBO J* 21: 1-11

Clark KM, Wetzel JD, Gu Y, Ebert DH, McAbee SA, Stoneman EK, Baer GS, Zhu Y, Wilson GJ, Prasad BVV, & Dermody TS (2006) Reovirus variants selected for resistance to ammonium chloride have mutations in viral outer-capsid protein σ3. *J Virol* 80: 671-681

Clarke P & Tyler KL (2003) Reovirus-induced apoptosis: a minireview. *Apoptosis* 8: 141-150

Coffey MC, Strong JE, Forsyth PA, & Lee PWK (1998) Reovirus therapy of tumors with activated Ras pathway. *Science* 282: 1332-1334

Coombs KM (1998) Stoichiometry of reovirus structural proteins in virus, ISVP, and core particles. *Virology* 243: 218-228

Coombs KM (2006) Reovirus structure and morphogenesis. *Curr Top Microbiol Immunol* 309: 117-167

Cumberlidge AG & Isono K (1979) Ribosomal protein modification in *Escherichia coli*. I. A mutant lacking the N-terminal acetylation of protein S5 exhibits thermosensitivity. *J Mol Biol* 131: 169-189

Danis C, Garzon S, & Lemay G (1992) Further characterization of the ts453 mutant of mammalian orthoreovirus serotype 3 and nucleotide sequence of the mutated S4 gene. *Virology* 190: 494-498

Danthi P, Kobayashi T, Holm GH, Hansberger MW, Abel TW, & Dermody TS (2008) Reovirus apoptosis and virulence are regulated by host cell membrane penetration efficiency. *J Virol* 82: 161-172

Denzler KL & Jacobs BL (1994) Site-directed mutagenic analysis of reovirus σ3 protein binding to dsRNA. *Virology* 204: 190-199

Dermody TS, Nibert ML, Wetzel JD, Tong X, & Fields BN (1993) Cells and viruses with mutations affecting viral entry are selected during persistent infections of L cells with mammalian reoviruses. *J Virol* 67: 2055-2063

Domínguez J, Lorenzo MDM, & Blasco R (1998) Green fluorescent protein expressed by a recombinant vaccinia virus permits early detection of infected cells by flow cytometry. *J Immunol Methods* 220: 115-121

Dryden KA, Wang G, Yeager M, Nibert ML, Coombs KM, Furlong DB, Fields BN, & Baker TS (1993) Early steps in reovirus infection are associated with dramatic changes in supramolecular structure and protein conformation: analysis of virions and subviral particles by cryoelectron microscopy and image reconstruction. *J Cell Biol* 122: 1023-1041

Dryden KA, Farsetta DL, Wang G, Keegan JM, Fields BN, Baker TS, & Nibert ML (1998) Internal structures containing transcriptase-related proteins in top component particles of mammalian orthoreovirus. *Virology* 245: 33-46

Dryden KA, Coombs KC, Yeager M (2008) The Structure of Orthoreoviruses. In *Segmented Double-stranded RNA Viruses: Structure and Molecular Biology,* Patton JT (ed) pp 3-35. Caister Academic Press: Norfolk, UK

Ebert DH, Wetzel JD, Brumbaugh DE, Chance SR, Stobie LE, Baer GS, & Dermody TS (2001) Adaptation of reovirus to growth in the presence of protease inhibitor E64 segregates with a mutation in the carboxy terminus of viral outer-capsid protein σ3. *J Virol* 75: 3197-3206

Ebert DH, Deussing J, Peters C, & Dermody TS (2002) Cathepsin L and cathepsin B mediate reovirus disassembly in murine fibroblast cells. *J Biol Chem* 277: 24609-24617

Ehrlich M, Boll W, Van Oijen A, Hariharan R, Chandran K, Nibert ML, & Kirchhausen T (2004) Endocytosis by random initiation and stabilization of clathrin-coated pits. *Cell* 118: 591-605

Faust M, Hastings KEM, & Millward S (1975) m7G5'ppp5'GmpCpUp at the 5' terminus of reovirus messenger RNA. *Nucleic Acids Res* 2: 1329-1343

Fecek RJ, Busch R, Lin H, Pal K, Cunningham CA, & Cuff CF (2006) Production of Alexa Fluor 488-labelled reovirus and characterization of target cell binding, competence, and immunogenicity of labelled virions. *J Immunol Methods* 314: 30-37

Fields B (1985) Genetics of reovirus virulence. *Trends Genet* 1: 284-287

Furlong DB, Nibert ML, & Fields BN (1988) Sigma 1 protein of mammalian reoviruses extends from the surfaces of viral particles. *J Virol* 62: 246-256

Georgi A, Mottola-Hartshorn C, Warner A, Fields B, & Chen LB (1990) Detection of individual fluorescently labelled reovirions in living cells. *Proc Natl Acad Sci U S A* 87: 6579-6583

Giantini M, Seliger LS, Furuichi Y, & Shatkin AJ (1984) Reovirus type 3 genome segment S4: nucleotide sequence of the gene encoding a major virion surface protein. *J Virol* 52: 984-987

Golden JW, Linke J, Schmechel S, Thoemke K, & Schiff LA (2002) Addition of exogenous protease facilitates reovirus infection in many restrictive cells. *J Virol* 76: 7430-7443

Golden JW, Bahe JA, Lucas WT, Nibert ML, & Schiff LA (2004) Cathepsin S supports acid-independent infection by some reoviruses. *J Biol Chem* 279: 8547-8557

Guglielmi KM, Johnson EM, Stehle T, & Dermody TS (2006) Attachment and cell entry of mammalian orthoreovirus. *Curr Top Microbiol Immunol* 309: 1-38

Hadžisejdić I (2005) Mammalian reovirus: characterization of outer capsid protein changes along virus to ISVP transition pathway. *M.Sc. thesis*. University of Manitoba, Winnipeg. Print.

Hadžisejdić I, Cheng K, Wilkins JA, Ens W, & Coombs KM (2006) High-resolution mass spectrometric mapping of reovirus digestion. *Rapid Commun Mass Spectrom* 20: 438-446

Harrison SJ, Farsetta DL, Kim J, Noble S, Broering TJ, & Nibert ML (1999) Mammalian reovirus L3 gene sequences and evidence for a distinct amino- terminal region of the λ1 protein. *Virology* 258: 54-64

Hashiro G, Loh PC, & Yau JT (1977) The preferential cytotoxicity of reovirus for certain transformed cell lines. *Arch Virol* 54: 307-315

Hayes EC, Lee PWK, Miller SE, & Joklik WK (1981) The interaction of a series of hybridoma IgGs with reovirus particles. Demonstration that the core portein λ2 is exposed on the particle surface. *Virology* 108: 147-155

Hazelton PR & Coombs KM (1999) The reovirus mutant tsA279 L2 gene is associated with generation of a spikeless core particle: Implications for capsid assembly. *J Virol* 73: 2298-2308

Hercher M, Mueller W, & Shapiro HM (1979) Detection and discrimination of individual viruses by flow cytometry. *J Histochem Cytochem* 27: 350-352

Hermann LL & Coombs KM (2004) Inhibition of reovirus by mycophenolic acid is associated with the M1 genome segment. *J Virol* 78: 6171-6179

Hitt DC, Booth JL, Dandapani V, Pennington LR, Gimble JM, & Metcalf J (2000) A flow cytometric protocol for titering recombinant adenoviral vectors containing the green fluorescent protein. *Appl Biochem Biotechnol* 14: 197-203

Hruby DE & Franke CA (1993) Viral acylproteins: greasing the wheels of assembly. *Trends Microbiol* 1: 20-25

Huang S, Wang H, Carroll CA, Hayes SJ, Weintraub ST, & Serwer P (2004) Analysis of proteins stained by alexa dyes. *Electrophoresis* 25: 779-784

Huismans H & Joklik WK (1976) Reovirus coded polypeptides in infected cells: isolation of two native monomeric polypeptides with affinity for single stranded and double stranded RNA, respectively. *Virology* 70: 411-424

Imani F & Jacobs BL (1988) Inhibitory activity for the interferon-induced protein kinase is associated with the reovirus serotype 1 σ3 protein. *Proc Natl Acad Sci U S A* 85: 7887-7891

Ivanovic T, Agosto MA, Zhang L, Chandran K, Harrison SC, & Nibert ML (2008) Peptides released from reovirus outer capsid form membrane pores that recruit virus particles. *EMBO J* 27: 1289-1298

Jané-Valbuena J, Nibert ML, Spencer SM, Walker SB, Baker TS, Chen Y, Centonze VE, & Schiff LA (1999) Reovirus virion-like particles obtained by recoating infectious subvirion particles with baculovirus-expressed σ3 protein: an approach for analyzing σ3 functions during virus entry. *J Virol* 73: 2963-2973

Jané-Valbuena J, Breun LA, Schiff LA, & Nibert ML (2002) Sites and determinants of early cleavages in the proteolytic processing pathway of reovirus surface protein σ3. *J Virol* 76: 5184-5197

Janossy G & Shapiro H (2008) Simplified cytometry for routine monitoring of infectious diseases. *Cytometry B Clin Cytom* 74: S6-S10

Jiang J & Coombs KM (2005) Infectious entry of reovirus cores into mammalian cells enhanced by transfection. *J Virol Methods* 128: 88-92

Joklik WK (1972) Studies on the effect of chymotrypsin on reovirions. *Virology* 49: 700-715

Joklik WK (1981) Structure and function of the reovirus genome. *Microbiol Rev* 45: 483-501

Kao C-, Wu M-, Chiu Y-, Lin J-, Wu Y-, Yueh Y-, Chen L-, Shaio M-, & King C- (2001) Flow cytometry compared with indirect immunofluorescence for rapid detection of dengue virus type 1 after amplification in tissue culture. *J Clin Microbiol* 39: 3672-3677

Kauffman RS, Wolf JL, & Finberg R (1983) The σ1 protein determines the extent of spread of reovirus from the gastrointestinal tract of mice. *Virology* 124: 403-410

Kedl R, Schmechel S, & Schiff L (1995) Comparative sequence analysis of the reovirus S4 genes from 13 serotype 1 and serotype 3 field isolates. *J Virol* 69: 552-559

Kobayashi T, Chappell JD, Danthi P, & Dermody TS (2006) Gene-specific inhibition of reovirus replication by RNA interference. *J Virol* 80: 9053-9063

Kobayashi T, Antar AAR, Boehme KW, Danthi P, Eby EA, Guglielmi KM, Holm GH, Johnson EM, Maginnis MS, Naik S, Skelton WB, Wetzel JD, Wilson GJ, Chappell JD, & Dermody TS (2007) A plasmid-based reverse genetics system for animal double-stranded RNA viruses. *Cell Host Microbe* 1: 147-157

Lal R, Harris D, Postel-Vinay S, & De Bono J (2009) Reovirus: rationale and clinical trial update. *Curr Opin Mol Ther* 11: 532-539

Lambeth CR, White LJ, Johnston RE, & De Silva AM (2005) Flow cytometry-based assay for titrating dengue virus. *J Clin Microbiol* 43: 3267-3272

Lee PWK, Hayes EC, & Joklik WK (1981) Protein σ1 is the reovirus cell attachment protein. *Virology* 108: 156-163

Lemay G & Danis C (1994) Reovirus λ1 protein: affinity for double-stranded nucleic acids by a small amino-terminal region of the protein independent from the zinc finger motif. *J Gen Virol* 75: 3261-3266

Lerner AM, Cherry JD, & Finland M (1963) Hemagglutination with reoviruses. *Virology* 19: 58-65

Liemann S, Chandran K, Baker TS, Nibert ML, & Harrison SC (2002) Structure of the reovirus membrane-penetration protein, μ1, in a complex with its protector protein, σ3. *Cell* 108: 283-295

Mabrouk T & Lemay G (1994) Mutations in a CCHC zinc-binding motif of the reovirus σ3 protein decrease its intracellular stability. *J Virol* 68: 5287-5290

Maratos-Flier E, Goodman MJ, Murray AH, & Kahn CR (1986) Ammonium inhibits processing and cytotoxicity of reovirus, a nonenveloped virus. *J Clin Invest* 78: 1003-1007

McCrae MA & Joklik WK (1978) The nature of the polypeptide encoded by each of the 10 double-stranded RNA segments of reovirus type 3. *Virology* 89: 578-593

McSharry JJ, Constantino R, Robbiano E, Echols R, Stevens R, & Lehman JM (1990) Detection and quantitation of human immunodeficiency virus-infected peripheral blood mononuclear cells by flow cytometry. *J Clin Microbiol* 28: 724-733

Mendez II, Hermann LL, Hazelton PR, & Coombs KM (2000) A comparative analysis of freon substitutes in the purification of reovirus and calicivirus. *J Virol Methods* 90: 59-67

Mendez II, She Y-, Ens W, & Coombs KM (2003) Digestion pattern of reovirus outer capsid protein σ3 determined by mass spectrometry. *Virology* 311: 289-304

Mendez II, Weiner SG, She Y-, Yeager M, & Coombs KM (2008) Conformational changes accompany activation of reovirus RNA-dependent RNA transcription. *J Struct Biol* 162: 277-289

Middleton JK, Severson TF, Chandran K, Gillian AL, Yin J, & Nibert ML (2002) Thermostability of reovirus disassembly intermediates (ISVPS) correlates with genetic, biochemical, and thermodynamic properties of major surface protein μ1. *J Virol* 76: 1051-1061

Miller JE & Samuel CE (1992) Proteolytic cleavage of the reovirus sigma 3 protein results in enhanced double-stranded RNA-binding activity: identification of a repeated basic amino acid motif within the C-terminal binding region. *J Virol* 66: 5347-5356

Morin MJ, Warner A, & Fields BN (1994) A pathway for entry of reoviruses into the host through M cells of the respiratory tract. *J Exp Med* 180: 1523-1527

Morin MJ, Warner A, & Fields BN (1996) Reovirus infection in rat lungs as a model to study the pathogenesis of viral pneumonia. *J Virol* 70: 541-548

Morrison LA, Sidman RL, & Fields BN (1991) Direct spread of reovirus from the intestinal lumen to the central nervous system through vagal autonomic nerve fibers. *Proc Natl Acad Sci U S A* 88: 3852-3856

Mustoe TA, Ramig RF, Sharpe AH, & Fields BN (1978) Genetics of reovirus: identification of the ds RNA segments encoding the polypeptides of the μ and σ size classes. *Virology* 89: 594-604

Nagafuku M, Kabayama K, Oka D, Kato A, Tani-Ichi S, Shimada Y, Ohno-Iwashita Y, Yamasaki S, Saito T, Iwabuchi K, Hamaoka T, Inokuchi J-, & Kosugi A (2003) Reduction of glycosphingolipid levels in lipid rafts affects the expression state and function of glycosylphosphatidylinositol-anchored proteins but does not impair signal transduction via the T cell receptor. *J Biol Chem* 278: 51920-51927

Nason EL, Wetzel JD, Erik SKM, Barton S, Venkataram Prasad BVV, & Dermody TS (2001) A monoclonal antibody specific for reovirus outer-capsid protein σ3 inhibits σ1-mediated hemagglutination by steric hindrance. *J Virol* 75: 6625-6634

Nguyen BD, Xia Z, Cutruzzolá F, Allocatelli CT, Brunori M, & La Mar GN (2000) Solution 1H NMR study of the influence of distal hydrogen bonding and N terminus acetylation on the active site electronic and molecular structure of aplysia limacina cyanomet myoglobin. *J Biol Chem* 275: 742-751

Nibert ML, Dermody TS, & Fields BN (1990) Structure of the reovirus cell-attachment protein: a model for the domain organization of σ1. *J Virol* 64: 2976-2989

Nibert ML, Furlong DB, & Fields BN (1991a) Mechanisms of viral pathogenesis. Distinct forms of reoviruses and their roles during replication in cells and host. *J Clin Invest* 88: 727-734

Nibert ML, Schiff LA, & Fields BN (1991b) Mammalian reoviruses contain a myristoylated structural protein. *J Virol* 65: 1960-1967

Nibert ML & Fields BN (1992) A carboxy-terminal fragment of protein µ1/µ1C is present in infectious subvirion particles of mammalian reoviruses and is proposed to have a role in penetration. *J Virol* 66: 6408-6418

Nibert ML, Odegard AL, Agosto MA, Chandran K, & Schiff LA (2005) Putative autocleavage of reovirus µ1 protein in concert with outer-capsid disassembly and activation for membrane permeabilization. *J Mol Biol* 345: 461-474

Nichols JE, Mock DJ, & Roberts Jr. NJ (1993) Use of FITC-labelled influenza virus and flow cytometry to assess binding and internalization of virus by monocytes-macrophages and lymphocytes. *Arch Virol* 130: 441-455

Noad L, Shou J, Coombs KM, & Duncan R (2006) Sequences of avian reovirus M1, M2 and M3 genes and predicted structure/function of the encoded µ proteins. *Virus Res* 116: 45-57

Norman KL & Lee PWK (2000) Reovirus as a novel oncolytic agent. *J Clin Invest* 105: 1035-1038

Norman KL, Hirasawa K, Yang A-, Shields MA, & Lee PWK (2004) Reovirus oncolysis: the Ras/RalGEF/p38 pathway dictates host cell permissiveness to reovirus infection. *Proc Natl Acad Sci U S A* 101: 11099-11104

Odegard AL, Chandran K, Zhang X, Parker JSL, Baker TS, & Nibert ML (2004) Putative autocleavage of outer capsid protein μ1, allowing release of myristoylated peptide μ1N during particle uncoating, is critical for cell entry by reovirus. *J Virol* 78: 8732-8745

Olland AM, Jané-Valbuena J, Schiff LA, Nibert ML, & Harrison SC (2001) Structure of the reovirus outer capsid and dsRNA-binding protein σ3 at 1.8 Å   resolution. *EMBO J* 20: 979-989

Organ EL & Rubin DH (1998) Pathogenesis of reovirus gastrointestinal and hepatobiliary disease. *Curr Top Microbiol Immunol* 233 II: 67-83

Parashar UD, Bresee JS, Gentsch JR, & Glass RI (1998) Rotavirus. *Emerg Infect Dis* 4: 561-570

Patick AK & Potts KE (1998) Protease inhibitors as antiviral agents. *Clin Microbiol Rev* 11: 614-627

Polevoda B & Sherman F (2000) N(α)-terminal acetylation of eukaryotic proteins. *J Biol Chem* 275: 36479-36482

Ramos-Alvarez M & Sabin Ab (1958) Enteropathogenic viruses and bacteria; role in summer diarrheal diseases of infancy and early childhood. *J Am Med Assoc* 167: 147-156

Reinisch KM, Nibert ML, & Harrison SC (2000) Structure of the reovirus core at 3.6 Å resolution. *Nature* 404: 960-967

Rivest P, Proulx M, Lonergan G, Lebel MH, & Bédard L (2004) Hospitalisations for gastroenteritis: The role of rotavirus. *Vaccine* 22: 2013-2017

Rodal SK, Skretting G, Garred O, Vilhard F, van Deurs B & Sandvig K (1999) Extraction of cholesterol with methyl-beta-cyclodextrin perturbs formation of clathrin-coated endocytic vesicles. *Mol Biol Cell* 10: 961-974

Roner MR & Roehr J (2006) The 3′ sequences required for incorporation of an engineered ssRNA into the Reovirus genome. *Virol Journal* 3: 1-11

Rosen L (1962) Reoviruses in animals other than man. *Ann N Y Acad Sci* 101: 461-465

Rubin DH, Kornstein MJ, & Anderson AO (1985) Reovirus serotype 1 intestinal infection: a novel replicative cycle with ileal disease. *J Virol* 53: 391-398

Sabin AB (1959) Reoviruses. *Science* 130: 1387-1389

Schiff LA, Nibert ML, Co MS, Brown EG, & Fields BN (1988) Distinct binding sites for zinc and double-stranded RNA in the reovirus outer capsid protein sigma 3. *Mol Cell Biol* 8: 273-283

Schiff LA (1998) Reovirus capsid proteins σ3 and μ1: interactions that influence viral entry, assembly, and translational control. *Curr Top Microbiol Immunol* 233 I: 179-183

Schiff LA, Nibert ML, Tyler KL (2007) Orthoreoviruses and their replication. In *Fields Virology,* Knipe DM & Howley PM (eds) pp 1853-1915. Lippincott Williams & Wilkins: Philadelphia

Selb B & Weber B (1994) A study of human reovirus IgG and IgA antibodies by ELISA and Western blot. *J Virol Methods* 47: 15-25

Sharpe AH & Fields BN (1982) Reovirus inhibition of cellular RNA and protein synthesis: role of the S4 gene. *Virology* 122: 381-391

Shatkin AJ & Sipe JD (1968) RNA polymerase activity in purified reoviruses. *Proc Natl Acad Sci U S A* 61: 1462-1469

Shatkin AJ, Sipe JD, & Loh P (1968) Separation of ten reovirus genome segments by polyacrylamide gel electrophoresis. *J Virol* 2: 986-991

Shatkin AJ & LaFiandra AJ (1972) Transcription by infectious subviral particles of reovirus. *J Virol* 10: 698-706

She RC, Preobrazhensky SN, Taggart EW, Petti CA, & Bahler DW (2009) Flow cytometric detection and serotyping of enterovirus for the clinical laboratory. *J Virol Methods* 162: 245-250

Sieczkarski SB & Whittaker GR (2002) Influenza virus can enter and infect cells in the absence of clathrin-mediated endocytosis. *J Virol* 76: 1055-1064

Silverstein SC, Schonberg M, Levin DH, & Acs G (1970) The reovirus replicative cycle: conservation of parental RNA and protein. *Proc Natl Acad Sci U S A* 67: 275-281

Silverstein SC, Astell C, Levin DH, Schonberg M, & Acs G (1972) The mechanisms of reovirus uncoating and gene activation in vivo. *Virology* 47: 797-806

Smith RE, Zweerink HJ, & Joklik WK (1969) Polypeptide components of virions, top component and cores of reovirus type 3. *Virology* 39: 791-810

Stanley NF (1967) Reoviruses. *Br Med Bull* 23: 150-154

Stoeckel J & Hay JG (2006) Drug evaluation: Reolysin - wild-type reovirus as a cancer therapeutic. *Curr Opin Mol Ther* 8: 249-260

Strong JE, Coffey MC, Tang D, Sabinin P, & Lee PWK (1998) The molecular basis of viral oncolysis: usurpation of the Ras signaling pathway by reovirus. *EMBO J* 17: 3351-3362

Sturzenbecker LJ, Nibert M, Furlong D, & Fields BN (1987) Intracellular digestion of reovirus particles requires a low pH and is an essential step in the viral infectious cycle. *J Virol* 61: 2351-2361

Tercero JC & Wickner RB (1992) MAK3 encodes an N-acetyltransferase whose modification of the L-A gag NH2 terminus is necessary for virus particle assembly. *J Biol Chem* 267: 20277-20281

Thirukkumaran CM, Nodwell MJ, Hirasawa K, Shi Z-, Diaz R, Luider J, Johnston RN, Forsyth PA, Magliocco AM, Lee P, Nishikawa S, Donnelly B, Coffey M, Trpkov K, Fonseca K, Spurrell J, & Morris DG (2010) Oncolytic viral therapy for prostate cancer: efficacy of reovirus as a biological therapeutic. *Cancer Res* 70: 2435-2444

Tyler KL, McPhee DA, & Fields BN (1986) Distinct pathways of viral spread in the host determined by reovirus S1 gene segment. *Science* 233: 770-774

Tyler KL, Clarke P, DeBiasi RL, Kominsky D, & Poggioli GJ (2001) Reoviruses and the host cell. *Trends Microbiol* 9: 560-564

Van Regenmortel MHV & Fauquet CM (2000) Advances in viral toxonomy. *Virologie* 4: 29-37

Virgin IV HW, Mann MA, Fields BN, & Tyler KL (1991) Monoclonal antibodies to reovirus reveal structure/function relationships between capsid proteins and genetics of susceptibility to antibody action. *J Virol* 65: 6772-6781

Virgin IV HW, Mann MA, & Tyler KL (1994) Protective antibodies inhibit reovirus internalization and uncoating by intracellular proteases. *J Virol* 68: 6719-6729

Wedemeyer N & Pötter T (2001) Flow cytometry: an 'old' tool for novel applications in medical genetics. *Clin Genet* 60: 1-8

Weiner HL, Drayna D, Averill Jr. DR, & Fields BN (1977) Molecular basis of reovirus virulence: role of the S1 gene. *Proc Natl Acad Sci U S A* 74: 5744-5748

Weiner HL, Powers ML, & Fields Fields BN (1980) Absolute linkage of virulence and central nervous system cell tropism of reoviruses to viral hemagglutinin. *J Infect Dis* 141: 609-616

Wetzel JD, Wilson GJ, Baer GS, Dunnigan LR, Wright JP, Tang DSH, & Dermody TS (1997) Reovirus variants selected during persistent infections of L cells contain mutations in the vital S1 and S4 genes and are altered in viral disassembly. *J Virol* 71: 1362-1369

Wiener JR, McLaughlin T, & Joklik WK (1989) The sequences of the S2 genome segments of reovirus serotype 3 and of the dsRNA-negative mutant ts447. *Virology* 170: 340-341

Wilson GJ, Nason EL, Hardy CS, Ebert DH, Wetzel JD, Venkataram Prasad BV, & Dermody TS (2002) A single mutation in the carboxy terminus of reovirus outer-capsid protein σ3 confers enhanced kinetics of σ3 proteolysis, resistance to inhibitors of viral disassembly, and alterations in σ3 structure. *J Virol* 76: 9832-9843

Wolf JL, Rubin DH, & Finberg R (1981) Intestinal M cells: a pathway for entry of reovirus into the host. *Science* 212: 471-472

Wolf JL, Dambrauskas R, Sharpe AH, & Trier JS (1987) Adherence to and penetration of the intestinal epithelium by reovirus type 1 in neonatal mice. *Gastroenterology* 92: 82-91

Xie D (2009) Fluorescent dye labelled influenza virus mainly infects innate immune cells and activated lymphocytes and can be used in cell-mediated immune response assay. *J Immunol Methods* 343: 42-48

Xu P, Miller SE, & Joklik WK (1993) Generation of reovirus core-like particles in cells infected with hybrid vaccinia viruses that express genome segments L1, L2, L3, and S2. *Virology* 197: 726-731

Yin P, Cheang M, & Coombs KM (1996) The M1 gene is associated with differences in the temperature optimum of the transcriptase activity in reovirus core particles. *J Virol* 70: 1223-1227

Zhang L, Chandran K, Nibert ML, & Harrison SC (2006) Reovirus µ1 structural rearrangements that mediate membrane penetration. *J Virol* 80: 12367-12376

Zhang X, Walker SB, Chipman PR, Nibert ML, & Baker TS (2003) Reovirus polymerase λ3 localized by cryo-electron microscopy of virions at a resolution of 7.6 Å . *Nat Struct Biol* 10: 1011-1018

Zhang X, Ji Y, Zhang L, Harrison SC, Marinescu DC, Nibert ML, & Baker TS (2005) Features of reovirus outer capsid protein µ1 revealed by electron cryomicroscopy and image reconstruction of the virion at 7.0 Å resolution. *Structure* 13: 1545-1557